UNDER THE INFLUENCE:

PF BACTERIOPHAGE MODULATE *PSEUDOMONAS AERUGINOSA* VIRULENCE & PATHOGENESIS

By

AMELIA KASS SCHMIDT

BScA, Quest University Canada, Squamish BC, V8B0N8, 2020

Dissertation

presented in partial fulfillment of the requirements
for the degree of

Doctor of Philosophy
in Cellular, Molecular, and Microbial Biology

The University of Montana
Missoula, MT

September 2024

Approved by:

Scott Whittenburg, Dean of The Graduate School
Graduate School

Dr. Patrick Secor, Chair
Division of Biological Sciences, University of Montana

Dr. Ekaterina Voronina
Division of Biological Sciences, University of Montana

Dr. Brandon S. Cooper
Division of Biological Sciences, University of Montana

Dr. Brent Ryckman
Division of Biological Sciences, University of Montana

Dr. Paul L. Bollyky
Division of Infectious Diseases and Geographic Medicine, Stanford University

ABSTRACT

Schmidt, Amelia Kass, Ph.D., 20240920 Cellular, Molecular, and Microbial Biology

Under the Influence: Pf Bacteriophage Modulate *Pseudomonas aeruginosa* Virulence & Pathogenesis

Chairperson: Dr. Patrick Secor

Pseudomonas aeruginosa is a gram-negative opportunistic bacterial pathogen which is as ubiquitous in the natural environment as it is within hospital settings, where it is a readily acquired nosocomial pathogen. Bacteriophages, viruses which infect bacteria, are a central component of the arsenal *P. aeruginosa* leverages to combat the stresses of infecting mammalian hosts. Over 60% of *P. aeruginosa* clinical isolates are chronically infected with temperate phages within the family of *Inoviridae.* These phages, referred to as Pf, have a filamentous virion structure which accommodates genome sizes between 10-20kbp. Pf is capable of integration into the bacterial chromosome where they can exist in a dormant prophage state, or excise and produce viral progeny which extrude from the bacterial host. Overproduction of Pf resulting from infection of a cell that already harbors a prophage; called superinfection, can lead to membrane stress and ultimately cell lysis. Temperate phages, such as Pf, typically encode superinfection exclusion mechanisms. Twitch motility is mediated by the classical bacterial virulence factor, Type IV Pili (T4P) which mediates bacterial adhesion allowing for biofilm formation. Importantly, T4P serve as the cell surface receptor for Pf, among other phages. We describe inhibition of Pf plaquing and twitch motility by a highly conserved Pf superinfection exclusion gene, *pfsE* (*PA0721)*. Furthermore, we determine that highly conserved aromatic residues facilitate PfsE localization to the inner membrane where PfsE binds to T4P structural subunit PilC, suppressing twitch motility. As most work on Pf phages focuses on Pf4 in the model *P. aeruginosa* strain PAO1, we sought to interrogate how Pf phage modulate virulence-associated phenotypes within diverse clinical isolate hosts. We describe a technique which targets the Pf lysogeny maintenance gene *pflM* (*PA0718*) and demonstrate that *pflM* deletion results in prophage excision but not replication, leading to total prophage loss. We identify conservation of a DUF5447 domain within all examined *pflM* alleles, implicating this domain in Pf lysis/lysogeny decision making. Next, we assess the effects different Pf phages have on virulence associated phenotypes and determine that although impacts on quorum sensing and biofilm formation appear to be strain-specific, nearly all Pf phages suppress pigment production and increase bacterial virulence against bacterivorous nematode *Caenorhabditis elegans.*

Collectively, this research advances our understanding of how filamentous Pf phages influence *P. aeruginosa* pathogenesis.

ACKNOWLEDGMENTS

I cannot fully express my gratitude for the countless people who have made this Ph.D. possible, we'd be here all day, but I would like to acknowledge (in a somewhat specific order):

Dr. Patrick R. Secor thank you for seeing me as a scientist, far before I saw myself as one. Thank you for your mentorship, enthusiasm, and time (lots of it!). My next boss has some big shoes (Chacos) to fill!

My committee members: Paul, Brandon, Brent, Katya – thank you for your support, wisdom, and encouragement over the past 4 years.

To Sarah Weldon, Dr. Luke White, and Dr. Mike Minnick -- thank you for making teaching fun. Sarah, thank you for the chats that took my mind of work, and letting me raid your chemical inventory on occasion. Sorry about the ice bucket that I stole. I think it's probably in Bozeman by now. Luke, thank you for guiding me as a wide-eyed first year through the frenzy that is General Microbiology. And Mike, thank you for steering me away from countless elephant traps, always encouraging me (often by example) to get outside, and for curing my friend Sadie's foot fungus.

Lab-mates past and present—thank you for making the lab a place I wanted to be, even on (some) warm sunny days. I would not be here without you. Thank you, Dr. Caleb Schwartzkopf, for gracefully laying the foundation I built this dissertation on. Thank you, Dr. Camilla de Mattos, Dr. Valery Roman-Cruz, Dr. Laura Jennings, Diane Brooks, Dr. Robert Brzozowski, Alison Coluccio, Mason Mazzola, Andrew Maciver, Autumn Robinson, Jared McGourty, Madilyn Head, Tyrza Lamma, Alex Joyce, Dr. DeAnna Bublitz, Elise Wells, Shelby Cole, Aubrey Schwartzkopf, Devin Hunt, and Lia Michaels.

Jill Burke, Ruth Johnson, Anne Tolo, and Janean Clark– Thank you for your guidance through the maze that is UMs bureaucracy, and for always picking up the phone or responding to my (barrage of) emails. I owe each of you a beer (or other beverage of choice!), redeemable at your convenience.

To my early mentors:

Dr. Marina Tourlakis, thank you for being your cool, funny, and whip-smart self. Your *second* most impactful lesson was a mandate to learn what each component of a reagent does before using it, which I still do. Your *first* was demonstrating to an impressionable teenager that science is a place where I can feel at home.

Prof. Dr. Martin Loessner, Dr. Samuel Kilcher, and Dr. Susanne Meile, thank you for letting me join your group on a whim and teaching me what doing 'research' meant. I am proud to say that I know how to spell *Bacillus* now.

Thank you to Dr. Margie Kinnersley, who possesses a depth of knowledge us mere mortals can only aspire to. I cannot express how grateful I am for your guidance in moments of uncertainty, and for encouraging me to pursue this dang degree. Tell your dogs I say hi.

Thank you to Dominick Faith, my comrade and confidant though the entirety of this degree. Thank you for lending an ear/hand even when I was interrupting (often), keeping up with the literature (one of us had to, and it sure wasn't me!), and for being my all-around role-model.

To my family–

First and foremost: Mom, Dad, thank you for your love, encouragement, and all that you both are to me. I quite literally would not be here without you, thank you for everything.

My siblings, Nina & Sutter (but mostly Nina because Sutter is an actual dog), thank you listening, chatting (not you Sutter, stop barking!), and loving me through all the phage talk.

Kristie, for being the picture of a chic badassery—I'm lucky to know you.

My grandparents—Hal, Liz, thank you for all your love, encouragement, and support.

And those who I deeply wish could be here today—

Nona & Poppy, thank you for enabling me to pursue my undergraduate degree, providing a blue-print for life-long learning, and for introducing me to Koffie Hopjes [Dutch coffee candies].

And Mugga. Thank you for always making me feel loved and imparting on me your ferocity for life. I really miss you.

Thank you to the *other* Dr. Schmidt (no relation). I would not be where I am or, more importantly, who I am without you. I cannot overemphasize my gratitude for your time, wisdom, and steady guiding hand.

My chosen family—Elsa, Brook, and Sadie. My queens! Thank you for making me laugh until I cry, pulling me out of more work dungeons than I can count, and not *ever* letting me forget who I am.

And finally, thank you to my partner, Ian. Thank you for your love, support, and patience through the many obscenely late nights in the lab and hearing me say *Be home in 30!* while knowing I probably mean an hour (or two). But more than anything, thank you for being my everything person. I love you.

Once more unto the breach, dear friends, once more[!]

TABLE OF CONTENTS

ABSTRACT.....iii

ACKNOWLEDGEMENTS.....iv

LIST OF TABLES.....ix

LIST OF FIGURES.....x

CHAPTER ONE Introduction and Context.....1

1.1. **The Filamentous Bacteriophage**.....1

1.1.1. Infection.....1

1.1.2. Replication.....2

1.1.3. Egress.....3

1.2. **Pf Phages**.....4

1.2.1. The Pf lifecycle.....5

1.2.2. Superinfection.....6

1.3. **The bacterial pathogen *Pseudomonas aeruginosa***.....8

1.4. **Pf Phages and *Pseudomonas aeruginosa***.....8

1.4.1. Modulation of Mammalian Immunity.....9

1.4.2. Biofilm formation.....9

1.4.3. Quorum sensing.....9

1.5. **Thesis Aims**.....10

CHAPTER TWO A Filamentous Bacteriophage Protein Inhibits Type IV pili to prevent superinfection of *Pseudomonas aeruginosa*.....11

2.1. **Abstract**.....11

2.1.1. Importance.....12

2.2. **Introduction**.....12

2.3. **Results**.....13

2.3.1. Type IV pili are transiently suppressed in response to Pf4 superinfection.....13

2.3.2. PfsE suppresses twitching motility and protects *P. aeruginosa* from superinfection.....14

2.3.3. T4P are not apparent on cells expressing PfsE.....15

2.3.4. PfsE protects *P. aeruginosa* from other T4P-dependent phage species.....16

2.3.5. Deletion of *pfsE* increases Pf4 virulence against *P. aeruginosa*.....17

2.3.6. Aromatic residues in PfsE are required to inhibit twitching motility and promote Pf4 resistance.....18

2.3.7. PfsE binds to the T4P inner-membrane protein PilC.....19

2.4. **Discussion**.....20

2.5. **Materials and Methods**.....22

2.5.1. Bacterial strains, plasmids, and growth conditions.....22

2.5.2. Construction of strain ΔPf4....22
2.5.3. Phage Expression Constructs....23
2.5.4. Twitch motility assays....23
2.5.5. Plaque assays....23
2.5.6. Pf4 phage virion quantitation by qPCR....23
2.5.7. Pf4 virion induction....24
2.5.8. Growth Curves....24
2.5.9. Transmission Electron Microscopy....24
2.5.10. Bacterial two-hybrid assays....24
2.5.11. PfsE modeling....25
2.5.12. Statistical analyses....26
2.6. **Acknowledgements**....26

CHAPTER THREE Targeted Deletion of Pf prophages from diverse *Pseudomonas aeruginosa* isolates has differential impacts on quorum sensing and virulence traits....27

3.1. **Abstract**....27
3.1.1. Importance....28
3.2. **Introduction**....28
3.3. **Results**....30
3.3.1. PA0718 (PflM) maintains Pf4 lysogeny in *P. aeruginosa* PAO1....30
3.3.2. The targeted deletion of pflM cures diverse *P. aeruginosa* isolates of their Pf prophages....32
3.3.3. Pf phages differentially modulate host quorum sensing....35
3.3.4. Pf phages have contrasting impacts on *P. aeruginosa* biofilm formation....36
3.3.5. Pf phages suppress *P. aeruginosa* pyocyanin production in most clinical isolates....37
3.3.6. Pf phages induce avoidance behavior in bacterivorous nematodes....38
3.4. **Discussion**....38
3.5. **Materials and Methods**....41
3.5.1. Strains, plasmids, primers, and growth conditions....41
3.5.2. Construction of Deletion Mutants....42
3.5.3. Excision Assays....43
3.5.4. Plaque assays....43
3.5.5. Quantitative PCR (qPCR) 43
3.5.6. Pyocyanin extraction and measurement....43
3.5.7. Quorum sensing reporters....44
3.5.8. *C. elegans* Growth Conditions....44
3.5.9. *C. elegans* Avoidance Assays....44
3.5.10. Whole Genome Sequencing & Annotation....44
3.5.11. Statistical analyses....45
3.6. **Acknowledgements**....45

CHAPTER FOUR Pf phage function as elements of bacterial pan-immune systems....46
4.1. **Introduction**....46
4.1.1. Filamentous Inoviruses influence *P. aeruginosa* pathogenesis....46
4.1.2. Filamentous Inoviruses and bacterial phage defense....47
4.1.3. Pf phages as elements of a *P. aeruginosa* pan-immune system....47
4.2. **Preliminary Results**....48
4.2.1. Identification of Pf Prophages in *P. aeruginosa* Clinical Isolate Genomes....48
4.2.1.1. Trimming Identified Pf Sequences....48
4.2.2. Characterization of Pf Accessory Genes....49
4.2.3. Pan-immune Trials....49
4.2.3.1. Trial v01....49
4.2.3.2. Trial v02....52
4.2.3.3. Suggested Methodology for Trial v03....56
4.3. **Discussion**....57
4.4. **Future Directions**....57
4.5. **Materials and Methods**....58
4.5.1. Strains, plasmids, and growth conditions....58
4.5.2. Construction of PAO1$^{\Delta Pf4/Pf6}$::pUC18-miniTn7-*gfp*....64
4.5.3. Construction of a pan-immune population....64
4.5.3.1. Trial v01....64
4.5.3.2. Trial v02....64
4.5.3.3. Suggested approach for Trial v03....65
4.5.4. Assembly of Clinical Isolate PacBio Whole-Genome sequencing....65
4.5.5. Identification of Pf genomes and prophage trimming....65
4.5.6. Genomic DNA Extraction and Quantification....66
4.5.7. DNA Library Preparation and Long Read Whole-Genome Sequencing....67
4.5.8. Pan-immune Whole-Genome Sequencing Quality Control and Analyses....67
4.5.9. Statistical Analyses and Graphing....67
CHAPTER FIVE Conclusions....68
SUPPLEMENTARY MATERIAL....70
REFRENCES....77

LIST OF TABLES

Table 2-1. Bacterial strains, phage, and plasmids used in this study.....25
Table 2-2. Primers used in this study.....26
Table 3-1. *P. aeruginosa* isolates and Pf prophage characteristics.....32
Table 3-2. Strains and plasmids used in this study.....41
Table 3-3. Primers used in this study.....41
Table 4-1. Strains, bacteriophage, and plasmids used in this study.....58
Table 4-2. Clinical Isolate Prophage Donor Strains, used in Trial v01.....58
Table 4-3. Clinical Isolate Prophage Donor Strains, used in Trial v02.....59
Table 4-4. Clinical metadata and prophage traits associated with strains used in Trial v01 and Trial v02.....59
Table 4-5. Clinical metadata and prophage traits associated with strains used in Trial v02.....61

LIST OF FIGURES

CHAPTER ONE

Figure 1- 1. Filamentous Inovirus virion structure....1
Figure 1- 2. Filamentous Inovirus adsorption....2
Figure 1- 3. Filamentous Inovirus egress....3
Figure 1- 4. Pf phage genomic organization....4
Figure 1- 5. Integration of Pf into the bacterial chromosome....5
Figure 1- 6. Excision and replication of Pf....6
Figure 1- 7. Model of tripartite PfsE interactions....7

CHAPTER TWO

Figure 2- 1. Pf4 superinfection transiently suppresses twitching motility and promotes resistance to Pf4-induced plaquing....13
Figure 2- 2. PfsE suppresses twitching motility and protects *P. aeruginosa* from Pf4 superinfection....14
Figure 2- 3. Type IV pili are not apparent on cells expressing PfsE....15
Figure 2- 4. Pf4 superinfection and expression of PfsE promotes resistance to type IV pili (T4P)-dependent bacteriophages....16
Figure 2- 5. Pf4 virions not encoding pfsE are more virulent against *P. aeruginosa*....17
Figure 2- 6. Conserved aromatic residues in PfsE are essential for the inhibition of type IV pili and resistance against Pf4 superinfection....18
Figure 2- 7. Divergent PfsE sequences inhibit twitching motility in various *P. aeruginosa* strains....20

CHAPTER THREE

Figure 3- 1. Graphical Abstract.... 28
Figure 3- 2. The Pf4 phage gene *PA0718* (*pflM*) maintains lysogeny....30
Figure 3- 3. Targeted deletion of *pflM*, or its Arc/mnt domain-containing isoform, cure diverse *P. aeruginosa* isolates of their Pf prophage infections....33
Figure 3- 4. Sequence and structural analysis of PflM....34
Figure 3- 5. Pf phage differentially modulates *P. aeruginosa* quorum sensing....35

Figure 3- 6. Pf prophage deletion has significant but variable effects on *P. aeruginosa* biofilm formation.....36
Figure 3- 7. Pyocyanin production is enhanced in Pf prophage deletion strains.....37
Figure 3- 8. *C. elegans* actively avoids *P. aeruginosa* Pf lysogens.....38

CHAPTER FOUR

Figure 4- 1. Depiction of the bacterial pan-immune system whereby genetic flux of mobile elements serve as a community resource.....47
Figure 4- 2. Pf phages in the clinical isolate population encode diverse defense systems.....49
Figure 4- 3. Experimental design employed to assess transmission of Pf phage from donor clinical isolates into a recipient population.....50
Figure 4- 4. Mitomycin C and exogenous polyamines increase phage mobilized from clinical isolates.....51
Figure 4- 5. Virulent phage predation reduces diversity of surviving recipient strains harboring prophages mobilized from clinical isolates.....52
Figure 4- 6. Generation of a pan-immune population allows for streamlined examination of selection outcomes.....53
Figure 4- 7. Trial v02 pan-immune population tolerant to ciprofloxacin, rifampin, and virulent phages DMS3*vir* and CMS1.....54
Figure 4- 8. Trial v02 sequencing reads mapped to pan-immune population backbone.....55
Figure 4- 9. Suggested approach to generate a pan-immune population for Trial v03.....56

SUPPLEMENTARY FIGURES

Figure S2- 1. Pf4 superinfection and expression of PfsE promotes resistance to type IV pili (T4P)-dependent lytic bacteriophages.....70
Figure S2- 2. PfsE expression does not affect swimming motility in *P. aeruginosa*.....70
Figure S2- 3. Wild-type PfsE protein is expressed in *E. coli*, but not the point mutants $PfsE^{Y16V}$ or $PfsE^{W20A}$.....71
Figure S3- 1. Prophage presence has variable impact on host growth.....71
Figure S3- 2. Pf4 modulates *P. aeruginosa* PAO1 quorum sensing.....72
Figure S3- 3. Pf6 modulates *P. aeruginosa* PAO1 quorum sensing.....72

Figure S3- 4. Pf4 and Pf6 modulate *P. aeruginosa* PAO1 quorum sensing.....73
Figure S3- 5. Pf phage modulate *P. aeruginosa* LESB58 quorum sensing.....73
Figure S3- 6. Pf phage modulate *P. aeruginosa* CPA0053 quorum sensing.....74
Figure S3- 7. Pf phage modulate *P. aeruginosa* CPA0087 quorum sensing.....74
Figure S3- 8. Pf phage modulate *P. aeruginosa* DDRC3 quorum sensing.....75
Figure S4- 1. Trial v02 pan-immune population tolerant to ciprofloxacin, rifampin, and virulent phages DMS3*vir* and CMS1.....76

CHAPTER ONE Introduction and Context

1.1. The Filamentous Bacteriophage

Bacteriophages, or 'phages', are viruses which infect bacteria, and are the most diverse and abundant biological entity on Earth. Filamentous phages, first identified in the early 1960's, are pervasive across earths biomes and infect archaeal and diverse bacterial hosts (18-21). This type of phage, which falls in the *Inoviridae* family, are characterized by a circular, positive-sense, single-stranded DNA (ssDNA) genomes encapsidated into long filament-like virions composed of several thousand major coat protein subunits and capped at either end by a few minor coat proteins (**Fig 1- 1**) (6, 21-24).

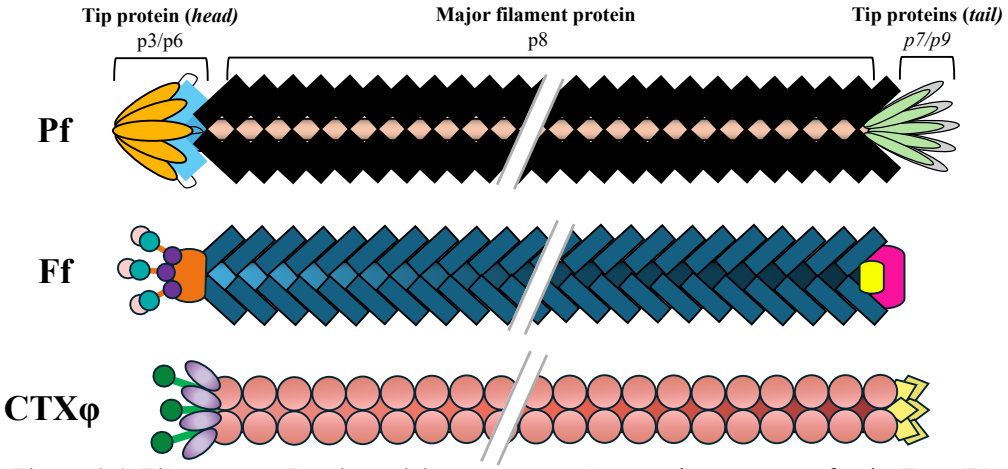

Figure 1-1. Filamentous Inovirus virion structure. Structural components for the Type IV Pili-dependent Pf phages of *Pseudomonas aeruginosa* (12), F-specific filamentous phages (Ff), which infect cells by binding to the F-pilus (synonymous with sex/conjugation pili) of *Escherichia coli* (6), and CTXφ which infects *Vibrio cholerae* through binding toxin-coregulated pili (TCP) via $p3^{CTX}$ (9, 10).

Typically, filamentous phage encode 7-15 proteins within a ~5-15kb genome (22). Their ssDNA genomes are packaged into filamentous virions between 60–70 Å in diameter but vary in length, between 800-2,000 nm, in a manner proportional to the size of the encapsidated genome (21-26). Despite the highly conserved genomic organization of filamentous phage, the genes, and proteins they encode have limited conservation in sequence (21, 23). For example, the major capsid proteins of *Escherichia* phage M13 and *Pseudomonas* phage Pf1 share a mere 17.0% identity, highlighting their functional diversity (27).

1.1.1. Infection

Infection of a susceptible bacterial host begins with adsorption to specific receptors on the bacterial cell surface, which are typically highly conserved. Filamentous phages within the *Inoviridae* family commonly rely on fimbriae[1] or pilus structures, such as Type IV Pili (T4P) and F-pili, as cell surface receptors (**Fig. 1- 2**) (6, 22, 28). Fimbriae are short hair-like appendages present on most Gram-negative and on some Gram-positive bacteria, facilitate adhesion to surfaces or other bacterial cells and resistance to flushing (29). Unlike other forms of pili,

[1] Fimbriae are referred to in some literature as pili or attachment pili.

fimbriae are numerous on the bacterial cell surface to the order of 1000 fimbriae appendages per cell (30). T4P, the receptor for *P. aeruginosa* Pf phage and CTXφ of *Vibrio cholerae*[2], undertake a broad range of functions, such as DNA uptake, electron transport, and twitch motility which enables adhesion to static surfaces (2, 9, 31-33). F-pili, also referred to as conjugation or sex pili, are responsible for cell-to-cell contact which mediates conjugation and DNA transfer and serve as the receptor for Ff phages of *E. coli* (6). Interactions with cognate cell surface receptors relies on phage coat proteins p3/p6 (**Fig. 1-1**) (27).

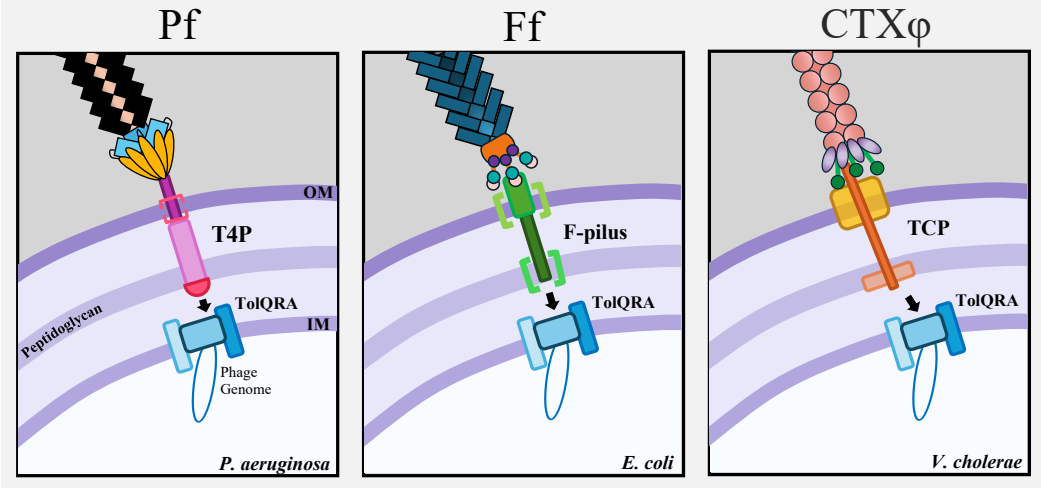

Figure 1- 2. Filamentous Inovirus adsorption. Filamentous Inoviruses adsorb to their bacterial hosts using conserved cell surface receptors such as Type IV Pili (Pf phages of *P. aeruginosa*), F-pili (Ff phages of *E. coli)* or the toxin-coregulated pilus (TCP) for *Vibrio cholerae* phage CTXφ (2). Following adsorption, virions move through the outer membrane (OM) as pili retract and enter the periplasm through the pilus pore (12). Translocation across the inner membrane (IM) is mediated by TolA through an unknown mechanism. As the major capsid proteins, pVIII for Ff and CoaB for Pf, are stripped off, they integrate into the cytoplasmic membrane unsheathing the circular-ssDNA phage genomes into the cytoplasm.

Although functionally distinct, these pili rely on retraction to achieve their respective functions. Adsorbed filamentous Inoviruses leverage this retraction to gain entrance to the periplasm, in a manner akin to reeling in a fish (**Fig 1- 2**) (12). Indeed, it has been spatially verified that the pore size formed by these receptors is large enough for entry of the phage into the periplasmic space (6, 22).

1.1.2. Replication

Once in the periplasm the minor coat-protein of filamentous Inoviruses, p3, interacts with the TolQRA as a secondary receptor (**Fig 1- 1**, **Fig 1- 2**) (6). The TolQRA complex spans the cytoplasmic membrane and is highly conserved within Gram-negative bacterial species. TolA serves as a crucial component of the Tol-Pal system which facilitates membrane invagination during cell division (22, 34, 35). The TolQRA complex anchors the virion in the inner membrane, unsheathing the circularized ssDNA phage genome into the cytoplasm (**Fig 1- 2**)(6, 22, 36, 37).

[2] The phage CTXφ, *Vibrio cholerae*, utilizes the toxin-coregulated pilus (TCP) for adsorption, which is classified as a type IVb pili (T4bP).

In the cytoplasm filamentous phages pirate replication machinery and nucleic/amino acids, imposing a significant metabolic burden on their bacterial hosts (27). To produce genomic copies or lysogenize, the circular ssDNA phage genome, referred to as infective form (IF) (22), must first become double-stranded DNA (dsDNA). To achieve this, filamentous phage rely on robust recruitment of RNA polymerase σ70 holoenzyme to mimicked bacterial -35 and -10 promoter sites, which it preferentially binds with increased affinity over a typical bacterial promotor (22, 38). Subsequent RNA polymerase-mediated synthesis of the + strand of the genome ends, creating a dsDNA primer (39). Host DNA polymerase recognizes and binds the dsDNA primer on IF completes synthesis of the + strand, forming circular dsDNA referred to as replicative form (RF) (40).

While the Ff phages of *E. coli* are generally episomal, the Pf phages of *P. aeruginosa* typically favor integration into the bacterial chromosome, termed lysogeny. When a filamentous phage such as Pf integrates, using either their own or a host-encoded integrase, the lysogen is stably maintained as a prophage and replicate passively with each bacterial cell division (21, 41). Certain environmental stimuli which result in activation of bacterial stress responses can prompt an abrupt exit from dormancy, and the prophage excises from the chromosome and circularizes into dsDNA RF. Multiple copies of a filamentous phage genome often exist simultaneously within a single bacterial cell, both episomally as RF, and in a dormant prophage state (21, 41). Although transcription can occur off RF or the prophage, is only off the RF that genomic replication through a rolling-circle mechanism occurs. However, some filamentous phage such as *Vibrio* phage CTXφ, utilize the chromosomally integrated prophage as a template for synthesis of viral ssDNA (42, 43). Regardless of mechanism, resulting transcripts are ultimately translated to form the structural components required virion assembly, while genomic ssDNA copies are packaged into filamentous virions.

1.1.3. Egress

A notable feature of filamentous phage is that they commonly shed virial particles continually without causing the death of their bacterial host (9, 44, 45). Egress begins with localization of major coat protein (p8) to the inner membrane, while IF DNA is

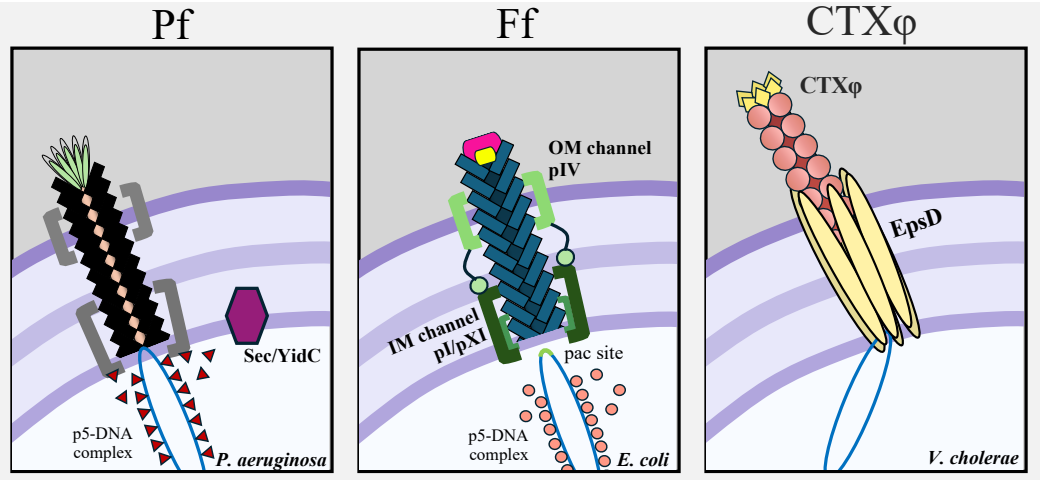

Figure 1- 3. Filamentous Inovirus egress. As Pf virions components are inserted into the inner-membrane assemble via host-encoded Sec/YidC machinery. ssDNA phage genomes, which are coated in a sheath of p5 (encoded by *PA0720* in Pf4) for transport, are assembled into virions as p5 is sloughed off and replaced by p8. Ff virions egress through phage-encoded cytoplasmic and outer membrane channels encoded by Ff genes pI/pXI and pIV, respectively (6). *Vibrio cholerae* phage CTXφ is relies on host-encoded secretin, EpsD, which is a native component of the type II secretion system responsible for extracellular protein secretion (Eps) (9, 10).

coated in p5 (encoded by *PA0720* in Pf4) for transport (**Fig. 1- 3**) (27). The virion is loaded with IF DNA and p5 is replaced with the major coat protein, p8, as the virion is assembled. Egress is facilitated by either host-encoded (as is the case with CTXφ and Pf) or phage encoded (Ff, among others) cytoplasmic and outer membrane channels (15, 46). Although filamentous Inoviruses do not directly lyse their bacterial hosts, localization of the major coat proteins to the inner membrane has been reported to cause significant bacterial membrane stress, ultimately leading to cell death (47-51). Thus, phage overproduction proves lethal to the bacterial host and must be tightly regulated (52).

It is well established that filamentous Inoviruses can increase bacterial virulence. CTXφ of *V. cholerae* is perhaps the clearest example of this, as the cholera-toxin, which causes the disease-state commonly known as cholera, is encoded by CTXφ (53). Ff phages of *E. coli*, are implicated in the dissemination of antibiotic resistance genes (16, 54). Furthermore, filamentous Inoviruses present in *Neisseria*, *Ralstonia*, and *Pseudomonas* phenotypically modulate their bacterial host, changing expression of virulence factors, bacterial motility, biofilm development and dispersal, and increase resistance to other phage, all of which serve to increase bacterial survival (17, 21, 22, 52, 55-63). Given the broad distribution of filamentous Inoviruses across domains of life, perhaps this unique co-dependency is not surprising. Nevertheless, the contribution of filamentous Inoviruses to bacterial virulence is of significant clinical concern, but also significant therapeutic potential.

1.2. Pf Phages

The filamentous Inoviruses which chronically infect 60-80% of *P. aeruginosa* clinical isolates, are called Pf phage (64). Pf phages typically have a genome ~12 kb in length, containing a 'core' genome spanning from the

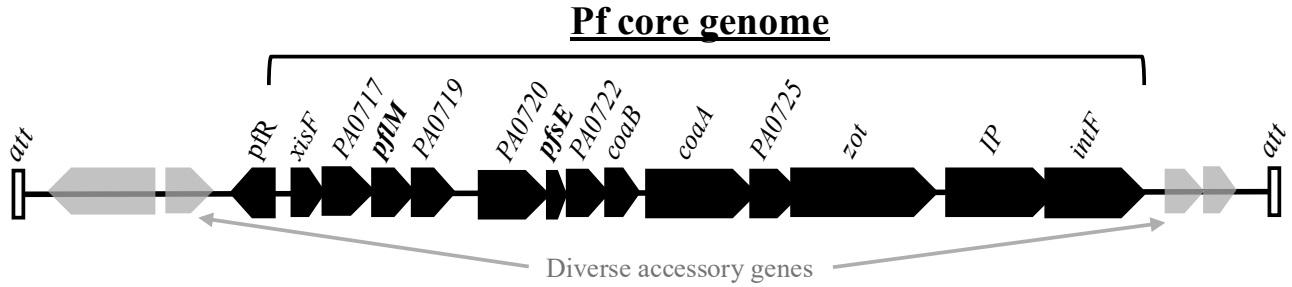

Figure 1- 4. Pf phage genomic organization. The core genome of Pf is often flanked by diverse accessory genes, and usually attachment (*att*) sites which bear homology to the region in the bacterial chromosome where the phage will integrate. The core genome of Pf phage begins with the repressor c gene, *pfR,* which is under the regulatory control of the OxyR transcriptional regulator (5). PfR suppresses excision through repression of the excisionase gene, *xisF*, and is inactivated through oxidation of the cysteine residues of OxyR which binds PfR to release the *xisF* promotor (3). XisF induces transcription of the operon encoding the integrase IntF and the initiator protein PA0727 which binds to the RF origin of replication, recruits the host enzymes DNA polymerase III, and the DNA repair helicase UvrD which commences rolling circle replication (15). The Pf lysogeny maintenance gene, *pflM*, suppresses excision of the prophage through a currently uncharacterized mechanism (16). The *PA0720* gene encodes the p5 protein, which coats IF ssDNA as it translocates into virions (17). The Pf superinfection exclusion gene, *pfsE*, binds the PilA which is the major subunit of T4P to prevent pilus extension and thus infection by other T4P-dependent phages (16). Virion structural subunits p3 and p8 are encoded by *coaA* and *coaB*, respectively.

repressor (Pfr) to the integrase (*intF*) (**Fig. 1-4**). Like other filamentous Inoviruses, they have a filamentous virion structure composed of repeating coat protein subunits which allow them to accommodate genomes of varying size (**Fig. 1-1**) (65). The flexible virion size allows Pf phages to accommodate diverse accessory genes, called morons because they add more-on, which flank the core genome (41).

1.2.1. The Pf lifecycle

As discussed above, Pf phages gain entry to their host via the T4P (22, 66). The minor coat protein, CoaA, binds T4P, adsorbing Pf to the cell. Following adsorption, the Pf phage genome, in its IF form, gains entry to the cell through the TolQRA complex as the major coat protein, CoaB, unsheaths and is stored in the inner membrane for reuse (22, 66). Like many filamentous Inoviruses, such as CTXφ, Pf phage undergo rolling circle replication (RCR) to reproduce (23). Some Pf phage, like Pf1, are incapable of lysogeny and remain in RF to replicate episomally (67). Pf that can integrate rely on a phage-encoded tyrosine recombinase, IntF, to catalyze lysogeny into a bacterial tRNA gene (**Fig. 1-5**). The integration site of the phage is dependent on what attachment (*att*) sites flank the phage genome; homology to the bacterial chromosome is required for integration (66). Chapter II of this work examines the model Pf phage, Pf4, which uses IntF4 to catalyze integration into the *P. aeruginosa* strain PAO1 in the tRNA-Gly gene *PA0729.1* (3, 66).

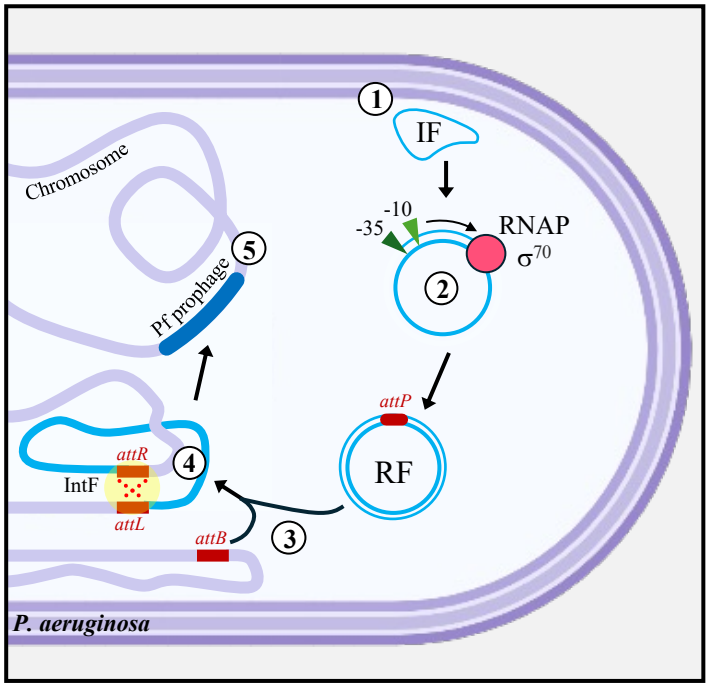

Figure 1- 5. Integration of Pf into the bacterial chromosome. **(1)** The circular-ssDNA infectious form (IF) phage genome enters the cytoplasm. **(2)** The -35 and -10 promoter elements encoded by the IF (*triangles*) are recognized by the RNA polymerase σ^{70} holoenzyme (*pink circle*) which synthesizes the complimentary strand to produce replicative form (RF) dsDNA (4) . **(3)** The freshly synthesized RF encodes an attachment (*att*) site (*attP*) homologous to a region within the bacterial chromosome (*attB*). **(4)** Recombination is facilitated by the tyrosine recombinase, IntF (*yellow circle*), resulting in **(5)** integration of the Pf genome, flanked by attachment Left (*attL*) and attachment Right (*attR*) sites into the bacterial chromosome (3).

Pf phage rely on extracellular factors such as nutrient limitation, bacterial population density, among other bacterial stresses, to determine whether to replicate or remain in a dormant prophage state (66, 68-71). Furthermore, in model strain PAO1 two H-NS family proteins, MvaT and MvaU, function to coordinately silence the expression of Pf phage (72, 73). MvaT and MvaU bind upstream of Pf structural genes, as well as to the *xisF* promotor site, preventing production of virion components and prophage excision, respectively (3, 12, 74-76). Pf phage are also under the control of transcriptional regulator OxyR (77). OxyR natively functions to regulate oxidative stress response and the presence of molecules such as hydrogen peroxide (H_2O_2) oxidizes OxyR

cystine residues and allows for binding of the Pf repressor c gene, *pfR* (5, 77). The repression PfR exerts is aimed at maintaining lysogeny through repression of the excisionase promoter (3). Thus, oxidation of OxyR lifts repression of the phage, allowing for production of XisF.

As repression of Pf is lifted, either by dephosphorylation of MvaU or oxidation of OxyR, replication kicks off with production of the excisionase. XisF catalyzes prophage excision into RF, and induces production of the IP, encoded by *PA0727*, as well as IntF (**Fig. 1- 6**) (3). The IP subsequently complexes with HU, a histone-like protein, which together bind the hairpin loop of the RF (+)*ori* and induce a single-stranded break (3). Next, host enzymes DNA polymerase III and UvrD are recruited to the RF, HU dissociates from IP, and the DNA Pol. III-IP-UvrD complex begin rolling circle replication (RCR) (78). UvrD, a host-encoded helicase, has been demonstrated to be vital for Pf replication, as it promotes replisome movement and participates in the restart of replication forks (15). Through RCR IF ssDNA and more copies of RF are synthesized. Off the RF, the ssDNA binding protein encoded by *PA0720* is produced and quickly coats the IF (66). Virion structural components, such as CoaA and CoaB, are also transcribed off the RF. CoaB's hydrophobic leader prompts localization to the inner membrane, where it is cleaved by Sec/YidC enzymes producing the mature CoaB peptide (66, 79). As CoaB subunits unite and extrude from the cell, the IF ssDNA is encapsidated via interaction with the C-terminus of CoaB which removes PA0720 as loading progresses (66, 80). As a result, the mature virion egresses from the bacterial cell.

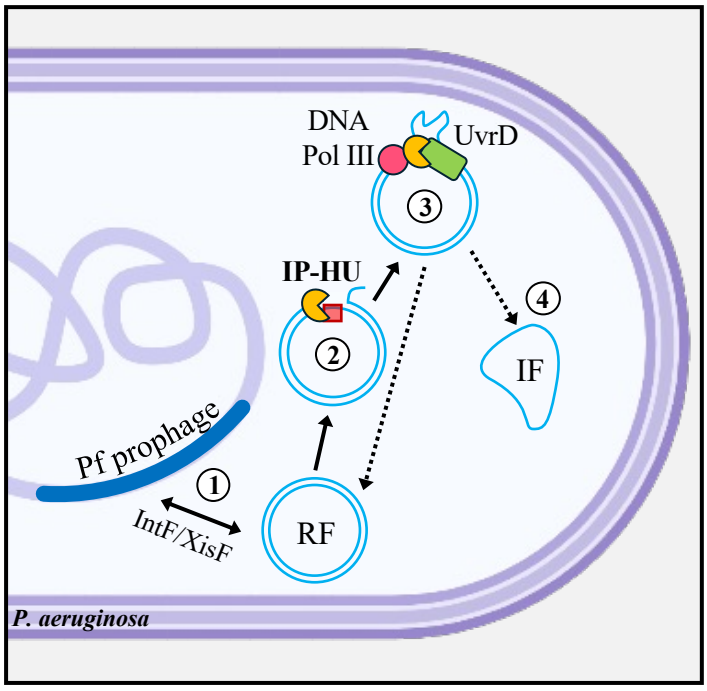

Figure 1- 6. Excision and replication of Pf. The circular-ssDNA infectious form (IF) phage genome enters the cytoplasm and is converted to dsDNA, known as the replicative form (RF). **(1)** If the phage genome is integrated in the bacterial chromosome as a prophage, it must first excise as outlined in Fig. 1- 5. **(2)** The IP (*PA0727*) (*orange semicircle*) and the histone-like protein HU (*red square*) complex and introduce a single-stranded break at the origin of replication, *ori*(+) of RF. **(3)** The IP-HU complex recruits host proteins DNA polymerase III and UvrD which together produce additional RF copies and IF through rolling-circle replication (RCR). **(4)** IF copies are coated with p5 (encoded by *PA0720*) to prevent degradation while transported to the inner membrane. Virion structural components produced off of RF are inserted into the inner membrane by the Sec/YidC machinery (3).

1.2.2. Superinfection

As a consequence of not lysing their bacterial host at the conclusion of their lifecycle, Pf virions accumulate outside of the cell during active replication. As extracellular virions accumulate, the odds of reinfecting a host increase. To mitigate reinfection, termed superinfection, many phages employ superinfection

exclusion mechanisms which typically target phage receptors (52, 81). There is ample evidence for superinfection exclusion via interreference with common cell-surface receptors such as T4P and the O-antigen of lipopolysaccharide (LPS) (52, 82, 83).

Superinfection, and the corollary superinfection exclusion, influence biofilm maturation and formation of phage resistant small colony variants (SCVs) (5, 57, 66, 84-87). Extracellular DNA resulting from superinfection-mediated lysis provides structural integrity to biofilms, while providing a framework on which electrons can be shuttled from the microaerophilic biofilm core to the aerobic periphery (85, 88-90). Furthermore, phage resistant SCVs which emerge from biofilms typically contain mutations in the repressor *c* gene, *pfR,* resulting in PfR which is unable to form a dimer and bind the *xisF* promoter to exert repression (5). Naturally, these mutations lead to overproduction of Pf in biofilms, and a heightened need to prevent superinfection (3, 5, 91). SCVs typically lack functional T4P as a means of superinfection exclusion (92-94). Interestingly, loss of T4P does not limit SCVs ability to attach or adhere but rather offers the significant advantage of increasing bacterial dispersion and proliferation (86).

The phage Pf4, of *P. aeruginosa* stain PAO1, limits superinfection through expression of the smallest protein it encodes, PfsE (**Fig. 1- 7**). PfsE interacts with the primary structural subunit of T4P, PilC, preventing pilus extension and abrogating twitch motility (**Fig. 1- 7**) (16). Work elaborating on this finding uncovered a fascinating tripartite interaction whereby PfsE also interacts with quorum sensing (QS) master regulator, PqsA (11).

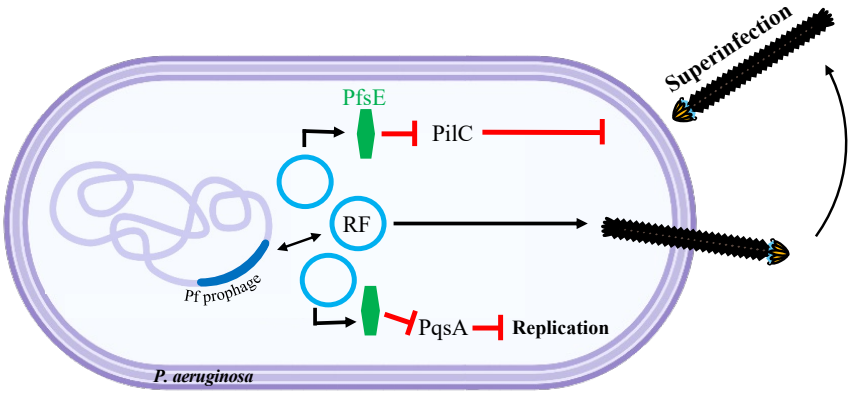

Figure 1- 7. Model of tripartite PfsE interactions. In *Pseudomonas aeruginosa*, Pf phage protein PfsE inhibits type IV pili by binding to PilC to protect its host from superinfection by other type IV pilus-dependent phages. Deleting the Pf4 prophage from *P. aeruginosa* has been demonstrated to upregulate PQS signaling, enhancing the production of the phenazine pigment pyocyanin. *P. aeruginosa* PQS signaling is involved in defending against phage infection as well as regulating production of redox-active pigments. Recently, it was demonstrated that PfsE also functions as an inhibitor of PQS signaling through binding to PqsA (11). Furthermore, it was shown that PfsE adopts a kinked conformation that orients conserved aromatic residues on PfsE into the hydrophobic catalytic pocket of PqsA. Inhibition of PqsA by PfsE results in more efficient Pf4 replication, suggesting that PQS signaling controls bacterial behaviors that defend against phage infection. Thus, the simultaneous inhibition of type IV pili and PQS signaling by PfsE may be a strategy to increase the susceptibility of the host while at the same time protecting it from competing phages.

1.3. The bacterial pathogen *Pseudomonas aeruginosa*

The γ-proteobacteria *Pseudomonas aeruginosa* is a gram-negative opportunistic bacterial pathogen that commonly infects medical hardware, diabetic ulcers, burn wounds and the lungs of cystic fibrosis patients (95). In comparison to other free-living bacteria, such as *Staphylococcus aureus* (2.8 Mbp) and *Escherichia coli* (4.6-5.5 Mbp), *P. aeruginosa* has a relatively large genome (5.5-7 Mbp) (96). As a result, *P. aeruginosa* displays a high degree of genomic plasticity which allows for the acquisition of new genes and the differential expression of existing ones with one of the many regulatory enzymes it encodes.

P. aeruginosa is implicated in 10-20% of nosocomial, hospital acquired, infections worldwide (97). Of increasing concern is the risk acquiring *P. aeruginosa* poses to patients with cystic fibrosis (CF). CF is a genetic condition caused by mutations in the cystic fibrosis transmembrane conductance regulator (CFTR) gene (98). These mutations result in the production of a misfolded protein which thickens mucus, reducing a patients sputum secretion. Patients with CF have immense difficulty irradicating bacterial pneumonias, requiring frequent treatment with antibiotics which give rise to microbial resistance. Compounding this issue, immunocompromised individuals, such as those with CF, frequent clinical settings where *P. aeruginosa* can be readily acquired. Indeed, patient-to-patient transmission of *P. aeruginosa* is common between individuals with CF in a hospital setting (99). Acquisition of *P. aeruginosa* often leads to chronic infection in individuals with CF, and significantly reduces patient lifespan (100).

Ultimately, the capacity of *P. aeruginosa* to form chronic infections, its prevalence as a nosocomial pathogen, and its increasing resistance to antibiotics pose a significant threat to human health, particularly those who are immunocompromised. The significance of this threat has been ratified by the World Health Organization, who designated *P. aeruginosa* as a ‘global priority pathogen’ in 2017, and it remains one as of late 2024 (101).

1.4. Pf Phages and *Pseudomonas aeruginosa*

Pf phages are central to the arsenal *P. aeruginosa* leverages to establish infection and evade immune detection (27). Pf phages are known to enhance *P. aeruginosa* infection pathogenesis by fortifying biofilm matrices, misdirecting mammalian innate immune cells, and preventing the phagocytosis and eradication of bacterial cells (102, 103). At sites of *P. aeruginosa* infection Pf virions are frequently present (57, 99). Pf phages are associated with increased chronicity of *P. aeruginosa* infections, increased bacterial tolerance of antibiotics, and ultimately worse disease outcomes for individuals with CF (66, 104).

1.4.1. Modulation of Mammalian Immunity

Pf is implicated in subversion of the eukaryotic immune system. Researchers demonstrated that Pf inhibit bacterial phagocytosis human and murine-derived dendritic cells and macrophages. In this model, Pf phages reduced TNF and cytokine production by host cells, which is understood to stimulate phagocytosis, while they increased type-I interferon and IL-12 secretion which prompt an antiviral immune response (66, 105). Thus, the presence of extracellular Pf virions prevents clearance of *P. aeruginosa* by prompting an antiviral, rather than an appropriate antibacterial, immune response.

1.4.2. Biofilm formation

A critical aspect of *P. aeruginosa* virulence is its ability to form biofilms, protective extracellular matrices, at sites of infection. Biofilms are composed of extracellular DNA (eDNA), and polymers such as the exopolysaccharides Pel, Psl, and alginate. Pf phage is well established as crucial components of the biofilm matrices. Pf has been demonstrated to switch from dormancy to active replication while biofilms form (106). Active replication results in a 100-fold increase in Pf titer; up to 10^{10} phage particles per mL (99, 106)! The resulting virions spontaneously assemble within the biofilm to form a viscous-liquid-crystal-like structure which provides structural integrity, increases resistance to desiccation and antibiotics, and increases adhesion (57, 86). The significance of Pf phage for biofilm maturation has been validated in a murine pneumonia model whereby Pf-null *P. aeruginosa* is efficiently cleared while Pf-positive progresses to chronic infection (84, 87, 105).

1.4.3. Quorum sensing

Broadly, quorum sensing (QS) is how bacterial cells speak to one another using small molecular messengers. QS allows kin-cells to collectively regulate behaviors and coordinately respond to their extracellular environment (107). The QS systems of *P. aeruginosa*, of which there are four major arms, all utilize autoinducers (AIs). AIs are secretory molecules that diffuse freely through the cellular membrane to interact with cognate receptors in the cytoplasm. QS is typically concentration dependent, the presence of more AIs results in a more robust phenotypic response. To limit sensing of their own secreted AIs, *P. aeruginosa* relies on antiactivators (108).

The *las* and *rhl* QS systems of *P. aeruginosa* together regulate nearly 10% of the *Pa* genome (109, 110). Both of these systems use synthesis of acyl-homoserine lactone (AHL) as AIs. AHLs are produced through autoinducer synthases, LasI and RhlI, respectively (111, 112). Each of these AIs interact with their receptors, LasR and RhlR, respectively. Transcriptional activity of the autoinducer synthases creates a positive feedback loop, more AI-receptor pairs increase transcription of AIs and their cognate receptors. LasR is known to influence transcription of the other QS circuits serving as the QS ‘master regulator’.

P. aeruginosa encodes two additional QS systems, which do not rely on AHL as an AI. The *Pseudomonas* quinolone signal (*pqs*) system relies on two molecules as AIs; PQS (2-heptyl-3-hydroxy-4-quinolone), and the precursor HHQ (4-hydroxy-2-heptylquinoline) (113, 114). PQS and HHQ interact with the receptor PqsR[3] to regulate genes involved in production of rhamnolipids, elastase, LecA, pyocyanin, and biofilm development (113). The regulatory region under *pqs* control overlaps with the *rhl* QS circuit (115-117).

The *iqs* (integrated quorum sensing signal) system is presently not well characterized. This system has an unidentified receptor which has been suggested to be involved in compensating for a loss of *las* function in low-phosphate conditions (110, 118, 119). Far too many genes fall under QS regulatory control to list them all here, however, important genes within the scope of this work include those involved in motility, biofilm formation, immune evasion, pigment production, and cytotoxicity (84, 109, 110, 120, 121). Some genes are regulated by more than one arm of *P. aeruginosa* QS, as is the case with production of potent redox-active virulence factors, called phenazines, which are regulated by both *rhl* and *pqs* (122). Among these aromatic molecules is pyocyanin which is responsible for the viridian color typical of *P. aeruginosa* (123). Pyocyanin functions as a terminal electron acceptor which allows for respiration in microaerophilic environments such as the biofilm core (89, 124). Because of its redox-active nature pyocyanin causes tissue damage and is often abundant in CF sputum (125, 126).

The complexity of QS mirrors the intricacy, and frustration, of learning a new language—as it is one. QS enables a sort of bacterial democracy, which allows concurrent phenotypic adaptation.

1.5. Thesis Aims

I undertook this research with the aim of elucidating the fundamental molecular biology which underpins the near ubiquity of Pf phage. This body of work; (1) uncovers a novel superinfection exclusion mechanism which interferes with function of the classical bacterial virulence factor Type IV Pili, (2) elucidates a conserved mechanism by which Pf phages maintain lysogeny and (3) present preliminary data supporting the role of Pf phages as fundamental elements of bacterial pan-immune systems. I undertook this work with the aim of elucidating the fundamental molecular biology which underpins the near ubiquity of Pf phage. Enjoy!

[3] PqsR is sometimes referred to as MfvR.

CHAPTER TWO A Filamentous Bacteriophage Protein Inhibits Type IV pili to prevent superinfection of *Pseudomonas aeruginosa*

Published January 18th, 2022, in mBio. DOI: 10.1128/mbio.02441-21.

Amelia K. Schmidt[1], Alexa D. Fitzpatrick[4], Caleb M. Schwartzkopf[1], Dominick R. Faith[1], Laura K. Jennings[1], Alison Coluccio[1], Devin J. Hunt[1], Lia A. Michaels[1], Dave W. Dorward[2], Jenny Wachter[3], Patricia A. Rosa[3], Karen L. Maxwell[4], and Patrick R. Secor[1#]

[1] Division of Biological Sciences, University of Montana
[2] Research Technologies Branch, & [3] Laboratory of Bacteriology, Rocky Mountain Laboratories, National Institute of Allergy and Infectious Diseases, National Institutes of Health
[4] Department of Biochemistry, University of Toronto
[#] Corresponding author: patrick.secor@mso.umt.edu

***Note**: My contribution to this work consisted of preforming twitch assays and plaque assays in Fig. 2- 1, Fig. 2- 2B/C and Fig. 2- 4 as well as construction of many Pf4 single-gene mutants (Fig. 2- 2), determining the impact of PfsE deletion on viral replication (Fig. 2-5), bioinformatic analyses of PfsE (Fig. 2- 6A/B) and construction and expression of aromatic residue point-mutants (Fig. 2- 6C/D). I was responsible for cloning and expression of bacterial adenylate cyclase two-hybrid (BACTH) system (Fig. 2- 6F) and cloning, expression, and twitch assays of PfsE variants from clinical isolates (Fig. 2- 7). Lastly, I wrote the manuscript and responded to reviewer comments.*

2.1. Abstract

Pseudomonas aeruginosa is an opportunistic pathogen that causes infections in a variety of settings. Many *P. aeruginosa* isolates are infected by filamentous Pf bacteriophage integrated into the bacterial chromosome as a prophage. Pf virions can be produced without lysing *P. aeruginosa*. However, cell lysis can occur during superinfection, which occurs when Pf virions successfully infect a host lysogenized by a Pf prophage. Temperate phages typically encode superinfection exclusion mechanisms to prevent host lysis by virions of the same or similar species. In this study, we sought to elucidate the superinfection exclusion mechanism of Pf phage. Initially, we observed that *P. aeruginosa* that survive Pf superinfection are transiently resistant to Pf-induced plaquing and are deficient in twitching motility, which is mediated by type IV pili (T4P). Pf utilize T4P as a cell surface receptor, suggesting that T4P are suppressed in bacteria that survive superinfection. We tested the hypothesis that a Pf-encoded protein suppress T4P to mediated superinfection exclusion, by expressing Pf proteins in *P. aeruginosa* and measuring plaquing and twitching motility. We found that the Pf protein PA0721, which we termed Pf superinfection exclusion (PfsE), promoted resistance to Pf infection and suppressed twitching motility by binding the T4P protein PilC. Because T4P play key roles in biofilm formation and virulence, the ability of Pf phage to modulate T4P via PfsE has implications in the ability of *P. aeruginosa* to persist at sites of infection.

2.1.1 Importance

Pf bacteriophage (phage) are filamentous viruses that infect *Pseudomonas aeruginosa* and enhance its virulence potential. Pf virions can lyse and kill P. aeruginosa through superinfection, which occurs when an already infected cell is infected by the same or similar phage. Here, we show that a small, highly conserved Pf phage protein (PA0721, PfsE) provides resistance to superinfection by phages that use the type IV pilus as a cell surface receptor. PfsE does this by inhibiting assembly of the type IV pilus via an interaction with PilC. As the type IV pilus plays important roles in virulence, the ability of Pf phage to modulate its assembly has implications for *P. aeruginosa* pathogenesis.

2.2. Introduction

Pseudomonas aeruginosa is an opportunistic pathogen that causes infection in wounds, on medical hardware, and in the airways of people with cystic fibrosis. *P. aeruginosa* itself can be infected by a variety of bacteriophages (phages). For example, many *P. aeruginosa* isolates are infected by temperate filamentous Pf phage, which can integrate into the bacterial chromosome as a prophage (17, 64). During *P. aeruginosa* growth as a biofilm or at sites of infection, the Pf prophage is induced, and filamentous virions are produced (99, 105, 106, 127). Like other filamentous phages, Pf can be extruded from the host cell without killing the host, allowing Pf virions to accumulate to high titers in biofilms (10^{11}/mL) (128) and infected tissues (10^{7}/gram) (57). However, cell lysis can occur when Pf superinfects *P. aeruginosa*, which occurs when multiple virions infect the same cell or when superinfective Pf variants emerge that contain mutations in the phage *c* repressor gene *Pf4r* (3, 128). Pf4-mediated cell lysis contributes to the maturation and dispersal stages of the *P. aeruginosa* biofilm lifecycle (102, 129-131).

Temperate phages typically encode superinfection exclusion mechanisms to stave off infection by competing phages in the environment. A common theme amongst superinfection exclusion mechanisms are proteins that inhibit or modify phage cell surface receptors such as type IV pili (T4P) (28), a common cell surface receptor for phages, including Pf4 (12). Many *P. aeruginosa* phages encode proteins that inhibit T4P to prevent superinfection (132). Specific examples include the Aqs1 protein encoded by phage DMS3 and the Tip protein encoded by phage D3112, which both inhibit T4P by binding to the T4P ATPase PilB (82, 83). Pf4 use T4P as a cell surface receptor (12); however, a superinfection exclusion mechanism has not been characterized for the Pf phages that reside in *P. aeruginosa* genomes.

In this study, we show that the smallest protein encoded by Pf4, which we call PfsE (Pf superinfection exclusion), transiently inhibits T4P assembly through an interaction with the T4P platform protein PilC, providing resistance to further infection by T4P-dependent phages. By introducing point mutations to PfsE, we identified

two aromatic residues (Y16 and W20) that may be required for PilC binding, T4P inhibition, and resistance to T4P-dependent phages. Furthermore, phage Pf4 engineered to lack the *pfsE* gene is able to kill *P. aeruginosa* more efficiently than the wild-type phage, demonstrating that this mechanism of superinfection reduces *P. aeruginosa* cell lysis. Filamentous Inoviruses such as Pf are widespread amongst Bacterial genomes with even a few examples infecting Archaea (133). Thus, the superinfection exclusion mechanism described here may be relevant to many species of filamentous phage that infect diverse bacterial hosts.

2.3. Results

2.3.1. Type IV pili are transiently suppressed in response to Pf4 superinfection

While working with phage Pf4 we noticed an interesting phenomenon where the surviving cells in a culture of PAO1 superinfected with Pf4 showed a decrease in twitching motility (**Fig 2-1A**). As Pf4 uses T4P as a cell surface receptor (12), we tested the ability of these non-twitching cells to mediate resistance to Pf4-induced plaquing. We found that these cells were highly resistant to lysis by Pf4 virions (**Fig 2-1B**) as compared to uninfected PAO1, which retain the ability to twitch (**Fig 2-1C**) and are sensitive to Pf4 superinfection (**Fig 2-1D**).

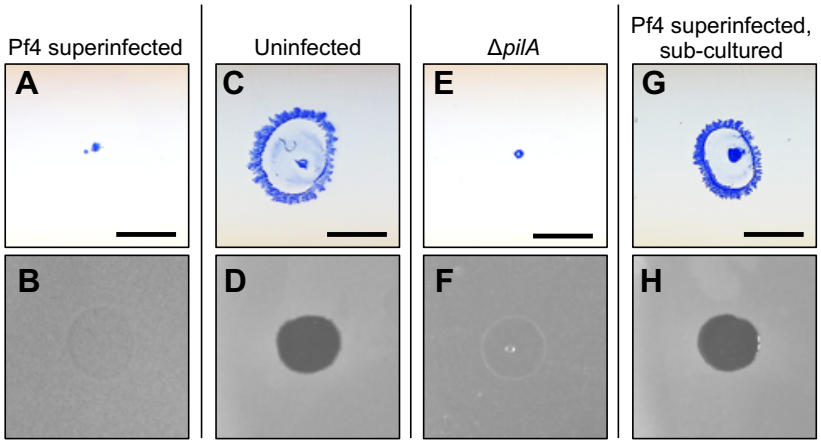

Figure 2- 1. Pf4 superinfection transiently suppresses twitching motility and promotes resistance to Pf4-induced plaquing. Twitch assays were performed by stabbing the indicated strain through the agar on a Petri dish to the plastic surface below. After 24h, the agar was removed and bacteria on the plastic dish were stained with Coomassie (upper panels **A, C, E & G**). To measure sensitivity of *P. aeruginosa* to Pf4 superinfection, lawns of the indicated strains were spotted with 10^6 PFUs of Pf4 in 3 µL (lower panels **B, D, F & H**). Strains tested include (**A and B**) PAO1 superinfected with Pf4, (**C and D**) uninfected PAO1, (**E and F**) the twitch-deficient type IV pili mutant Δ*pilA*, and (**G and H**) Pf4 superinfected PAO1 that was sub-cultured in phage-free broth and re-plated. Scale bar 5 mm.

The resistance observed was similar to that seen for a PAO1 Δ*pilA* mutant, which completely lacks pilus on the cell surface (**Fig 2-1E and F**). To determine if Pf4 superinfection selected for T4P-null mutants or transiently suppressed T4P expression, bacteria collected from Pf4-resistant lawns were sub-cultured in phage-free growth medium for 18 hours and then their ability to twitch and sensitivity to Pf4-induced plaquing was tested. Twitching motility and sensitivity to Pf4 superinfection was restored in sub-cultured bacteria (**Fig 2-1G and H**), indicating that heritable mutations in T4P genes were not responsible for the twitch-deficient and Pf4-resistance phenotypes.

2.3.2. PfsE suppresses twitching motility and protects *P. aeruginosa* from superinfection

Many temperate phages possess superinfection exclusion mechanisms that prevent re-infection of an already infected cell (134). We hypothesized that a Pf4-encoded protein would suppress T4P as a mechanism to prevent Pf4 superinfection and lysis of the host cell. To test this hypothesis, we first deleted the Pf4 prophage from our in-house PAO1 strain (PAO1$^{\Delta Pf4}$). Pf4 proteins encoded by *PA0717-PA0728* in the core Pf4 genome (**Fig 2-2A**) were then expressed individually from a plasmid in PAO1$^{\Delta Pf4}$ and twitching motility and sensitivity to Pf4-mediated lysis were then assessed. We identified two proteins, PA0721 and PA0724, that suppressed twitching motility when overexpressed (**Fig 2-2B**) and promoted resistance to Pf4 plaquing (**Fig 2-2C**). PA0721 is a small 30 residue uncharacterized protein and PA0724 is the Pf4 minor coat protein CoaA, which is involved in receptor binding during the initial steps of infection (17). These results were consistent with a previous study that found these proteins promote resistance to T4P-dependent long-tailed dsDNA phages DMS3m and JBD30 (133).

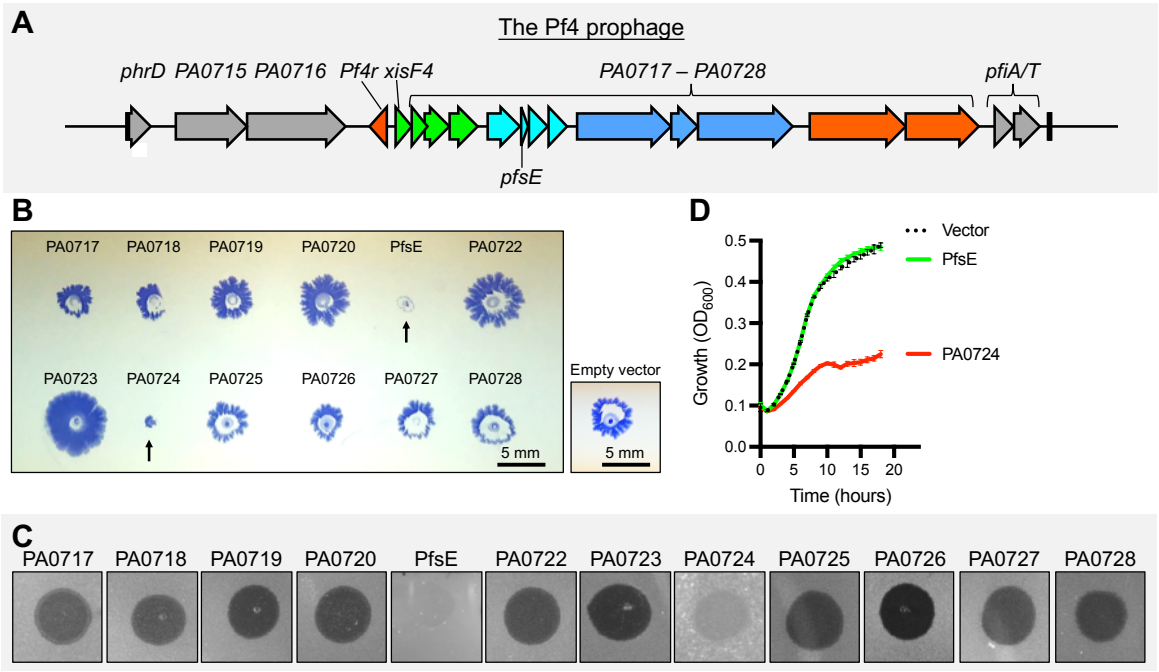

Figure 2- 2. PfsE suppresses twitching motility and protects *P. aeruginosa* from Pf4 superinfection. (**A**) The Pf4 prophage is composed of core genes that are essential for the phage to complete its lifecycle (*Pf4r* to *PA0728*) and flanking moron regions (gray) that add "more on" to the core genome (1). (**B**) Genes *PA0717–PA0728* in the core Pf4 genome were placed under the control of an arabinose-inducible promoter and expressed individually in *P. aeruginosa* PAO1$^{\Delta Pf4}$. Twitching was measured in the indicated strains after 24 hours; arrows indicate strains with reduced twitching motility. Bar 5 mm. (**C**) 10^6 PFUs of Pf4 were spotted onto lawns of PAO1$^{\Delta Pf4}$ expressing the indicated phage protein. (**D**) Growth curves in liquid culture for PAO1$^{\Delta Pf4}$ bacteria carrying the indicated expression vector. Cultures were grown in LB supplemented with 0.1% arabinose. Results are the mean ±SEM of three experiments.

To determine if the observed twitching inhibition and phage resistance was a direct result of the biological function of these proteins or was due to toxicity of the overexpressed proteins, we examined the growth rates of cells expressing these proteins. We found that PAO1$^{\Delta Pf4}$ expressing PA0724 grew poorly compared to cells

expressing PA0721 or PAO1$^{\Delta Pf4}$ carrying an empty expression vector (**Fig 2-2D**). These observations suggest that PA0724 expression is toxic to *P. aeruginosa,* and it is possible that the twitch-deficient and phage resistance phenotypes associated with PA0724 expression are a result of this toxicity rather than a specific superinfection exclusion mechanism. Therefore, we turned our attention towards characterizing PA0721, which we refer to herein as PfsE (Pf superinfection exclusion).

2.3.3. T4P are not apparent on cells expressing PfsE

Twitching motility requires bacteria to extend their pili outwards from the cell surface and then retract them to move along solid surface. Thus, PfsE could inhibit twitching motility by either preventing pilus retraction or extension. If PfsE inhibits T4P retraction, cells are anticipated to have a piliated or hyperpiliated morphology. If PfsE inhibits T4P extension, then cells are expected to have few or no pili. To determine if PfsE interferes with extension or retraction we used transmission electron microscopy to look for the presence of pili on the cell surface. We found that cells expressing PfsE showed no visible pili on the surface (**Fig 2-3**) while wild-type PAO1 cells had structures consistent with T4P (**Fig 2-3**). The lack of pili observed on the cells expressing PsfE was similar to a PAO1 Δ*pilA* mutant (**Fig 2-3**), which is known to completely lack surface piliation (135). These data suggest that PfsE inhibits T4P extension rather than retraction.

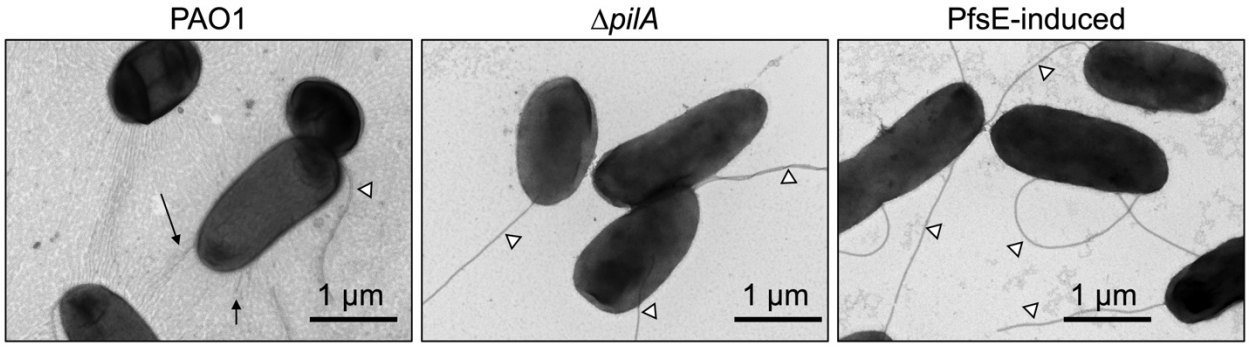

Figure 2- 3. Type IV pili are not apparent on cells expressing PfsE. Transmission electron microscopy of the indicated strains of *P. aeruginosa* was performed. Mid-logarithmic cells were washed, fixed, placed on a grid, and negatively stained with uranyl acetate. Arrows indicate potential pili on PAO1 cells. White triangles indicate flagella.

2.3.4. PfsE protects *P. aeruginosa* from other T4P-dependent phage species

Many phages use the T4P as a cell surface receptor to infect bacteria (28). We hypothesized that the transient T4P suppression by PfsE that protected against Pf4 superinfection would also protect *P. aeruginosa* from non-filamentous phages. To test this hypothesis, we examined the ability of phage JBD26, a temperate long-tailed dsDNA phage that uses the pilus as a cell surface receptor, to form plaques on lawns of PAO1, PAO1 Δ*pilA*, PAO1 superinfected with Pf4, PAO1 superinfected with Pf4 and then sub-cultured in phage-free media, or PAO1 expressing PfsE from a plasmid.

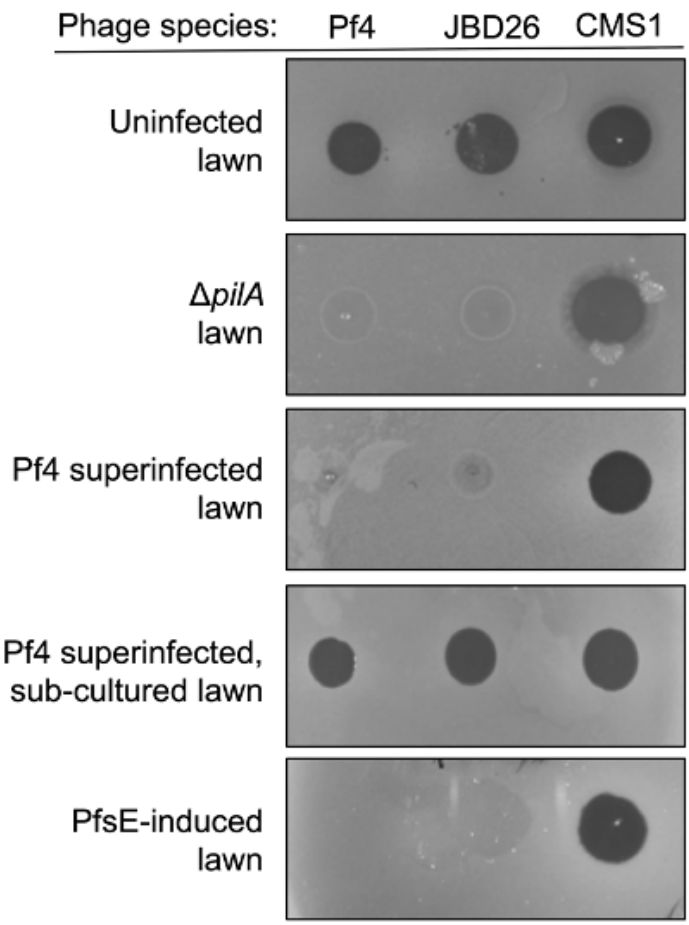

Figure 2- 4. Pf4 superinfection and expression of PfsE promotes resistance to type IV pili (T4P)-dependent bacteriophages. Representative images of *P. aeruginosa* PAO1 lawns spotted with 10^6 PFUs of Pf4, JBD26 (both T4P-dependent phages), or CMS1 (a T4P-independent phage). See also Figure S2-1.

Like Pf4, JBD26 was not able to infect cells that were superinfected by Pf4 or cells expressing PfsE (**Fig 2-4**). We also tested the ability of phage CMS1, which does not depend on the pilus for infection, to form plaques on these strains. As expected, the plaquing ability of these phages was not affected by the absence of T4P (Δ*pilA*), expression of PsfE, or superinfection by Pf4 (**Fig 2-4**).

Furthermore, Pf4 superinfection and expression of PfsE was able to prevent infection by phage OMKO, a lytic pili-dependent phage, but not LPS-5, another pili-independent phage species (**Fig S2-1**). These results demonstrate that PfsE protects *P. aeruginosa* from T4P-dependent phage species.

2.3.5. Deletion of *pfsE* increases Pf4 virulence against *P. aeruginosa*

To definitively show that PsfE expression from Pf phage provides resistance to superinfection, we attempted to delete the *pfsE* gene from Pf4. All attempts to delete *pfsE* from the Pf4 prophage integrated into the PAO1 chromosome failed. We hypothesized that inactivating *pfsE* resulted in unregulated replication of Pf4, killing *pfsE* mutants, similar to how Pf4 kills *P. aeruginosa* PAO1 when the global repressors *mvaT* and MvaU are both disabled (12). To test this hypothesis, we attempted to delete *pfsE* from the PAO1 Δ*intF4* background. IntF4 (PA0728) is a Pf4-encoded site-specific tyrosine recombinase that catalyzes Pf4 prophage integration and excision (3, 57). In Δ*intF4*, the Pf4 prophage is trapped in the chromosome, preventing infectious virions from being produced (12, 57). We were successful in deleting *pfsE* from Δ*intF4* creating the double mutant Δ*intF4/pfsE*, suggesting that when *pfsE* is inactivated, Pf4 replication kills *P. aeruginosa*.

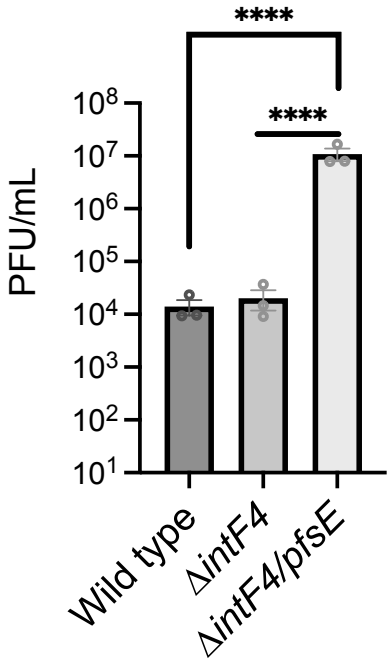

Figure 2- 5. Pf4 virions not encoding pfsE are more virulent against *P. aeruginosa*. Wild-type and mutant Pf4 virions were induced by expressing both the Pf4 excisionase (*xisF4*) and integrase (*intF4*) *in trans* in wild type, Δ*intF4*, or Δ*intF4/pfsE* backgrounds. Note that deletion of *pfsE* alone from the Pf4 prophage was not possible. Wild-type, Δ*intF4*, and Δ*intF4/pfsE* Pf4 virion titers were measured by qPCR and normalized to $6.95x10^7$ virions per mL. Virions were then spotted as a 10x dilution series on lawns of ΔPf4 to enumerate PFUs. Results are mean ± SEM of three experiments, unpaired Student's *t* test, ****P<0.0001.

We hypothesized that Δ*intF4/pfsE* Pf4 virions that lack the *pfsE* gene would not be able to regulate superinfection of the host bacterium, increasing host cell lysis. To test this, we induced and collected Pf4 virions from wild-type, Δ*intF4*, and Δ*intF4/pfsE P. aeruginosa*. To induce Pf4 virions from these strains, the Pf4 excisionase XisF4 was expressed *in trans* from a plasmid under the control of an arabinose-inducible promoter (3). To complement the Δ*intF4* mutation, IntF4 was also expressed from a plasmid in all strains tested. After overnight growth (18h) in LB supplemented with 0.1% arabinose, bacterial supernatants were filtered, DNase-treated, and Pf4 titers measured by qPCR, as previously described (136). Phage titers in each supernatant (wild-type, Δ*intF4*, and Δ*intF4/pfsE*) were normalized to $6.95x10^7$ virions per mL and were plated on a lawn of $PAO1^{\Delta Pf4}$ to determine how infective the mutant phages were. While the Δ*intF4* mutant phage titer was equal to wild-type Pf4, the Δ*intF4/pfsE* mutant phage was approximately 1,000-fold more infective (**Fig 2-5**), indicating that *pfsE* restricts Pf4 infection and thereby protects the bacterial host from lysis.

2.3.6. Aromatic residues in PfsE are required to inhibit twitching motility promote Pf4 resistance

PfsE contains a conserved cluster of aromatic residues, **YAWGW** (**Fig 2-6A and B**). Clusters of aromatic residues often facilitate protein-protein binding interactions (137, 138). Therefore, we hypothesized that the cluster of aromatic residues in PfsE is required for suppression of twitching motility and resistance to T4P-dependent phages. To test this hypothesis, we introduced into PfsE the following point mutations: PfsE^{Y16V}, PfsE^{W18A}, PfsE^{W20A}, and PfsE$^{Y16V/W18A/W20A}$. The mutant proteins were then expressed in PAO1$^{\Delta Pf4}$ and twitching motility and phage resistance were measured. PfsE^{Y16V}, PfsE^{W20A}, and PfsE$^{Y16V/W18A/W20A}$ all lost the ability to suppress twitching motility (**Fig 2-6C**) and did not promote resistance to the T4P-dependent phages Pf4 or JBD26 (**Fig 2-6D**). PfsE^{W18A}, however, only partially suppressed both twitch motility and infection by T4P-dependent phages, indicating residue W18 is not critical for PfsE to inhibit T4P. The difference in phenotypes between the point mutants may be related to the location of the aromatic residues on the PfsE α-helix; Y16 and W20 are located on the same side of the PfsE α-helix while W18 is oriented in the opposite direction (**Fig 2-6E**). We also tested the ability of PfsE to inhibit flagellum-dependent swimming motility. PAO1$^{\Delta Pf4}$ expressing wild-type PfsE

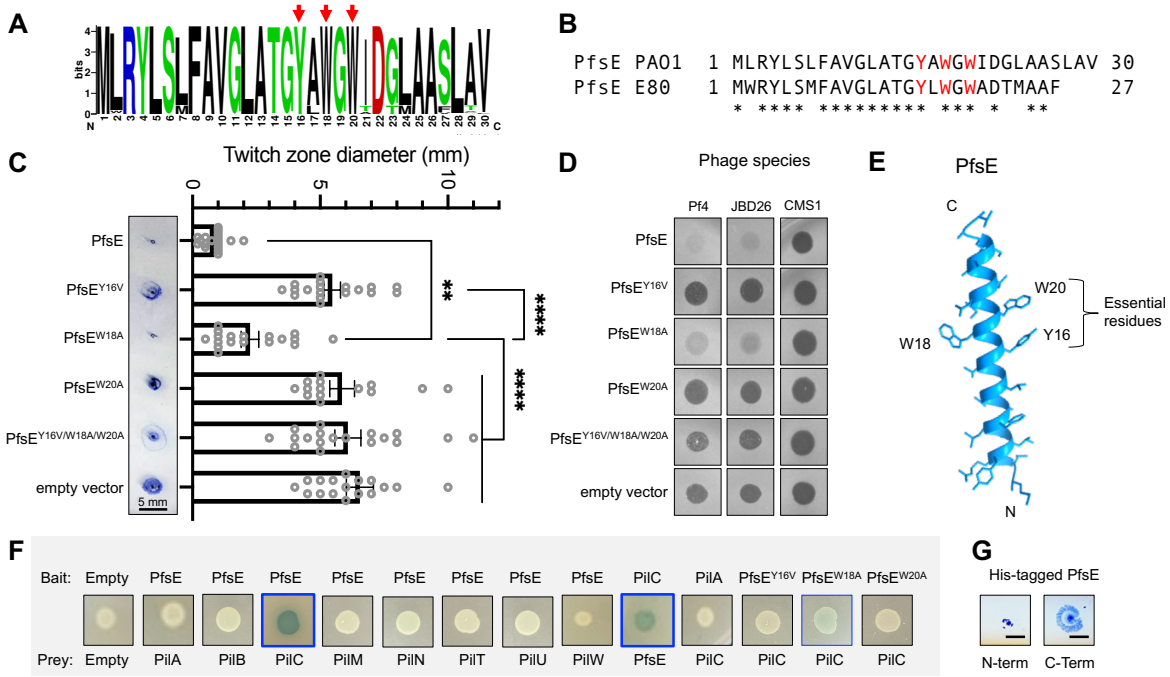

Figure 2- 6. Conserved aromatic residues in PfsE are essential for the inhibition of type IV pili and resistance against Pf4 superinfection. (**A**) WebLogo (7) was used to construct a protein sequence logo for 312 PfsE sequences from Pf prophages infecting *P. aeruginosa* strains in the *Pseudomonas* genome database (8). Note that aromatic residues in the YXWGW motif (residues 16-20) are conserved (arrows). (**B**) There is 66% sequence identity (20/30) between two of the most highly diverged PfsE homologues found in Pf prophages residing in the *P. aeruginosa* PAO1 or E80 chromosomes. (**C**) Twitch motility was measured in PAO1$^{\Delta Pf4}$ expressing wild-type or modified PfsE. Results are mean ± SEM of 16 experiments, unpaired Student's *t* test, **p<0.01, ****p<0.0001. (**D**) Lawns of PAO1$^{\Delta Pf4}$ carrying the indicated expression vectors were induced with 0.01% arabinose and spotted with 3 µl of 10^9 PFU/ml stocks of Pf4, JBD26 (pili-dependent phages), or CMS1 (a pili-independent phage). (**E**) AlphaFold (13) was used to predict the structure of PfsE. (**F**) A bacterial adenylate cyclase two-hybrid (BACTH) assay (14) was used to detect interactions between PfsE and the indicated T4P proteins. Interactions between bait and prey proteins are detected by β-galactosidase activity, as indicated by the production of blue pigment. Representative colonies are shown. (**G**) A 6x-His tag was added to the N- or C-terminus of PfsE, expressed in PAO1$^{\Delta Pf4}$, and twitching was measured. Scale bar 5mm.

or PfsE point mutants did not affect swimming motility compared to PAO1$^{\Delta Pf4}$ carrying an empty expression vector (**Fig S2-2**), indicating that PfsE does not affect flagellum-dependent swimming motility, which is consistent with our previous observation that Pf4 superinfection does not affect swimming motility in *P. aeruginosa* PAO1 (127).

2.3.7. PfsE binds to the T4P inner-membrane protein PilC

The T4P complex consists of four subcomplexes: the outer membrane complex, an alignment complex that spans the periplasm, and two inner membrane complexes (31). Because PfsE is predicted to localize in the inner membrane (8), we hypothesized that PfsE would interact with inner membrane proteins of the T4P complex or proteins that interact with the T4P inner membrane complex. To test this hypothesis, we used a bacterial adenylate cyclase two-hybrid (BACTH) assay (14) to detect interactions between PfsE and the T4P proteins PilA, PilB, PilC, PilM, PilN, PilT, PilU, or PilW. In the BACTH assay, interactions between bait (PfsE) and prey (pili proteins) is detected by β-galactosidase activity. High levels of β-galactosidase activity were observed only when PfsE was expressed with PilC (**Fig 2-6F**), an inner membrane protein essential for T4P pilus biogenesis (139). Similar activity was observed with PilC as bait and PfsE as prey (**Fig 2-6F**).

In an attempt to map residues that are important for the PsfE/PilC interaction, we examined the PfsE protein sequence and identified a conserved cluster of aromatic residues, YAWGW (**Fig. 2-6A and B**). As clusters of aromatic residues often facilitate protein-protein binding interactions (137, 138), we hypothesized that these residues may be required for suppression of twitching motility and resistance to T4P-dependent phages. To test this hypothesis, we introduced into PfsE the following point mutations: PfsE^{Y16V}, PfsE^{W18A}, PfsE^{W20A}, and PfsE$^{Y16V/W18A/W20A}$. These variant proteins were expressed in PAO1$^{\Delta Pf4}$, and twitching motility and phage resistance were measured. PfsE^{Y16V}, PfsE^{W20A}, and PfsE$^{Y16V/W18A/W20A}$ all lost the ability to suppress twitching motility (**Fig. 2-6C**) and did not promote resistance to the T4P-dependent phages Pf4 or JBD26 (**Fig. 2-6D**). PfsE^{W18A} partially suppressed both twitch motility and infection by T4P-dependent phages. When the PfsE^{Y16V} or PfsE^{W20A} point mutants were used as bait with PilC as the prey, β-galactosidase activity was not detected. The PfsE^{W18A} mutant showed some β-galactosidase activity in the BACTH assay, consistent with its intermediate twitch and phage resistance phenotypes. To determine if the loss of twitching and phage resistance was due to loss of the protein interaction or to instability of the protein, we used a Western blot to examine the steady-state levels of 6-His-tagged wild-type PfsE, PfsE^{Y16V}, and PfsE^{W20A} in *E. coli*. While we were able to detect wild-type PfsE using an anti-His antibody, we were unable to detect the PfsE^{Y16V} or PfsE^{W20A} point mutants (**Fig. S2-3**), suggesting that the loss of twitching motility, phage resistance, and the PilC interaction were due to low protein

levels in the cell. These data suggest that Y16 and W20 play a role in stabilizing the PfsE protein fold or promoting its proper insertion into the membrane.

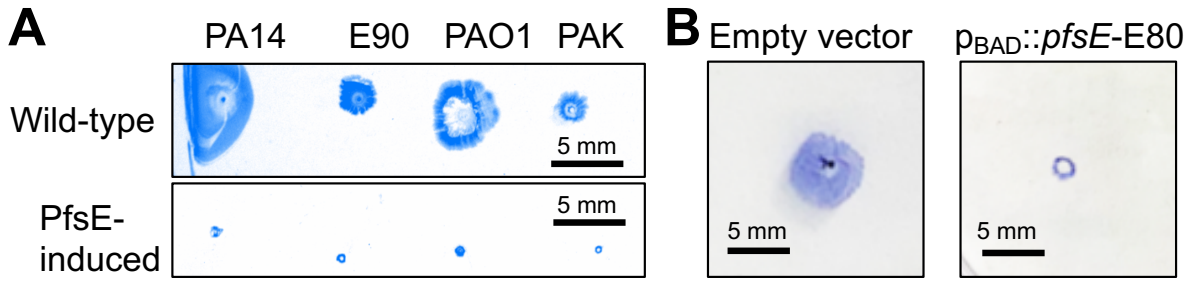

Figure 2- 7. Divergent PfsE sequences inhibit twitching motility in various *P. aeruginosa* strains. (A) PfsE was expressed *in trans* in the indicated strains of *P. aeruginosa* and twitching motility measured after 24h. Representative images are shown. **(B)** Twitching motility was assessed in PAO1$^{\Delta Pf4}$ carrying either the empty vector pHERD20T or p_{BAD}-*pfsE*-E80 by standard twitch assay. Representative images are shown.

The binding of PfsE to the inner membrane protein PilC is consistent with the prediction that PfsE is itself an inner membrane protein. To determine the orientation that PfsE inserts itself into the inner membrane, we tagged the N- or C-terminus of PfsE with a poly-histidine (His) tag, which is positively charged and unable to insert into lipid membranes. Tagged PfsE was expressed in PAO1$^{\Delta Pf4}$ and twitching motility measured. The N-terminal His tag had no impact on the ability of PfsE to inhibit twitching, while the C-terminal His tag prevented PfsE-mediated twitching inhibition (**Fig. 2-6G**). These results suggest that PfsE inserts into the inner membrane with the N-terminus oriented toward the cytoplasm.

As PilC is highly conserved across many different strains of *P. aeruginosa* (139), we tested the ability of PfsE to inhibit twitching motility in *P. aeruginosa* strains PA14, PAK, and E90. We found that the PfsE sequence from Pf4 inhibited twitching in each of these strains (**Fig. 2-7A**). When the divergent PfsE sequence from *P. aeruginosa* strain E80 (see **Fig. 2-6B**) was expressed in *P. aeruginosa* PAO1$^{\Delta Pf4}$, twitching motility was similarly inhibited (**Fig. 2-7B**). These results indicate a conserved mechanism of action.

2.4. Discussion

Many *P. aeruginosa* isolates are Pf lysogens (i.e., they harbor one or more Pf prophage in their chromosome) (17, 64). Lysogenized bacteria defend against infection by the same or similar phage through a mechanism called superinfection exclusion. For example, previously characterized superinfection exclusion mechanisms employed by *P. aeruginosa* phages include proteins Aqs1 from phage DMS3 (82) and Tip from phage D3112 (83), both of which inhibit T4P by binding to the T4P assembly ATPase PilB, which energizes pilus extension (139). This is the first report, to our knowledge, of a phage protein binding PilC to suppress T4P and

prevent superinfection. Our data support a model where the Pf-encoded protein PfsE mediates superinfection exclusion by transiently suppressing T4P by binding to PilC to prevent pilus extension, which inhibits twitching motility and prevents infection by T4P-dependent phages. PfsE interactions with PilC may inhibit T4P by either blocking PilC from rotating, PilA loading, or by interfering with interactions between PilC and other pili proteins such as PilB.

To our knowledge, a transient superinfection exclusion phenotype has not previously been described for a phage. However, transient superinfection exclusion has been observed in animal viruses such as the RNA Pestivirus that causes bovine viral diarrhea (140). The transient nature of PfsE-mediated T4P inhibition may be related to highly stable PfsE-PilC binding interactions. If true, then if PfsE is downregulated as Pf re-enters the lysogenic replication lifecycle, tight binding interactions between PfsE and PilC may titrate out PfsE as the cells divide, restoring T4P function. Alternatively, the conserved acidic residue D22 (see **Fig 2-6A**) may pull the C-terminus of PfsE into the periplasmic space where PfsE could interact with periplasmic proteins that could disrupt PfsE-PilC binding (e.g., a periplasmic protease could degrade PfsE).

Our data suggest that PfsE inhibits pili extension. By inhibiting extension of the T4P cell surface receptor, PfsE may reduce the number of Pf virions that are "wasted" on non-productive infections of an already infected host. This would allow Pf virions to accumulate in the environment, allowing Pf phage to spread and infect naïve *P. aeruginosa* hosts. *P. aeruginosa* also benefits from the accumulation of filamentous Pf virions in the environment—as Pf virions accumulate in polymer-rich environments such as the biofilm matrix or host secretions (e.g., mucus), they spontaneously align, creating a large liquid crystalline lattice that protects *P. aeruginosa* from desiccation and some antibiotics (57, 103, 141). When encountered by immune cells, Pf virions induce a type I interferon antiviral response, which reduces the phagocytic uptake of bacteria by macrophages (105). Collectively, these phenotypes help explain why in *P. aeruginosa* PAO1 deleting the Pf4 prophage from the chromosome reduces bacterial virulence in murine lung (102) and wound (105) infection models.

PfsE inhibition of T4P may affect other bacterial behaviors. For example, in *P. aeruginosa*, T4P play important roles in virulence and biofilm formation (94, 142). T4P are critical virulence determinants in *P. aeruginosa* (142) and inhibition of T4P by PfsE could affect *P. aeruginosa* virulence potential. This possibility is consistent with our previous work demonstrating that Pf4 superinfection promotes a non-invasive infection phenotype *in vivo* (127). Under some conditions such as nutrient limitation, suppression of T4P is thought to contribute to biofilm dispersion (143). Pf4 superinfection contributes to the biofilm lifecycle as well by inducing cell death and lysis, which produces the characteristic voids in the center of mature microcolonies of biofilms grown in flow cells (102, 129, 130). In dispersed cell populations, Pf4 gene expression is upregulated while T4P genes are downregulated (143, 144). Thus, it is possible that in response to Pf4 superinfection, PfsE expression

contributes to biofilm dispersal by suppressing T4P.

Phage therapy holds great potential in combating multidrug-resistant bacterial infections in several settings (145-150). Unfortunately, bacteria can develop resistance to therapeutic phages causing treatment failure ((151) and references therein). In some cases, heritable phage resistance mutations cannot account for phage therapy failure as bacteria remain sensitive to phage infection *ex vivo* (151-154). Because Pf prophages are prevalent amongst *P. aeruginosa* clinical isolates and PfsE is encoded by all Pf lysogens, it is possible that PfsE could cause some phage therapies to fail. Conversely, PfsE could be leveraged as a therapeutic. Recent work demonstrates that the Tip protein from phage D3112 inhibits T4P by blocking the activity of PilB (83). A peptide mimic of the Tip protein inhibits T4P *in vitro,* and when given topically to *P. aeruginosa*, the peptide reduced virulence in a *Drosophila* infection model (155). This approach could potentially be adapted to PfsE by synthesizing a peptide that contains the aromatic amino acid motif YAWGW.

2.5. Materials and Methods

2.5.1. Bacterial strains, plasmids, and growth conditions

Strains, plasmids and their sources are listed in **Table 2-1** and primers are listed in **Table 2-2.** Unless indicated otherwise, bacteria were grown in lysogeny broth (LB) at 37 °C with shaking and supplemented with antibiotics (Sigma) or 0.1% IPTG when appropriate. Unless otherwise noted, antibiotics were used at the following concentrations: gentamicin (10 or 30 μg ml^{-1}), ampicillin (100 μg ml^{-1}), kanamycin (50 μg ml^{-1}), carbenicillin (50 μg ml^{-1}).

2.5.2. Construction of strain ΔPf4

The Pf4 prophage was deleted from the PAO1 chromosome by allelic exchange (156), producing a clean and unmarked ΔPf4 deletion with the Pf4 att site intact. All primers used for strain construction are given in **Table 2- 2**. The Pf4 prophage contains a toxin-antitoxin (TA) pair (157). The presence of the Pf4-encoded PfiTA system likely explains the low efficiency at which the Pf4 prophage can be deleted from the PAO1 chromosome (102); deletion of the Pf4 prophage results in loss of the antitoxin gene *pfiA* and cells without the antitoxin are killed by the longer-lived toxin PfiT (157). Thus, the *pfiT* toxin gene was first deleted from PAO1 by allelic exchange (156). Briefly, the upstream region of *pfIT (pfiT')* and the downstream region of *pfIT ('pfiT)* were amplified using the primer pairs attB1-pfiT-UpF/pfiT-UpR and PfiT-DownF/attB2-PfiT-DownR, respectively (**Table 2- 2**). These were then assembled using SOE-PCR. The resulting fragment was cloned into pENTRpEX18-Gm, transformed into *Escherichia coli* S17λ*pir*, and subsequently mobilized into *P. aeruginosa* PAO1 via biparental mating. Merodiploid *P. aeruginosa* was selected on Vogel-Bonner minimal medium (VBMM) agar containing 60 μg ml^{-}

[1] gentamicin, followed by recovery of deletion mutants on no-salt LB (NSLB) medium containing 10% sucrose. Candidate mutants were confirmed by PCR and sequencing using primer pair PfiT seq F/PfiT seq R. The remaining Pf4 prophage was then deleted from Δ*pfiT* using the same allelic exchange strategy described for Δ*pfiT* using primers Pf4-UpF-GWL, Pf4-UpR-GM, Pf4-DnF-GM, and Pf4-DnR-GWR (**Table 2- 2**), producing an unmarked clean deletion of Pf4 with an intact att site. Candidate mutants were confirmed by PCR using primer pair pf4-out F/pf4-out R and sequenced confirmed. Supernatants collected from overnight cultures this ΔPf4 strain did not produce detectable plaques on lawns of PAO1 or ΔPf4 and the ΔPf4 genotype was routinely PCR confirmed prior to experiments using this strain to avoid re-infection by exogenous Pf4 virions in the laboratory environment.

2.5.3. Phage Expression Constructs

The indicated Pf4 genes or *pfsE* point mutant genes were cloned into the arabinose-inducible expression constructs pHERD20T or pHERD30T (158) were obtained from reference (133) or made by Genewiz (**Table 2-1**). Final constructs were all sequence verified.

2.5.4. Twitch motility assays

Twitching motility was assessed by stab inoculating the indicated strains through a 1.5% LB agar plate to the underlying plastic dish. Agar was supplemented with 0.1% arabinose or antibiotics when appropriate. After incubation for 24 h, the agar was carefully removed, and the zone of motility on the plastic dish was visualized and measured after staining with 0.05% Coomassie brilliant blue, as previously described (159). Twitch zones were measured by placing the plastic dish onto a ruler and imaging with a BioRad GelDoc GO imaging system using preset parameters for Coomassie-stained gels.

2.5.5. Plaque assays

Plaque assays were performed using ΔPf4 or isogenic PAO1 as indicator strains grown on LB plates. Phage in filtered supernatants were serially diluted 10x in PBS and spotted onto lawns of the indicated indicator strain. Plaques were imaged after 18h of growth at 37°C.

2.5.6. Pf4 phage virion quantitation by qPCR

Pf4 virion copy number was measured using qPCR as previously described (136). Briefly, filtered supernatants were treated with DNase I (10 µL of a 10mg/ml stock per mL supernatant) followed by incubation at 70°C for 10 minutes to inactivate the DNase. Ten µL reaction volumes containing 5 µl SYBR Select Master Mix (Life Technologies, Grand Island, NY), 100 nM of primer attR-F and attL-R (**Table 2-2**), and 2 µl supernatant. Primers attR-F and attL-R amplify the re-circularization sequence of the Pf4 replicative form and

thus, do not amplify linear Pf4 prophage sequences that may be present in contaminating chromosomal DNA. Cycling conditions were as follows: 50°C 2min, 95°C 2min, (95°C, 15 sec, 60°C 1 minute) x 40 cycles. A standard curve was constructed using plasmids containing the template sequence at a known copy number per milliliter. Pf4 copy numbers were then calculated by fitting Ct values of the unknown samples to the standard curve.

2.5.7. Pf4 virion induction

P. aeruginosa strains PAO1, Δ*intF4*, and Δ*intF4/pfsE* were made competent by 300 mM sucrose washes (160) and electroporated with the arabinose-inducible expression vectors pHERD20T-*xisF4* and pHERD30T-*intF4.* Double transformants were grown in LB supplemented with gentamicin and carbenicillin to an OD_{600} of 0.3 and induced with 0.1% arabinose. Bacteria were grown for 18h, pelleted by centrifugation, and supernatants were filtered through a 0.22μm filter (Millipore Millex GP) followed by DNase treatment. Pf4 virion titers were measured by qPCR, as described above. Pf4 copy numbers in each supernatant were normalized to the same titer by diluting with PBS.

2.5.8. Growth Curves

Overnight cultures were diluted to an OD_{600} of 0.05 in 96-well plates containing LB and if necessary, the appropriate antibiotics. Over the course of 24h, OD_{600} was measured in a CLARIOstar (BMG Labtech) plate reader at 37C with shaking prior to each measurement.

2.5.9. Transmission Electron Microscopy

Cells were grown to mid-log (OD_{600} 0.4), washed with PBS, fixed with 4% formamide, and placed on a grid and negatively stained with uranyl acetate. Cells were imaged on a Hitachi H-7800 120 kV TEM.

2.5.10. Bacterial two-hybrid assays

Bacterial two-hybrid assays were performed as described previously (14). PfsE was cloned into plasmid constructs (pKT25, pUT18C) using relevant primers (**Table 2-2**). *Escherichia coli* BTH101 cells were co-transformed with plasmid constructs containing different sets of genes. Three independent colonies were grown overnight at 30°C in LB media containing the appropriate selection, 2μl of each was plated onto X-gal and MacConkey agar plates containing the appropriate selection and 1mM IPTG and incubated at 30°C for 48 hours. A colour change on both plates indicates an interaction between the genes encoded in the plasmids.

2.5.11. PfsE modeling

AlphaFold (13) was used to predict the secondary structure of PfsE. The .pdb file was downloaded for PfsE 'model one' and visualized using UCSF ChimeraX (161).

Table 2-1. Bacterial strains, phage, and plasmids used in this study.

Strain	Description	Source
Escherichia coli		
DH5α	New England Biolabs	(12)
S17	λpir-positive strain	(12)
P. aeruginosa		
PAO1	Wild type	(162)
PAO1 Δ*pilA*	Clean deletion of *pilA* from PAO1	(163)
PAO1 Δ*intF4*	Clean deletion of *intF4* from PAO1	(57)
PAO1 Δ*intF4/pfsE*	Clean deletion of *pfsE* from PAO1 Δ*intF4*	This study
PAO1 ΔPf4	Clean deletion of the Pf4 prophage from PAO1	This study
PA14	Wild type	(164)
PAK	Wild type	ATCC 25102
E90	Clinical CF *P. aeruginosa* isolate	(165)
Bacteriophage Strains		
Pf4	Inoviridae	(57)
JBD26	Siphoviridae	(134)
CMS1	Podoviridae	This study
DMS3	Siphoviridae	(166)
OMK01	Myoviridae	(167)
LPS-5	Podoviridae	Felix Biotech
Plasmids		
pHERD20T	AmpR, expression vector with araC-P_{BAD} promoter	(158)
pHERD30T	GmR, expression vector with araC-P_{BAD} promoter	(158)
pHERD30T-*PA0717*	pBAD::*PA0717*	(133)
pHERD30T-*PA0718*	pBAD::*PA0718*	(133)
pHERD30T-*PA0719*	pBAD::*PA0719*	This study
pHERD30T-*PA0720*	pBAD::*PA0720*	(133)
pHERD30T-*pfsE*	pBAD::*pfsE*	(133)
pHERD30T-*PA0722*	pBAD::*PA0722*	This study
pHERD30T-*PA0723*	pBAD::*PA0723*	This study
pHERD30T-*PA0724*	pBAD::*PA0724*	This study
pHERD30T-*PA0725*	pBAD::*PA0725*	(133)
pHERD30T-*PA0726*	pBAD::*PA0726*	This study
pHERD30T-*PA0727*	pBAD::*PA0727*	This study
pHERD30T-*intF4*	pBAD::*intF4*	This study
pHERD20T-*xisF4*	pBAD::*xisF4*	(3)
pKT25	BACTH construct	(14)
pUT18C	BACTH construct	(14)
pHERD20T-*pfsE*	pBAD::*pfsE*	This study
pHERD20T- *pfsE* ^{Y16V}	pBAD:: *pfsE* ^{Y16V}	This study
pHERD20T- *pfsE* ^{W18A}	pBAD:: *pfsE* ^{W18A}	This study
pHERD20T- *pfsE* ^{W20A}	pBAD:: *pfsE* ^{W20A}	This study
pHERD20T- *pfsE* $^{Y16A/W18A/W20A}$	pBAD:: *pfsE* $^{Y16A/W18A/W20A}$	This study

Table 2-2. Primers used in this study.

Purpose/Name	Sequence (5'-3')
Cloning	
PfsE_p18CFwd	TACGTCTAGAGCTCCGCTATCTCTCGCTGTTCGCGGTAGG
PfsE_p18CRev	TACGGGTACCTCAAACAGTCAGGGAGGCCGCTAGG
PfsE_Y16VFwd	CTGGCCACCGGCGTGGCCTGG
PfsE_Y16VRev	CCAGCCCCAGGCCACGCCGGT
PfsE_W18AFwd	ACCGGCTACGCCGCCGGCTGG
PfsE_W18ARev	TCGATCCAGCCGGCGGCGTAGC
PfsE_W20AFwd	TACGCCTGGGGCGCCATCGACG
PfsE_W20ARev	CTAGGCCGTCGATGGCGCCCCAGG
Δ*pfiT* primers	
attB1-pfiT-UpF	ggggataagtttgtacaaaaaagcaggcttcTTCAACCCGCTCATAGGTT
pfiT-UpR	TCAGGAGTAGAAAGCCATCACATTAAACCTCCTTATTCTGG
PfiT-DownF	TGATGGCTTTCTACTCCTGA
attB2-PfiT-DownR	ggggaccactttgtacaagaaagctgggtaAGCCGCTCAACCCGATCTA
PfiT seq F	CCACACGTTCGCCAGTCACTT
PfiT seq R	AATGCCGGCCACTTCATCGAC
ΔPf4 primers	
Pf4-UpF-GWL	tacaaaaaagcaggctTCTGGGAATACGACGGGGGC
Pf4-UpR-GM	tcagagcgcttttgaagctaattcgGATCCCAATGCAAAAGCCCC
Pf4-DnF-GM	aggaacttcaagatccccaattcgCGTCATGAGCTTGGGAAGCT
Pf4-DnR-GWR	tacaagaaagctgggtTGGCAGCAGACCCAGGACGC
pf4-out F	AGTGGCGGTTATCGGATGAC
pf4-out R	TCATTGGGAGGCGCTTTCAT

2.5.12. Statistical analyses

Differences between data sets were evaluated by an unpaired Student's *t* test, using GraphPad Prism version 5.0 (GraphPad Software, San Diego, CA). P values of < 0.05 were considered statistically significant.

2.6. Acknowledgements

We are grateful to Joe Bondy-Denomy, Adair Borges, and Xiaoxue Wang for sharing the inducible Pf plasmids indicated in Table 2-1. We thank Paul Turner and Felix Biotechnology, Inc. for sharing phages OMK01 and LPS-5. PRS was supported by NIH grants R01AI138981 and P20GM103546. DWD, JW and PAR were supported by the Intramural Research Program of the National Institute of Allergy and Infectious Diseases, National Institutes of Health.

CHAPTER THREE Targeted Deletion of Pf prophages from diverse *Pseudomonas aeruginosa* isolates has differential impacts on quorum sensing and virulence traits

Published April 30th, 2024, in the Journal of Bacteriology. DOI: 10.1128/jb.00402-23.

Amelia K. Schmidt[1], Caleb M. Schwartzkopf[1], Julie D. Pourtois[2], Elizabeth Burgener[2], Dominick R. Faith[1], Alex Joyce[1], Tyrza Lamma[1], Geetha Kumar[3], Paul L. Bollyky[2], and Patrick R. Secor[1#]

[1] Division of Biological Sciences, University of Montana, Missoula, Montana, USA
[2] Division of Infectious Diseases and Geographic Medicine, Department of Medicine, Stanford University School of Medicine, Stanford, CA, USA.
[3] School of Biotechnology, Amrita Vishwa Vidyapeetham, Amritapuri, Kerala, India
[#] Correspondence: Patrick.secor@mso.umt.edu

Note: With the assistance of laboratory technicians Alex Joyce and Tyrza Lamma, this work was entirely undertaken by me. I relied on the guidance of Julie D. Pourtois and Dominick R. Faith for bioinformatic analyses. As with all science, the conception of many of the experiments below were collaborative discissions with Caleb M. Schwarzkopf, Elizabeth Burgener, Paul L. Bollyky and Patrick R. Secor. Stains used in this work were the generous gifts of the Kumar Lab and Bollyky Lab.

3.1. Abstract

Pseudomonas aeruginosa is an opportunistic bacterial pathogen that commonly causes medical hardware, wound, and respiratory infections. Temperate filamentous Pf phages that infect *P. aeruginosa* impact numerous virulence phenotypes. Most work on Pf phages has focused on Pf4 and its host *P. aeruginosa* PAO1. Expanding from Pf4 and PAO1, this study explores diverse Pf phage infecting *P. aeruginosa* clinical isolates. We describe a simple technique targeting the Pf lysogeny maintenance gene, *pflM* (*PA0718*), that enables the effective elimination of Pf prophages from diverse *P. aeruginosa* hosts. The *pflM* gene shows diversity amongst different Pf phage isolates; however, all examined *pflM* alleles encode the DUF5447 domain. We demonstrate that *pflM* deletion results in prophage excision but not replication, leading to total prophage loss, indicating a role for lysis/lysogeny decisions for the DUF5447 domain. This study also assesses the effects different Pf phages have on host quorum sensing, biofilm formation, pigment production, and virulence against the bacterivorous nematode *Caenorhabditis elegans*. We find that Pf phages have strain-specific impacts on quorum sensing and biofilm formation, but nearly all suppress pigment production and increase *C. elegans* avoidance behavior. Collectively, this research not only introduces a valuable tool for Pf prophage elimination from diverse *P. aeruginosa* isolates, but also advances our understanding of the complex relationship between *P. aeruginosa* and filamentous Pf phages.

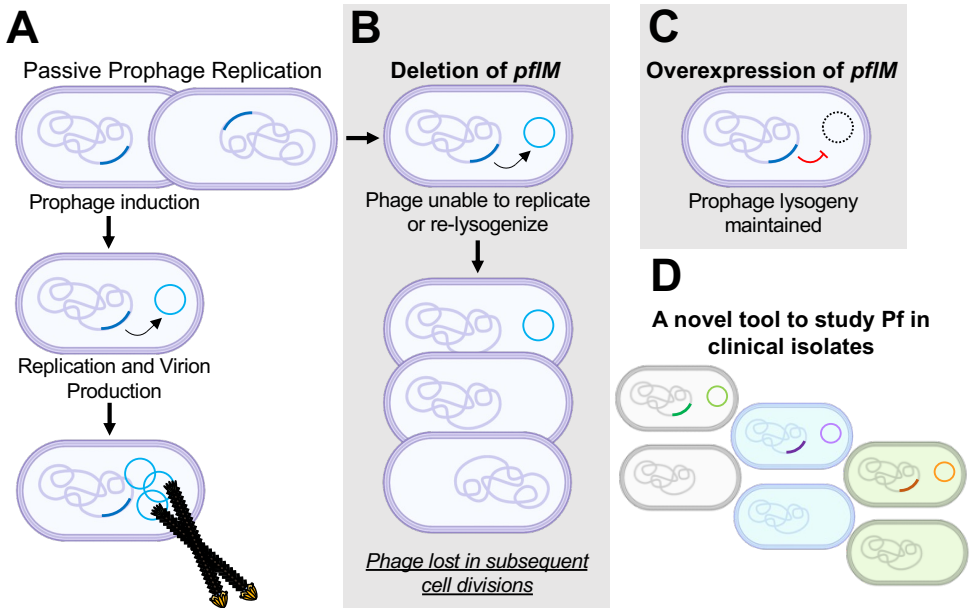

Figure 3- 1. Graphical Abstract. Deletion of *PA0718 (pflM)* causes prophage excision, halts mature virion production and Pf4 genome replication while overexpression maintains prophage lysogeny. (**A**) Filamentous Inoviruses either replicate passively as a lysogen in a prophage state or are induced to excise from the bacterial chromosome and replicate through rolling circle replication. (**B**) Deletion of Pf4 gene PA0718, renamed *pflM* (Pf-lysogeny-Maintenance) causes prophage excision, and halts replication resulting in loss of the native prophage in subsequent cell divisions. **(C)** Overexpression of *pflM* results in increased lysogenic conversion of Pf, where it remains stably in a prophage state. **(D)** PflM can be leveraged as a tool to study phage:host interactions contributing to clinical isolate virulence.

3.1.1. Importance

Pseudomonas aeruginosa is an opportunistic bacterial pathogen that is frequently infected by filamentous Pf phages (viruses) that integrate into its chromosome, affecting behavior. While prior work has focused on Pf4 and PAO1, this study investigates diverse Pf in clinical isolates. A simple method targeting the deletion of the Pf lysogeny maintenance gene *pflM* (*PA0718*) effectively eliminates Pf prophages from clinical isolates. The research evaluates the impact Pf prophages have on bacterial quorum sensing, biofilm formation, and virulence phenotypes. This work introduces a valuable tool to eliminate Pf prophages from clinical isolates and advances our understanding of *P. aeruginosa* and filamentous Pf phage interactions.

3.2. Introduction

Pseudomonas aeruginosa is an opportunistic bacterial pathogen that commonly infects medical hardware, diabetic ulcers, burn wounds, and the airways of cystic fibrosis patients (95). *P. aeruginosa* isolates are often infected by filamentous viruses (phages) called Pf (17, 64, 168). Pf phages live a temperate lifestyle and integrate into the bacterial chromosome as a prophage, passively replicating with each bacterial cell division. When induced, the Pf prophage is excised from the chromosome forming a circular double-stranded episome called the

replicative form (129). Pf replicative form copy numbers increase in the cytoplasm where they serve as templates for viral transcription. The replicative form is also a template for rolling circle replication which generates circular single-strand DNA genomes that are packaged into filamentous virions as they are extruded from the cell (15, 17).

Filamentous Pf virions are associated with enhanced *P. aeruginosa* virulence potential by promoting biofilm formation (57) and inhibiting phagocytic uptake by macrophages (99, 127). Pf virions also carry a high negative charge density allowing them to sequester cationic antimicrobials such as aminoglycoside antibiotics and antimicrobial peptides (57, 103, 169). Additionally, Pf phages enhance the virulence potential of *P. aeruginosa* by modulating the secretion of the quorum-regulated virulence factor pyocyanin (170, 171). These properties may explain why the presence of Pf virions at sites of infection is associated with more chronic lung infections and antibiotic resistance in cystic fibrosis patients (99) and why *P. aeruginosa* strains cured of their Pf infection are less virulent in murine models of pneumonia (102) and wound infection (105).

Most studies to date have focused on interactions between Pf isolate Pf4 and its host *P. aeruginosa* PAO1. (17, 102, 103, 127). Despite the clear link between Pf4 and the virulence of *P. aeruginosa* PAO1, the effects diverse Pf that infect *P. aeruginosa* clinical isolates have on virulence phenotypes remains unclear. This is in part due to the significant challenge of 'curing' clinical isolates of their Pf prophage infections. Prior efforts to delete Pf4 from PAO1 relied on the integration of a selectable marker into the integration site used by Pf4 (102), which precludes complementation studies that re-introduce the Pf4 prophage to the host chromosome. In prior work, we were able to generate a clean Pf4 deletion strain by first deleting the *pfiTA* toxin-antitoxin module encoded by Pf4 followed by deletion of the rest of the prophage (172).

Here, we find that the Pf4 gene *PA0718* maintains Pf4 in a lysogenic state; we therefore refer to *PA0718* as the Pf lysogeny maintenance gene *pflM*. Deletion of *PA0718* or homologous alleles from Pf prophages in clinical *P. aeruginosa* isolates LESB58, CPA0053, CPA0087, and the multidrug resistant strain DDRC3 resulted in the complete loss of Pf prophages from each strain. Furthermore, we observe that some substrains of PAO1 are lysogenized by two Pf phages, Pf4 and Pf6, and we successfully cured PAO1 of both Pf4 and Pf6 prophages. We compare phenotypic differences between wild-type and ΔPf prophage mutants by assessing Las, Rhl, and PQS quorum sensing activity, biofilm formation, and pyocyanin production. We also examine how Pf prophages impact virulence phenotypes in a *Caenorhabditis elegans* avoidance model. Overall, we present a new methodology for efficiently curing *P. aeruginosa* strains of their resident Pf prophages and leverage this tool to gain insight into the diverse impacts Pf phages have on their bacterial hosts.

3.3. Results

3.3.1. PA0718 (PflM) maintains Pf4 lysogeny in *P. aeruginosa* PAO1

While making single gene deletions from the core Pf4 genome (*pf4r-intF4)* in *P. aeruginosa* PAO1 (**Fig. 3-2A**), we noted that deleting either the *Pf4r* repressor or the *PA0718* gene results in the complete excision of the Pf4 prophage from the *P. aeruginosa* chromosome (**Fig. 3-2B**, upper bands). Prior work demonstrates that deletion of the *Pf4r* repressor induces Pf4 prophage excision and virion replication (3), but how *PA0718* is

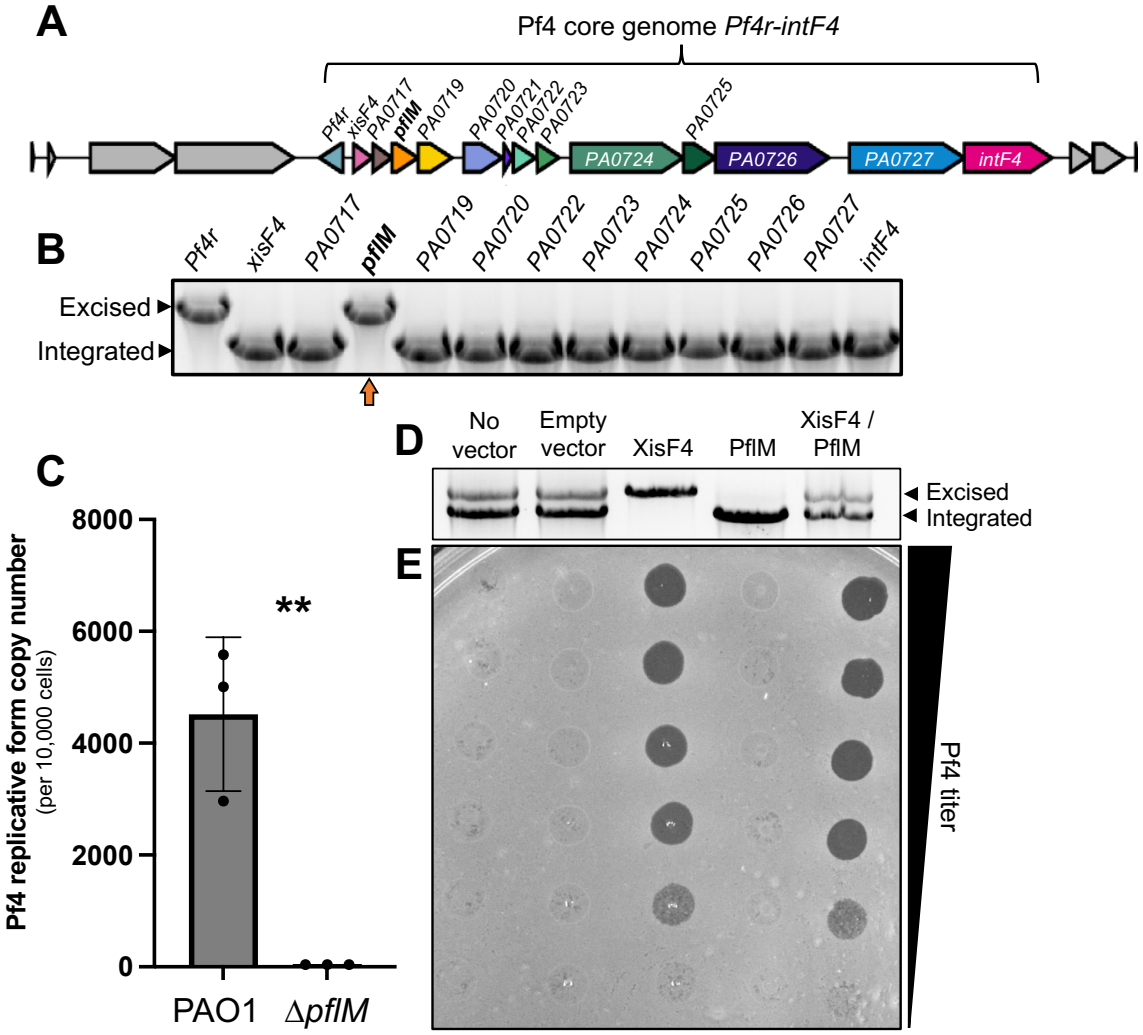

Figure 3- 2. The Pf4 phage gene PA0718 (pflM) maintains lysogeny. (A) Schematic of the Pf4 prophage (PA0715-PA0729) integrated into the tRNA-Gly gene PA0729.1 in P. aeruginosa PAO1. The core genome that is conserved amongst Pf isolates is indicated. Color coding corresponds to predicted function of gene products as in Fiedoruk et al., 2020. **(B)** Multiplex PCR was used to measure Pf4 prophage integration and excision from the PAO1 chromosome in the indicated Pf4 single-gene mutants. Excision and integration are differentiated by the size of the PCR product produced. Note that that deleting PA0721 (pfsE) from the Pf4 prophage is lethal to P. aeruginosa (16) explaining why pfsE is not included in the assay. A representative gel is shown. **(C)** Quantitative PCR (qPCR) was used to measure episomal Pf4 replicative form in PAO1 or ΔPA0718 cells after 18 hours of growth in LB broth. Data are the mean of three replicate experiments, ΔPA0718 values were below the limit of detection for the assay (37 copies per microliter of input material). **(D)** PflM and/or XisF4 were expressed from inducible plasmids in P. aeruginosa PAO1. After 18 hours of growth in LB broth, Pf4 integration and excision was measured by multiplex PCR. **(E)** Filtered supernatants collected from the indicated bacterial strains were titered via 10X dilution series on lawns of PAO1ΔPf4 and imaged after 18 hours of growth. Axis label indicates dilution of supernatant.

involved in Pf4 excision is not known.

After excision, Pf4 replicates as a circular episome called the replicative form (129). We used qPCR to measure circular Pf4 replicative form copy number in wild-type and Δ*PA0718* cells. In wild-type cells, approximately 4,400 replicative form copies were detected for every 10,000 cells; however, the Pf4 replicative form was not detected in Δ*PA0718* cells (**Fig. 3-2C**), indicating that Pf4 genome replication is not initiated, and the replicative form is lost as cells divide. These results indicate that PA0718 maintains the Pf4 prophage in a lysogenic state and that deleting *PA0718* induces Pf4 prophage excision, but not replication, curing PAO1 of its Pf4 infection. Herein, we refer to *PA0718* as the Pf lysogeny maintenance gene *pflM*.

The observation that 4,400 Pf4 replicative form copies are detected for every 10,000 wild-type cells (**Fig. 3-2C**) indicates Pf4 is actively replicating in a subpopulation of cells. We used a multiplex PCR excision assay to measure Pf4 prophage excision and integration in *P. aeruginosa* populations. In PAO1 populations with no expression vector or those carrying an empty expression vector, both Pf4 prophage integration and excision are observed (**Fig. 3-2D**, two bands are present); however, infectious virions were not detected in supernatants by plaque assay suggesting that Pf4 is replicating at low levels during planktonic growth in LB broth, consistent with prior results (173).

The Pf4 excisionase XisF4 regulates Pf4 prophage excision (3) and expressing XisF4 in *trans* induces complete Pf4 prophage excision (**Fig. 3-2D**) and robust virion replication (**Fig. 3-2E**). In contrast, expressing PflM in *trans* maintains the entire population in a lysogenic state (**Fig. 3-2D**) and virion replication is not detected (**Fig. 3-2E**). When PflM and XisF4 are expressed together, both Pf4 integration and excision products are observed (**Fig. 3-2D**) and infectious virions are produced at titers comparable to cells where XisF4 was expressed by itself (**Fig. 3-2E**). These results indicate that expressing PflM is not sufficient to inhibit XisF4-mediated Pf4 prophage excision and replication, but that PflM can maintain some cells in a lysogenic state during active viral replication.

3.3.2. The targeted deletion of *pflM* cures diverse *P. aeruginosa* isolates of their Pf prophages

We hypothesized that deleting *pflM* would provide a convenient way to cure *P. aeruginosa* clinical isolates of their Pf prophages. To test this hypothesis, we deleted *pflM* from the Pf prophages in cystic fibrosis isolate LESB58, two cystic fibrosis isolates from the Stanford Cystic Fibrosis Clinic (CPA0053 and CPA0087), and the multidrug-resistant urine isolate DDRC3 (**Table 3-1**).

Strain	Accession	Source	Mucoid?	Pf name / lineage	Pf integration site	Pf prophage length (kb)
PAO1	GCF_000006765.1	Lab strain	No	Pf4 / I	tRNA-Gly	12.4
				Pf6 / I	tRNA-Met	12.1
LESB58	FM209186.1	CF isolate, Liverpool, United Kingdom	No	Pf-LESB58 / II	Direct repeat	10.5
CPA0053	CP137561	CF isolate, Stanford, CA, USA	No	Pf-CPA0053/ II	Direct repeat	10.4
CPA0087	CP137562	CF isolate, Stanford, CA, USA	No	Pf-CPA0087/ II	tRNA-Gly	11.1
DDRC3	CP137563	Urine isolate, Trivandrum, Kerala, India	No	Pf-DDRC3/ II	tRNA-Gly	15.5

Table 3-1. *P. aeruginosa* isolates and Pf prophage characteristics.

Pf prophage loss in PAO1 was screened by multiplex PCR (**Fig. 3-3A/C**) and confirmed in all strains by long-read whole-genome sequencing. Targeting *pflM* successfully cured all the above clinical *P. aeruginosa* isolates of their Pf prophages (**Fig. 3-3B, D–G**). Of the Pf prophages we deleted, four were integrated into tRNA genes (three in tRNA-Gly and one in tRNA-Met) and two were integrated into direct repeats (**Table 3-1**). Further, Pf prophages fall into two main lineages (I and II, **Table 3-1**) (168) and we were successful in deleting representatives from each lineage with an efficiency rate of approximately 17%. These observations indicate integration site nor lineage have influence on *pflM*-mediated Pf prophage deletion.

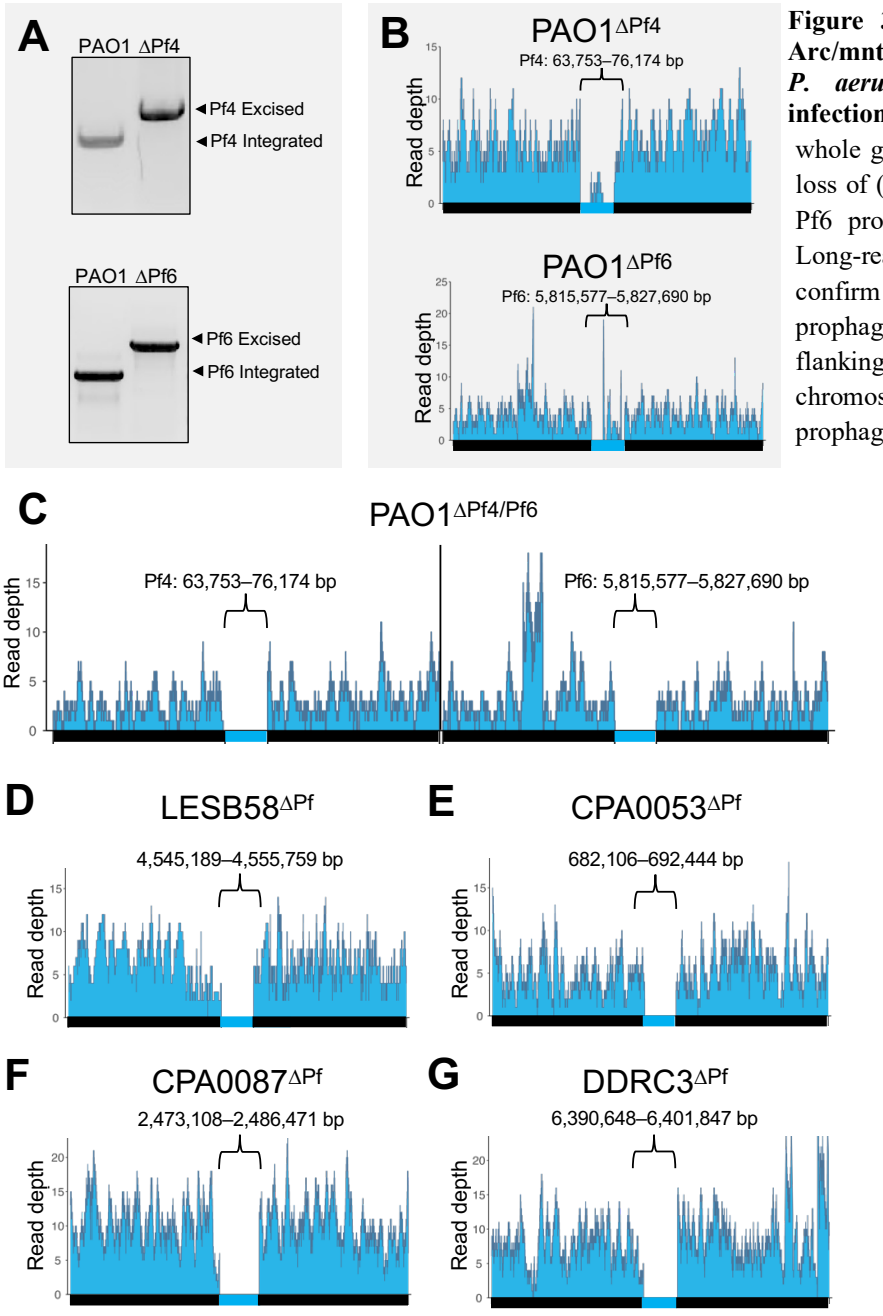

Figure 3- 3. Targeted deletion of pflM, or its Arc/mnt domain-containing isoform, cure diverse *P. aeruginosa* isolates of their Pf prophage infections. A multiplex PCR assay and long-read whole genome sequencing were used to confirm the loss of (A and B) the Pf4 prophage or (C and D) the Pf6 prophage from the PAO1 chromosome. (E-I) Long-read whole genome sequencing was used to confirm the successful deletion of the indicated Pf prophages. Reads were aligned to 50 kb sequences flanking the Pf prophage insertion sites in the parental chromosome. The genomic coordinates for each Pf prophage are shown above each bracket.

To determine if prophage loss impacts bacterial growth, we performed growth curves over 18 hours and compared parental and prophage mutant strains (**Fig. S3-1**). In strains PAO1, CPA0053 and DDRC3 deletion of the Pf prophage has no significant impact on bacterial growth (**Fig. S3-1A-C**). For strains CPA0087 and LESB58, prophage presence significantly reduces or increases growth rates, respectively ($P<0.0001$) (**Fig. S3-1 D-E**). The decreased growth of strain CPA0087$^{\Delta Pf}$ may be related to the large increase in pyocyanin production, which could negatively impact bacterial growth. The increased growth rate of LESB58$^{\Delta Pf}$ may be explained by relieving the metabolic burden of Pf phage replication. Alternatively, differences in Pf prophage insertion loci in different *P. aeruginosa* strains could affect bacterial growth dynamics.

Many *P. aeruginosa* strains are infected by one or more Pf prophages (17). For example, some *P. aeruginosa* PAO1 sub-isolates are infected by Pf4 and Pf6 (174). Deleting *pflM* from Pf4 results in the loss of the Pf4 prophage, as does deleting *pflM* from Pf6 (**Fig. 3-3B and D**). Furthermore, we were able to delete Pf6 from ΔPf4, producing a PAO1$^{\Delta Pf4/Pf6}$ double mutant (**Fig. 3-3E**). This observation indicates that *pflM* from one Pf prophage is specific to that prophage and does not compensate for the loss of *pflM* from another Pf prophage residing in the same host.

PflM specificity may be explained by the diversity in the operon encoding *pflM* or in the *pflM* allele itself (**Fig 3-4A**). All *pflM* sequences examined contain a predicted DUF5447 domain (pfam17525), which, as pointed out in prior work, appears to originate from a disrupted gene encoding the Mnt (PHA01513) domain (41). The Mnt protein encoded by *Salmonella* phage P22 governs lysis-lysogeny decisions by binding phage operator sequences (175, 176), suggesting PflM may regulate Pf lysis-lysogeny decisions by a similar mechanism. In the Pf DDRC3 *pflM* allele, the Mnt domain is present and is fused to the DUF5447 domain while in Pf4, Pf LESB58, Pf CPA0087, and Pf6, *pflM* is truncated by a 5' insertion of a gene of unknown function (*PA0717* in Pf4) (**Fig. 3-4A**). Structural prediction and sequence alignments indicate that, despite the different isoforms PflM present within different Pf prophages, residues which are predicted to form an anti-parallel β-sheet characteristic of the DUF5447 domain are conserved (**Fig. 3-4B and C**).

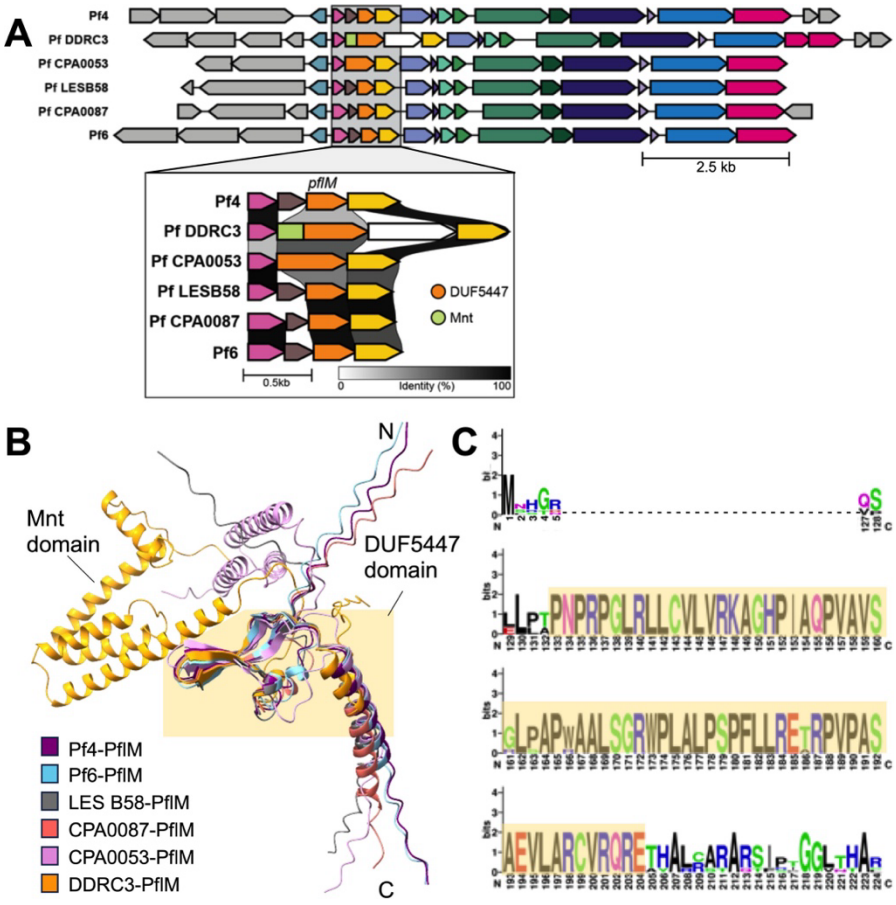

Figure 3- 4. Sequence and structural analysis of PflM. (**A**) Pf prophage annotation was performed with Rapid Annotation using Subsystem Technology (RAST). Inset: Clinker was used to generate alignments of the *pflM* loci spanning from *xisF* to *PA0719* in the Pf4 reference sequence. DUF5447 and mnt domains in *pflM* are indicated by orange or green, respectively, in the inset. (**B**) PflM structures were predicted using AlphaFold2and aligned using ChimeraX. The highlighted region indicates the DUF5447 domain and the Mnt domain is indicated for the PflM sequence from strain DDRC3. (**C**) A protein sequence logo for PflM was generated with WebLogo3 (v. 2.8.2); dashes represent variable residues. The DUF5447 domain is highlighted.

3.3.3. Pf phages differentially modulate host quorum sensing

Pf4 is known to suppress PQS and Rhl quorum sensing in *P. aeruginosa* PAO1 (170, 171, 177). We hypothesized that Pf phages would likewise modulate quorum sensing in the Pf deletion strains we constructed here. To test this, we used fluorescent transcriptional reporters (170) to measure Las (*rsaL*), Rhl (*rhlA*), and PQS (*pqsA*) transcriptional activity in parental strains and Pf mutants.

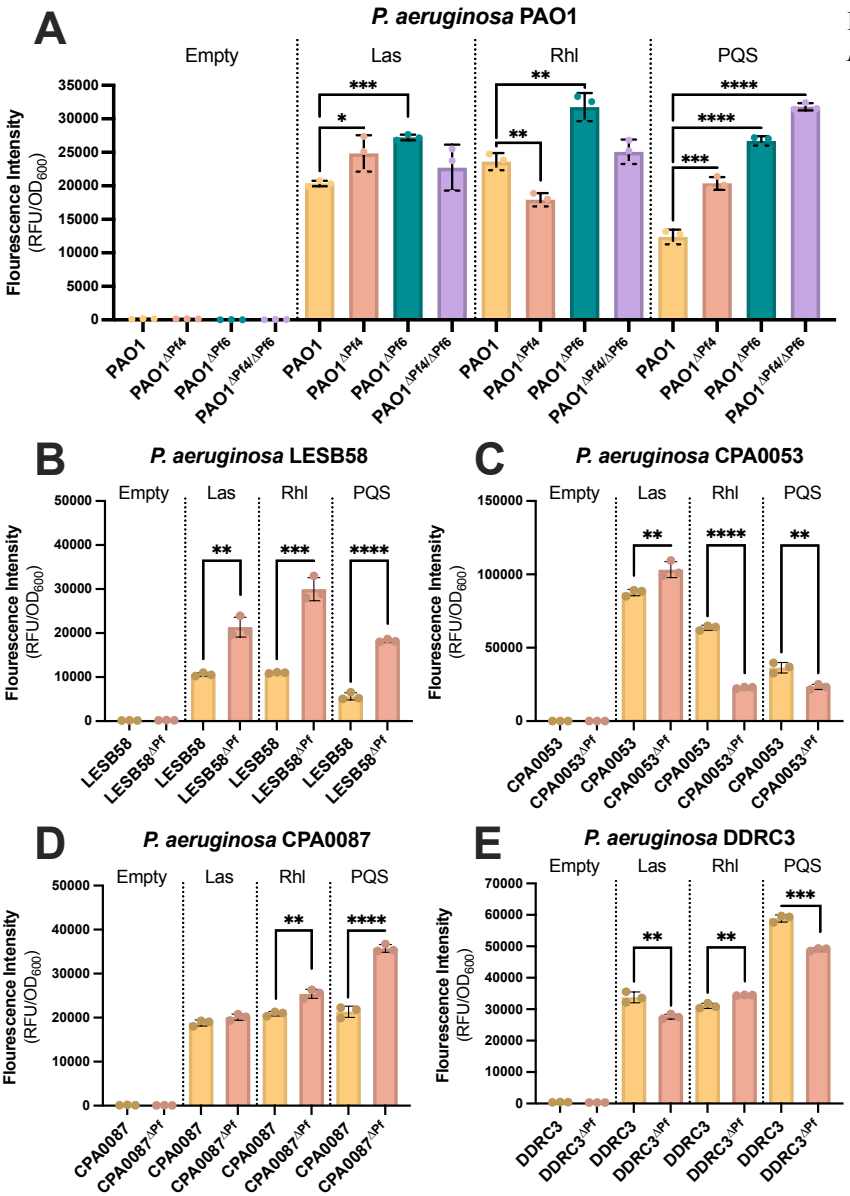

Figure 3- 5. Pf phage differentially modulates *P. aeruginosa* quorum sensing. Fluorescence from the transcriptional reporters P_{rsaL}-*gfp* (Las), P_{rhlA}-*gfp* (Rhl), or P_{pqsA}-*gfp* (PQS) was measured in the indicated strains after 18 hours of growth. Reporter fluorescence intensity was normalized to cell density (OD_{600}) at each time point. Data are the mean ± SEM of seven replicates. $^{*}P < 0.05$, $^{**}P < 0.01$, $^{***}P < 0.001$, $^{****}P < 0.0001$, Student's *t*-test comparing ΔPf strains with the wild-type parent at each time point.

Over an 18-h growth period, we find that differences in Las, Rhl, and PQS quorum sensing activity vary by Pf phage and *P. aeruginosa* host (**Fig. S3-2–S3-8**). The general trends for each quorum sensing reporter hold over 18 h; however, for clarity, we show only the 18-h time point in **Figure 3-5**. After 18 h, PAO1$^{\Delta Pf4}$ Las and PQS signaling are significantly upregulated (P<0.01 and P<0.0001, respectively) while Rhl transcription is downregulated (**Fig. 3-5A**). Pf6 differentially affects PAO1 quorum sensing—Las, Rhl, and PQS signaling are

all upregulated in PAO1$^{\Delta Pf6}$ compared to the parental strain (**Fig. 3-5A**). Deleting both Pf4 and Pf6 had no significant impact on Las or Rhl signaling, but PQS signaling was significantly upregulated in PAO1$^{\Delta Pf4/Pf6}$ compared to the parental strain (**Fig. 3-5A**), which is consistent with prior work (170, 178).

After 18h, PQS transcriptional activity is also significantly (P<0.001) upregulated in LESB58$^{\Delta Pf}$, as are Las and Rhl (**Fig 3-5B**). In strain CPA0053$^{\Delta Pf}$, Las signaling was significantly upregulated (P<0.001) while Rhl and PQS transcription is reduced when the Pf prophage is deleted (**Fig. 3-5C**). PQS and Rhl are upregulated in CPA0087$^{\Delta Pf}$ while Las and signaling is not significantly affected (**Fig. 3-5D**). Finally, in DDRC3$^{\Delta Pf}$, Las and PQS signaling are significantly downregulated (P<0.001) while Rhl signaling is significantly upregulated (P<0.001) (**Fig. 3-5E**). Taken together, these data indicate that Pf phages have diverse and complex relationships with host quorum sensing pathways that vary significantly by strain.

3.3.4. Pf phages have contrasting impacts on *P. aeruginosa* biofilm formation

Pf4 is known to promote *P. aeruginosa* PAO1 biofilm assembly and function (17, 57, 102, 103, 128, 129, 179). To test if other Pf isolates similarly affect biofilm formation, we used the crystal violet biofilm assay (180) to measure biofilm formation of lysogenized *P. aeruginosa* isolates compared to the Pf prophage deletion mutants. In PAO1, deletion of either Pf4 or Pf6 significantly (P<0.001) reduce biofilm formation by 1.79- and 2.33-fold, respectively, while deletion of both Pf4 and Pf6 reduces biofilm formation by 7.14-fold (**Fig. 3-6A**). This result indicates both Pf4 and Pf6 contribute to PAO1 biofilm formation, which is consistent with prior observations (57, 102, 103, 128, 129, 179). The clinical isolates in general did not form as robust biofilms as the PAO1 laboratory strain under the *in vitro* conditions tested. Even so, deleting the Pf prophage from strains CPA0053 and DDRC3 modestly but significantly (P<0.05) reduced biofilm formation (**Fig. 3-6C and E**). In contrast, biofilm formation was significantly (P<0.01) increased in strains LESB58$^{\Delta Pf}$ and CPA0087$^{\Delta Pf}$ compared to the parental strains (**Fig. 3-6B and D**). The variation in biofilm formation phenotypes is perhaps not surprising

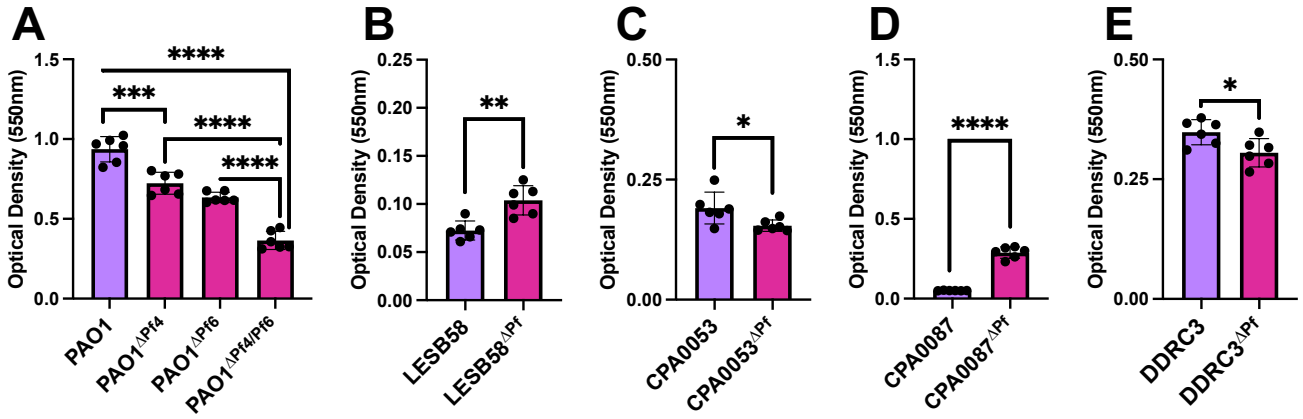

Figure 3- 6. Pf prophage deletion has significant but variable effects on *P. aeruginosa* biofilm formation. Crystal violet biofilm assays were performed to measure biofilm formation of the indicated strains after 48h incubation. Data are the mean ±SEM of six replicates. *P<0.05, **P<0.01, ***P<0.001, ****P<0.0001, Student's t-test.

given the variation inherent in the strains examined here, ranging from lab adapted strains to CF-lung adapted *P. aeruginosa* isolates. Although quorum sensing regulation varies between Pf lysogens and their corresponding Pf prophage mutants, there is no clear trend of modified QS expression and biofilm formation (**Fig. 3-6**).

3.3.5. Pf phages suppress *P. aeruginosa* pyocyanin production in most clinical isolates

Pyocyanin is a redox-active quorum-regulated virulence factor (181). Deleting the Pf4 prophage from PAO1 enhances pyocyanin production (182). We observed increased pyocyanin production in all ΔPf strains tested except CPA0053, which did not produce much pyocyanin under any condition tested (**Fig. 3-7A-E**). We confirmed that the *pqsABCD* operon nor *pqsR* encoded by CPA0053 is not mutated, nor is *lasI, lasR, rhlI, or rhlR*, indicating other factors/signaling pathways are contributing to reduced pyocyanin production by this strain. These results suggest that some Pf prophages encode gene(s) that inhibit host pyocyanin production.

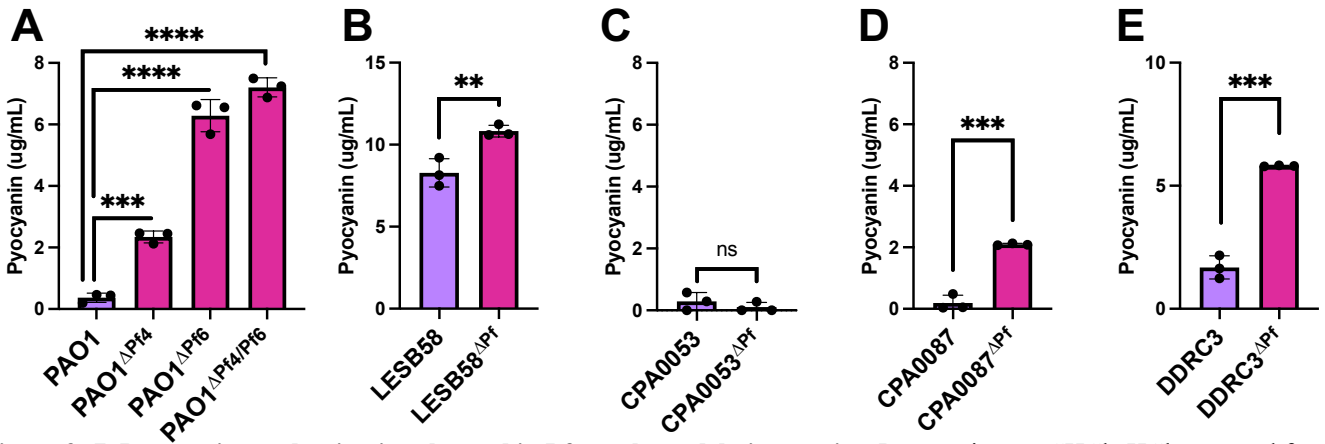

Figure 3- 7. Pyocyanin production is enhanced in Pf prophage deletion strains. Pyocyanin was $CHCl_3$-HCl extracted from the supernatants of the indicated cultures after 18h of incubation. Pyocyanin concentration was measured (Abs 520nm). Data are the mean ±SEM of three replicates. **P<0.01, ***P<0.001, ****P<0.0001, Student's *t*-test.

3.3.6. Pf phages induce avoidance behavior in bacterivorous nematodes

In the environment, bacterivores impose high selective pressures on bacteria (183, 184). Pf4 modulation of quorum-regulated virulence factors increases *P. aeruginosa* fitness against the bacterivorous nematode *Caenorhabditis elegans* (170). We hypothesized that Pf prophages in *P. aeruginosa* clinical isolates would similarly protect *P. aeruginosa* from predation by *C. elegans*. To test this, we employed *C. elegans* avoidance assays (185-188) as a metric of bacterial fitness when confronted with nematode predation (**Fig. 3-8A**). *C. elegans* avoided all Pf lysogens, preferring to associate with the ΔPf strains in every case (**Fig. 3-8B**). Note that nematode survival was over 95% over the course of the experiment (8 hours) in all experiments (**Fig. 3-8B**, triangles). Collectively, our results suggest that Pf modulates *P. aeruginosa* virulence phenotypes in ways that repel *C. elegans*.

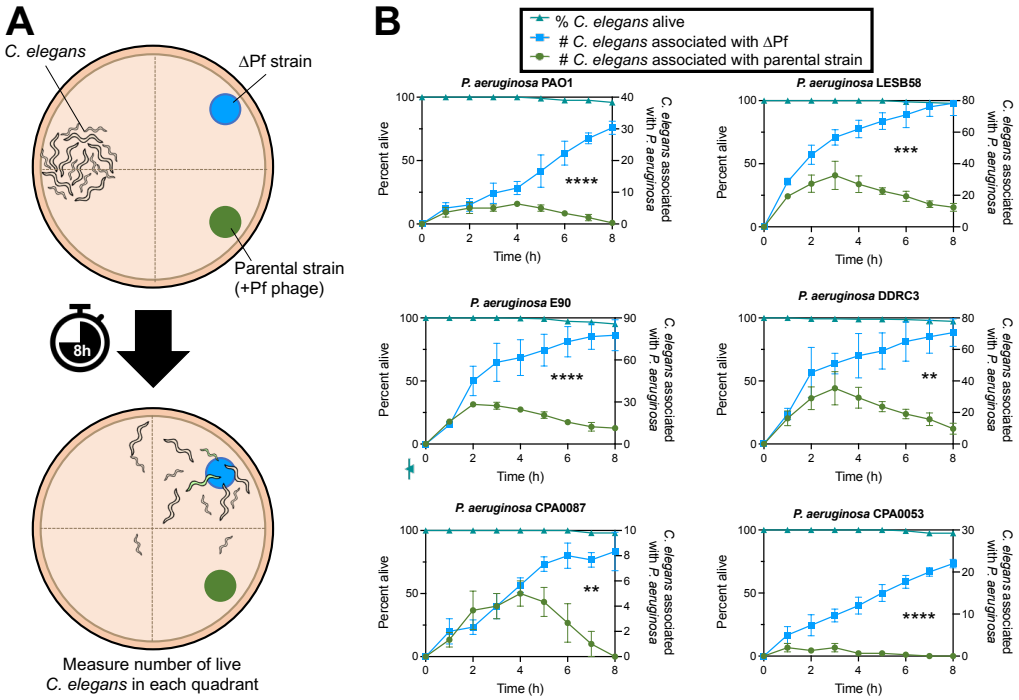

Figure 3- 8. *C. elegans* actively avoids *P. aeruginosa* Pf lysogens. (**A**) Experimental design: *P. aeruginosa* and isogenic ΔPf mutants were spotted on normal nematode growth medium (NNGM) plates with wild-type N2 *C. elegans* at the indicated locations. *C. elegans* localization to the indicated quadrants was measured hourly. (**B**) *C. elegans* association with *P. aeruginosa* (circles) or isogenic ΔPf mutants (squares) in the indicated strain backgrounds was measured hourly over 8 hours (three experiments with $N = 30$ per replicate [90 animals total]). *P* values were calculated by two-way ANOVA (analysis of variance) comparing ΔPf strains with the parental strains using the Šidák correction (95% confidence interval threshold), $^{**}P < 0.01$, $^{***}P < 0.001$, $^{****}P < 0.0001$.

3.4. Discussion

This study describes a convenient method to cure *P. aeruginosa* isolates of their Pf prophage infections and explores relationships between diverse Pf phages and their *P. aeruginosa* hosts. Overall, different Pf isolates exhibit varying effects on host quorum sensing and biofilm formation. One commonality between all Pf isolates examined is their ability to suppress pyocyanin production and repel *C. elegans* away from *P. aeruginosa*, protecting their host from predation.

Our results indicate that PflM maintains Pf in a lysogenic state and that deleting the *pflM* gene induces Pf prophage excision, but not replication. In Pf4, the site-specific tyrosine recombinase IntF4 catalyzes Pf4 prophage integration into and excision from the chromosome while the Pf4 excisionase XisF4 regulates Pf4 prophage

excision by promoting interactions between IntF4 and Pf4 attachment sites as well as inducing the expression of the replication initiation protein PA0727 (3, 168). In response to stimuli such as oxidative stress (189), these coordinated events induce Pf4 prophage excision and initiate episomal replication, allowing Pf4 to complete its lifecycle.

While it is presently not known how PflM maintains Pf lysogeny, it is possible that PflM regulates the IntF recombinase or inhibits the XisF excisionase, causing the Pf prophage to excise from the chromosome without concurrently inducing the replication initiation protein PA0727 (15), thus resulting in Pf prophage excision without initiating episomal Pf replication. Additionally, the DUF5447 domain (pfam17525) encoded by PflM originates from the lysogeny maintenance system of Salmonella phage P22, as pointed out in prior work(41). The DUF5447 domain bears homology to the Mnt repressor, which functions to suppress transcription of the anti-repressor Ant, maintaining the prophage in a dormant state. Taken together, this implicates PflM as a conserved component of a *bona fide* lysogeny maintenance system of Pf.

Our study highlights a role for Pf phages in manipulating *P. aeruginosa* quorum sensing. Pf phages have varying effects on host quorum sensing; broadly, we determine that Pf phage modulate quorum sensing activity and quorum-regulated phenotypes in all bacterial strains tested. These findings imply that different Pf isolates interact with host quorum sensing networks in diverse ways, indicating a complex interplay between Pf phages and host regulatory systems.

Quorum sensing regulates *P. aeruginosa* biofilm formation and Pf4 contributes to biofilm formation in PAO1 (57, 102, 129, 173, 190). Consistently, we find that both Pf4 and Pf6 contribute to PAO1 biofilm formation. Interestingly, the impact of Pf prophage deletion on biofilm formation varies among clinical isolates, which may be related to different quorum sensing hierarchies present in clinical P. *aeruginosa* isolates (38). Alternatively, Pf prophage encode accessory genes that may modulate host quorum sensing systems.

Despite differences in interactions between Pf phages and host quorum sensing, deleting Pf prophages from the host chromosome enhances pyocyanin production in all strains tested except for strain CPA0053, which produces low levels of pyocyanin compared to all other strains tested. As pyocyanin is the terminal signaling molecule in *P. aeruginosa* quorum sensing networks (181), these results suggest this inhibition is the ultimate goal of Pf phages and may be beneficial to Pf phages during active replication. Pyocyanin and other redox-active phenazines are toxic to bacteria; it is possible that stress responses that are induced by pyocyanin-producing *P. aeruginosa* are detrimental to Pf replication.

We recently discovered that Pf phages encode a protein called PfsE (PA0721), that inhibits PQS signaling by binding to the anthranilate-coenzyme A ligase PqsA and that this results in enhanced Pf replication (171). Increase in growth rate of LESB58$^{\Delta Pf}$ could be explained by metabolic burden of phage infection. In strain CPA0087$^{\Delta Pf}$ we observe a dramatic increase in pyocyanin production which can negatively impact bacterial growth. To gain insight into the observed growth defect in CPA0087$^{\Delta Pf}$, we compared sequencing of the prophage mutant to its parental strain confirming that strain CPA0087$^{\Delta Pf}$ possesses no genomic mutations apart from prophage loss. It is possible that the loss of PfsE in the ΔPf strains is responsible for the observed increase in pyocyanin production, however further investigation is required to parse the differential impacts of increased pigment production on bacterial growth.

Pf lysogens induce avoidance behavior by *C. elegans*, which prefers to associate with the ΔPf strains. Strikingly, although strains lacking Pf prophages are less virulent in a nematode infection model and attract *C. elegans* in the model described here, the reduced virulence of ΔPf strains contrasts with their high pyocyanin virulence factor production. This discrepancy may be partly explained by our prior findings that Pf4 suppresses pyocyanin and other bacterial pigment production as a means to avoid detection by innate host immune responses (170) that are regulated by the aryl hydrocarbon receptor (191, 192).

In summary, this research reveals the crucial role of the PflM gene in maintaining Pf lysogeny, demonstrates strain-specific effects on quorum sensing and biofilm formation, reveals the consistent inhibition of pyocyanin production by Pf phages, and suggests a role for Pf phages in protecting *P. aeruginosa* against nematode predation.

3.5. Materials and Methods

3.5.1. Strains, plasmids, primers, and growth conditions

Strains, plasmids, and their sources are listed in **Table 3- 2**. Unless otherwise indicated, bacteria were grown in lysogeny broth (LB) at 37℃ with 230 rpm shaking and supplemented with gentamicin (Sigma) where appropriate, at either 10 or 30 μg ml^{-1}.

Table 3-2. Strains and plasmids used in this study.

Strain	Description	Source
Escherichia coli		
DH5α	Cloning strain	New England Biolabs
S17	Donor strain	(12)
OP50	*C. elegans* food source	PMID 4366476
P. aeruginosa		
PAO1	Wild type	(102)
PAO1 ΔPf4	Deletion of Pf4 prophage from PAO1	This study
PAO1 ΔPf4 ΔPf6	Deletion of Pf4 and Pf6 prophage from PAO1	This study
LES B58	Liverpool Epidemic strain B58	(193)
LES B58 ΔPf	Deletion of Pf prophage from LESB58	This study
CPA0053	CF clinical isolate	Gift from Paul Bollyky, Stanford University
CPA0053 ΔPf	Deletion of Pf prophage from CPA0053	This study
CPA0087	CF clinical isolate	Gift from Paul Bollyky, Stanford University
CPA0087 ΔPf	Deletion of Pf prophage from CPA0087	This study
DDRC3	MDR clinical isolate	Gift from Geetha Kumar, Amrita University
DDRC ΔPf	Deletion of Pf prophage from DDRC3	This study
C. elegans		
N2	Wild type	*Caenorhabditis* Genetic Center
Plasmids		
CP59 pBBR1-MCS5 *rsaL-gfp*	GFP *lasI* transcriptional reporter	(194)
CP57 pBBR1-MCS5 *rhlA-gfp*	GFP *rhlA* transcriptional reporter	(194)
CP53 pBBR1-MCS5 *pqsA-gfp*	GFP *pqsA* transcriptional reporter	(195)
CP1 pBBR-MCS5- Empty	GFP empty vector control	(194)
pHERD30T - *pflM*	Cloning vector with *pflM* insert, GmR	This study
pENTRpEX18-Gm:Δ*PA0718*	Allelic exchange vector for the deletion of *pflM*	(156)
pLM61	pENTR221L1L2-RFqPCRstandard	This study
pUC57-*rplU*	qPCR standard for *rplU*	(196)

Table 3-3. Primers used in this study.

Name	Tm° (C)	Sequence
Construction of pENTRpEX18-Gm:Δ*PA0718*		
Δ*pflM* UP*attB1*-Fwd	62.1	ggggacaagtttgtacaaaaaagcaggcttcCTAATGCCACGAATAGTGACGG
Δ*pflM* UP-Rev	65.3	TCAGCCCTCCAGTTGGAATGCGTAGGGACTGGCGGCCAT
Δ*pflM* DOWN-Fwd	63.2	GCATTCCAACTGGAGGGCTGA
Δ*pflM* DOWN*attB2*-Rev	62.1	ggggaccactttgtacaagaaagctgggtaAAAGTGATTTGTCGGGCGATCC

Δ*pflM* Seq-Fwd	57.5	TTTTTGGGGCCGATTTTCTTG
Δ*pflM* Seq-Rev	56.3	ATTGGACCGAGGCGTGA
Quantitative PCR		
RF-Fwd	60.5	TAGGCATTTCAGGGGCTTGG
RF-Rev	62.5	GAGCTACGGAGTAAGACGCC
rplU-Fwd	52.4	CAAGGTCCGCATCATCAAGTT
rplU-Rev	52.6	GGCCCTGACGCTTCATGT
Prophage Mutant Screening		
16SRNA-F	59.5	TGGTTCAGCAAGTTGGATGTG
16SRNA-R	59.5	GTTTGCTCCCCACGCTTTC
pfsE-F	56.3	ATGCTCCGCTATCTCTCG
pfsE-R	58.4	TCAAACAGCCAGGGAGGC
Excision Assays		
Pf4-Fwd1	62.5	GGATATGGAGCGTGGTGGAG
Pf4-Fwd2	59.9	AGTGGCGGTTATCGGATGAC
Pf4-Rev	61.4	TCATTGGGAGGCGCTTTCAT
Pf6-Fwd1	60.5	GTGATCCACGTGTCCAACAG
Pf6-Fwd2	60.5	CCCAGTGCAGATGACTTGGT
Pf6-Rev	60.5	CGCCACTGGTCATTGATCCT
LES B58-Fwd1	59.8	AGCGACAGCCGCCAGCA
LES B58-Fwd2	61.6	GCTTGCCGAACTGCTGGTG
LES B58-Rev	62.5	CGGGTTTCGTCGGTCATCAC
CPA0053-Fwd1	52.8	GCAGGTCGAGGTAGTAG
CPA0053-Fwd2	60	TTCGTCGCTGAACATGACCA
CPA0053-Rev	51.6	CCTCGATCATGTTGAAGT
CPA0087-Fwd1	52.8	GCAGGTCGAGGTAGTAG
CPA0087-Fwd2	60	TTCGTCGCTGAACATGACCA
CPA0087-Rev	51.6	CCTCGATCATGTTGAAGT
DDRC3*gly*-Fwd1	60.1	GCTTTCTACTCCTGAGCATGTA
DDRC3*gly*-Fwd2	59.8	CGCTGCGGAACACCGTG
DDRC3*gly*-Rev	59.5	ACCGTGAAGTACCTGCAGC

3.5.2. Construction of Deletion Mutants

We used allelic exchange to delete alleles from *P. aeruginosa* (156). Briefly, to delete *pflM* (*PA0718),* upstream and downstream homologous sequences (~500bp) were amplified through PCR from PAO1 genomic DNA using the UP and DOWN primers listed in **Table 3- 3**. These amplicons were then ligated through splicing-by-overlap extension (SOE)-PCR to construct a contiguous deletion allele. This amplicon was then run on a 0.5% agarose gel, gel extracted (*New England Biolabs #T3010L*), and cloned (Gateway, Invitrogen) into a pENTRpEX18-Gm backbone to produce the deletion construct. The deletion construct was then transformed into DH5α, mini-prepped (*New England Biolabs #T1010L*), and sequenced (Plasmidsaurus.com). Sequencing-confirmed vectors were then transformed into *E. coli* S17 Donor cells for biparental mating with the recipient *P. aeruginosa* strain. Single crossovers were isolated on VBMM agar supplemented with 30 µg/mL gentamicin followed by selection of double crossovers on no salt sucrose. The final obtained mutants were confirmed by

excision assay (see below), Sanger sequencing of excision assay products, and whole genome sequencing.

3.5.3. Excision Assays

Excision assays were designed as described previously (197). Briefly, a multiplex PCR assay was designed to produce amplicons of distinct sizes if the Pf prophage was integrated (primers Fwd_1 and Rev produce a smaller band) or excised (primers Fwd_2 and Rev produce a larger band) using Phusion Plus PCR Mastermix (Thermo Scientific # F631L). Primers were used at a final concentration of 0.5μM and are listed in **Table 3- 3**.

3.5.4. Plaque assays

Plaque assays were performed using ΔPf4 as the indicator strain grown on LB plates. Phage in filtered supernatants were serially diluted 10x in PBS and spotted onto lawns of $PAO1^{\Delta Pf4}$. Plaques were imaged after 18h of growth at 37℃. PFUs/mL were then calculated.

3.5.5. Quantitative PCR (qPCR)

Cultures were grown overnight in LB broth with shaking at 37°C. Following 18h incubation, cultures were pelleted at 16,000xg for 5 minutes, washed 3x in 1X PBS, and treated with DNase at a final concentration of 0.1 mg/mL. qPCR was performed using SsoAdvanced Universal SYBR Green Supermix (BioRad #1725270) on the BioRad CFX Duet. For the standard curves, the sequence targeted by the primers were inserted into vectors pLM61 and pUC57-*rplU,* respectively*,* and 10-fold serial dilutions of the standard were used in the qPCR reactions with the appropriate primers (**Table 3- 3**). Normalization to chromosomal copy number was performed as previously described (196) using 50S ribosomal protein gene *rpIU*.

3.5.6. Pyocyanin extraction and measurement

Pyocyanin was measured as previously described (41, 198). Briefly, 18-hour cultures were treated with chloroform at 50% vol/vol. Samples were vortexed vigorously and the organic phase separated by centrifuging samples at 6,000xg for 5 minutes. The chloroform layer was removed to a fresh tube and 20% the volume of 0.1 N HCl was added and the mixture vortexed vigorously. Once separated, the aqueous fraction was aliquoted to a 96-well plate and absorbance measured at 520 nm. The concentration of pyocyanin, expressed as μg/ml, was obtained by multiplying the OD_{520} nm by 17.072, as described previously (198).

3.5.7. Quorum sensing reporters

Competent *P. aeruginosa* cells were prepared by washing overnight cultures in 300 mM sucrose followed by transformation by electroporation (199) with the plasmids CP1 PBBR-MCS5 *Empty*, CP53 PBBR1-MCS5 *pqsA-gfp*, CP57 PBBR1-MCS5 *rhlA-gfp*, CP59 PBBR1-MCS5 *rsaL-gfp* listed in **Table 3- 2**. Transformants were selected by plating on the appropriate antibiotic selection media. The indicated strains were grown in buffered LB containing 50 mM MOPS and 100 μg ml^{-1} gentamicin for 18 hours. Cultures were then sub-cultured 1:100 into fresh LB MOPS buffer and grown to an OD_{600} of 0.3. To measure reporter fluorescence, each strain was added to a 96-well plate containing 200 μL LB MOPS with a final bacterial density of OD_{600} 0.1 and incubated at 37℃ in a CLARIOstar BMG LABTECH plate reader. Prior to each measurement, plates were shaken at 230 rpm for a duration of two minutes. A measurement was taken every 15 minutes for both growth (OD_{600}) or fluorescence (excitation at 485–15 nm and emission at 535–15 nm). End-point measurements at 18h were normalized to cell density.

3.5.8. *C. elegans* Growth Conditions

Synchronized adult N2 *C. elegans* were propagated on Normal Nematode Growth Medium (NNGM) agar plates with *E. coli* OP50 as a food source.

3.5.9. *C. elegans* Avoidance Assays

C. elegans avoidance assays were performed as previously described (187). Briefly, synchronized adult N2 worms were propagated at 24°C on 3.5 cm NNGM agar plates with *E. coli* OP50 for 48h, collected, and washed 4x to remove residual OP50. NNGM agar was spotted with 20 μL of *P. aeruginosa* (Pf lysogens and their isogenic ΔPf mutant) overnight cultures (LB broth) as shown in Fig 7A and grown for 18 hours at 37°C. Worms were plated in in triplicate and incubated at 24°C. *C. elegans* migration was monitored hourly for 8h.

3.5.10. Whole Genome Sequencing & Annotation

DNA extraction was performed using NEB Monarch gDNA isolation kits (NEB #T3010). Whole genome sequencing was performed by Plasmidsaurus using an Oxford Nanopore GridION device and corresponding flow-cells to >30x coverage. Reads were filtered using Filtlong (v0.2.1), assembled using Flye (v2.9.1) and/or Velvet (v7.0.4). Contigs polished using Medaka (v1.8.0), and annotated using Bakta (v1.6.1), Bandage (v0.8.1), and RAST (https://rast.nmpdr.org/). Domain analysis was performed using PfamScan (https://www.ebi.ac.uk/Tools/pfa/pfamscan/) against the library of Pfam HMM using an e-value cutoff of 0.01. Supporting domain models were obtained from Conserved Domain Database, and Defense Finder (200). Raw

sequencing reads and assemblies for parental strains introduced in this study (**Table 3- 2.**) have been deposited as part of BioProject PRJNA1031220 in the NCBI SRA database.

3.5.11. Statistical analyses

Differences between data sets were evaluated with a Student's *t*-test (unpaired, two-tailed), or two-way ANOVA using the Šidák correction (95% CI threshold) where appropriate. P values of < 0.05 were considered statistically significant. GraphPad Prism version 9.4.1 (GraphPad Software, San Diego, CA) was used for all analyses.

3.6. Acknowledgements

This work was supported by NIH grants R01AI138981 and P20GM103546 to PRS. DRF was supported by NSF GRFP grant 366502. The funders had no role in study design, data collection and analysis, decision to publish, or preparation of the manuscript. The authors report no conflicts of interest.

CHAPTER FOUR Pf phage function as elements of bacterial pan-immune systems

Unpublished work.

Amelia K. Schmidt[1]

[1]Division of Biological Sciences, University of Montana, Missoula, Montana, USA

4.1. Introduction

Bacterial interactions with bacteriophages, viruses which infect bacteria, affect antibiotic sensitivity, virulence phenotypes, and ultimately, infectious disease outcomes. Bacterial defense against bacteriophages, commonly referred to as phages, is reliant on the presence of the appropriate phage defense system. Because ineffective defense against virulent phage results in bacterial cell death, phage defense systems are subject to strong selection (151, 201). Phages are the most diverse biological entity on the planet; most anti-phage defense systems only protect against specific phage types. It is untenable for bacteria to harbor enough systems to defend against all phage threats. Natural selection of bacteria capable of surviving phage threats favors constant genetic recombination of diverse defense systems between closely related bacterial strains. This defense-sharing, which relies on mobilization of defense genes, was recently termed 'bacterial pan-immunity' (202) and enables rapid reassortment of mechanisms to respond to specific but ever-changing threats.

4.1.1. Filamentous Inoviruses influence *P. aeruginosa* pathogenesis

Filamentous Inoviruses infecting the opportunistic bacterial pathogen *Pseudomonas aeruginosa* are called Pf phages. Pf phages are central to the arsenal *P. aeruginosa* leverages in combat with the stresses of infecting mammalian hosts. Pf phages chronically infect 60-80% of *P. aeruginosa* clinical isolates (17, 64, 168). It is well established that Pf phages enhance *P. aeruginosa* fitness and resistance stresses exerted on the cell in contexts relevant to human infection.

Induction of Pf replication and virion production has been demonstrated to occur in *P. aeruginosa* infected lungs and wounds in both humans and murine models (57, 99). Presence of Pf in sputum is correlated with antibiotic resistance of *P. aeruginosa* in cystic fibrosis airway infections (99). Pf phages influence bacterial pathogenesis by promoting colonization (127) and biofilm formation (57), and inhibiting immune cell phagocytic uptake (105, 127). The presence of Pf enhances the virulence potential of *P. aeruginosa* in murine lung (102) and wound (105) infection models and a nematode infection model (170).

4.1.2. Filamentous Inoviruses and bacterial phage defense

Filamentous Inovirus prophages, such as Pf, are found integrated into genomes of a wide range of bacteria and even some Archaea (133). These viruses encode a variety of phage defense systems, toxin-antitoxin modules, and numerous genes of unknown function, some of which may benefit the bacterial host under stressful conditions beyond phage infection. When induced, filamentous Inovirus virions are extruded from the host cell without causing cell death (17), making them an effective vehicle for the horizontal dissemination of diverse defense systems among closely related bacterial populations.

4.1.3. Pf phages as elements of a *P. aeruginosa* pan-immune system

The role of mobile genetic elements (MGEs) in the evolution of bacterial pathogens is well established (203). MGEs encode antibiotic resistance genes, toxins, and cooperative genes (204, 205). MGEs also readily harbor 'defense islands' which are localized hot-spots of phage defense genes (206) (**Figure 4- 1**). Phage resistance can result from mutation to a cell surface receptor or bacterial expression of an endogenous defense system, such as a restriction modification system, toxin-antitoxin system, CRISPR-Cas9, or any of the new phage defense systems recently identified (202, 206-210). Pf phages encode highly diverse accessory genes, called morons because they add more-on, which flank genes within their highly conserved 'core' genome [genes *PA0716.1-PA0728]* (41). Many Pf morons are predicted to be involved in bacterial phage defense (**Figure 4- 2**).

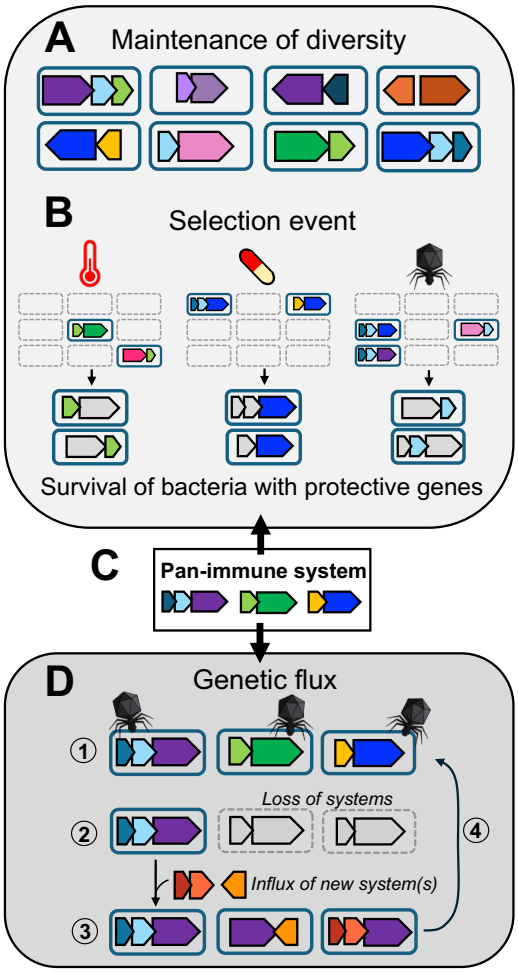

Figure 4- 1: Depiction of the bacterial pan-immune system whereby genetic flux of mobile elements serve as a community resource. (A) Within a community of microorganisms, closely related *P. aeruginosa* strains possess diverse Pf phage encoding diverse anti-phage defenses and antibiotic resistance genes— this is the maintained diversity present in the pan-immune system. **(B)** A selection event such as introduction of an antibiotic or phage infection result in a bottleneck where bacterial species which harbor Pf phage(s) encoding advantageous genes overcome the event and survive. **(C)** Members of the population can acquire advantageous genes mobilized by Pf phage. **(D)** By design, the pan-immune system is always in flux. Selective events, such as phage infection (D, 1) can reduce population diversity, but members encoding a specific defense system [light blue] survive (D, 2). However, new systems can be acquired through HGT via Pf infection, and recombine with existing Pf-encoded systems to create novel defenses (D, 3). The cycle repeats (D, 4). *Figure adapted from Bernheim & Sorek (2020).*

Filamentous Inoviruses, like Pf, are pervasive across earths biomes (133). A role for Inoviruses as mediators of bacterial immunity could explain their wide distribution. Filamentous Inovirus virions are composed of repeating subunits which enable them to accommodate genomes of varied size, which are extruded from the bacterial cell without killing it (17). Importantly, a fundamental

requirement bacterial pan-immune elements is that they need to be able to spread and fluctuate in dominance in response to specific but ever-changing threats (202). Taken together, Inoviruses like Pf are an ideal vehicle of horizontal dissemination for diverse defense systems amongst populations of related bacteria like *P. aeruginosa*.

4.2. Preliminary Results

4.2.1 Identification of Pf Prophages in *P. aeruginosa* Clinical Isolate Genomes

Clinical isolate strains used in Trial v01 (**Table 4- 2**, **Table 4- 4**) were a gift of the Bollyky Lab (Stanford University) and were sequenced by Felix Biotech using PacBio short-read sequencing. With this dataset, we observed that many assemblers struggled to produce complete contigs containing prophage sequences, and speculated that the attachment (*att*) sites, composed of~20 bp which repeat on either side of the prophage contributed to their limitation. To address this challenge, we developed a new prophage identification and trimming methodology and generated used it to produce a dataset of assemblies with complete prophage sequences (see Methods 4.5.4). Briefly, raw reads were reassembled using Trycycler (211, 212), which utilizes the assemblers minimap2, Raven, Velvet, and Flye. Assemblies were then visually assessed and manually curated in Bandage, polished using Medaka, and annotated using Bakta and RAST (*https://rast.nmpdr.org/*).

Clinical isolate strains used in Trial v02 were a combination of strains from Trial v01 (**Table 4-4**), new sequenced clinical isolates from the Bollyky Lab (**Table 4- 5**), and unsequenced clinical isolate strains generously gifted to us by Prof. Geetha Kumar of Amrita University (**Table 4- 3**).

4.2.1.1. Trimming Identified Pf Sequences

Identified prophages were trimmed in R studio (*v. 2023.12.1+402*) using either characterized attachment (*att*) sites or by detecting repeating sequences ~20bp in length which flank the core genome. R code available in Methods 4.5.5.

The location of novel *att* sites required validation through alignment of contigs to the established Pf 'core' genome which spans from the repressor gene (*pfR*) to the initiation protein (IP) encoded by gene *PA0727*. Validated *att* sites yielded a prophage genome of ~12kb. Domain analysis of trimmed prophage sequences was performed using PfamScan against the library of Pfam HMM using an e-value cutoff of 0.01. Supporting domain models were obtained from Conserved Domain Database, and Defense Finder (200). Trimmed prophage sequences were concatemerized with *N-1000-N* spacers and reads from Trial v01 were mapped back to the prophage concatemers.

4.2.2 Characterization of Pf Accessory Genes

A recent publication examines the prevalence phage defense systems within defense islands harbored by *P. aeruginosa* and finds that RM systems are present in >70% of isolates, followed by CRISPR-Cas (35%), CBASS (16%), and Gabija (10%) (213). Three of the four defense islands identified by Johnson *et al.* are proximal to mobile elements such as transposons and prophage. Based on these observations, we hypothesized that Pf phage sequences from our clinical isolate pool would harbor diverse accessory genes flanking the 'core' Pf genome. Analysis of nearly 200 clinical isolate *P. aeruginosa* sequences with Padloc, and domain annotation as previously described, revealed that 58% of Pf phages harbor putative phage defense accessory genes (**Figure 4-2**, **Table 4- 4**, **Table 4- 5**).

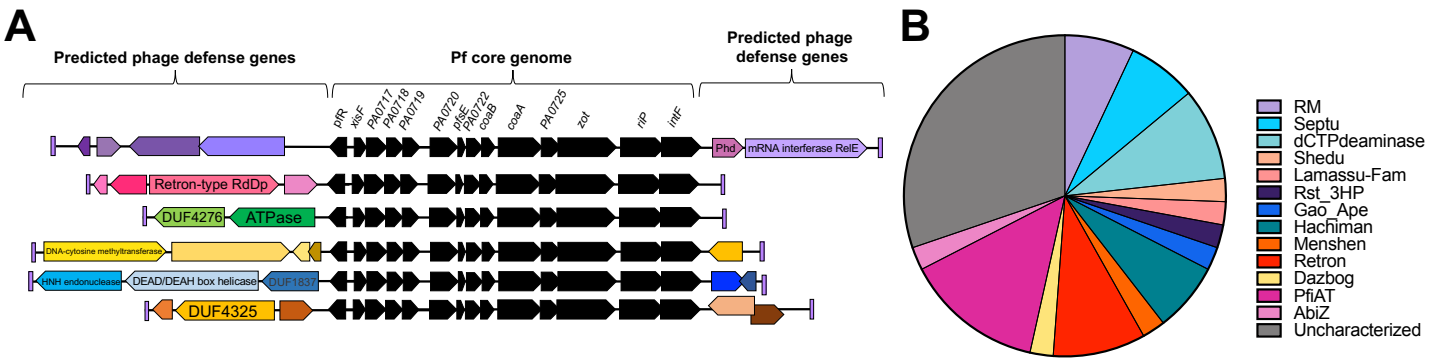

Figure 4- 2. Pf phages in the clinical isolate population encode diverse defense systems. (A) Pf phages have a conserved core genome and highly variable 5' and 3' ends, called morons. Six representative Pf genomes are shown. **(B)** Defined defense systems were identified using Padloc for 138 Pf phages that infect *P. aeruginosa* clinical isolates. Nineteen out of 138 are defined; most are uncharacterized.

4.2.3 Pan-immune Trials

4.2.3.1. Trial v01

To determine if exchange of phage or phage accessory genes (morons) occurs between susceptible hosts we constructed a phage-free recipient strain (PAO1$_{\Delta Pf4/Pf6}$::pUC18-miniTn7Gm-*gfp*) harboring a resistance cassette to gentamycin. We tested all prophage-positive clinical isolate strains, as determined in 4.2.1, for resistance to gentamycin at 30 μg/ml^{-1}. Susceptible strains (**Table 4- 2**) were individually propagated overnight, cells were pelleted, washed to remove any exogenous phage particles, and resuspended in an LB Glycerol solution. Resuspended cultures were combined in equal volume (**Figure 4- 3A**) and immediately aliquoted and frozen (-80ºC) to prevent competition. For each following experiment, tubes were thawed in biological triplicate,

revived in LB for 30 minutes, and then combined at a 1:3 ratio with the recipient strain (PAO1$_{\Delta Pf4/Pf6}$::pUC18-miniTn7Gm-*gfp*) at OD_{600} 0.2 (**Figure 4- 3A**).

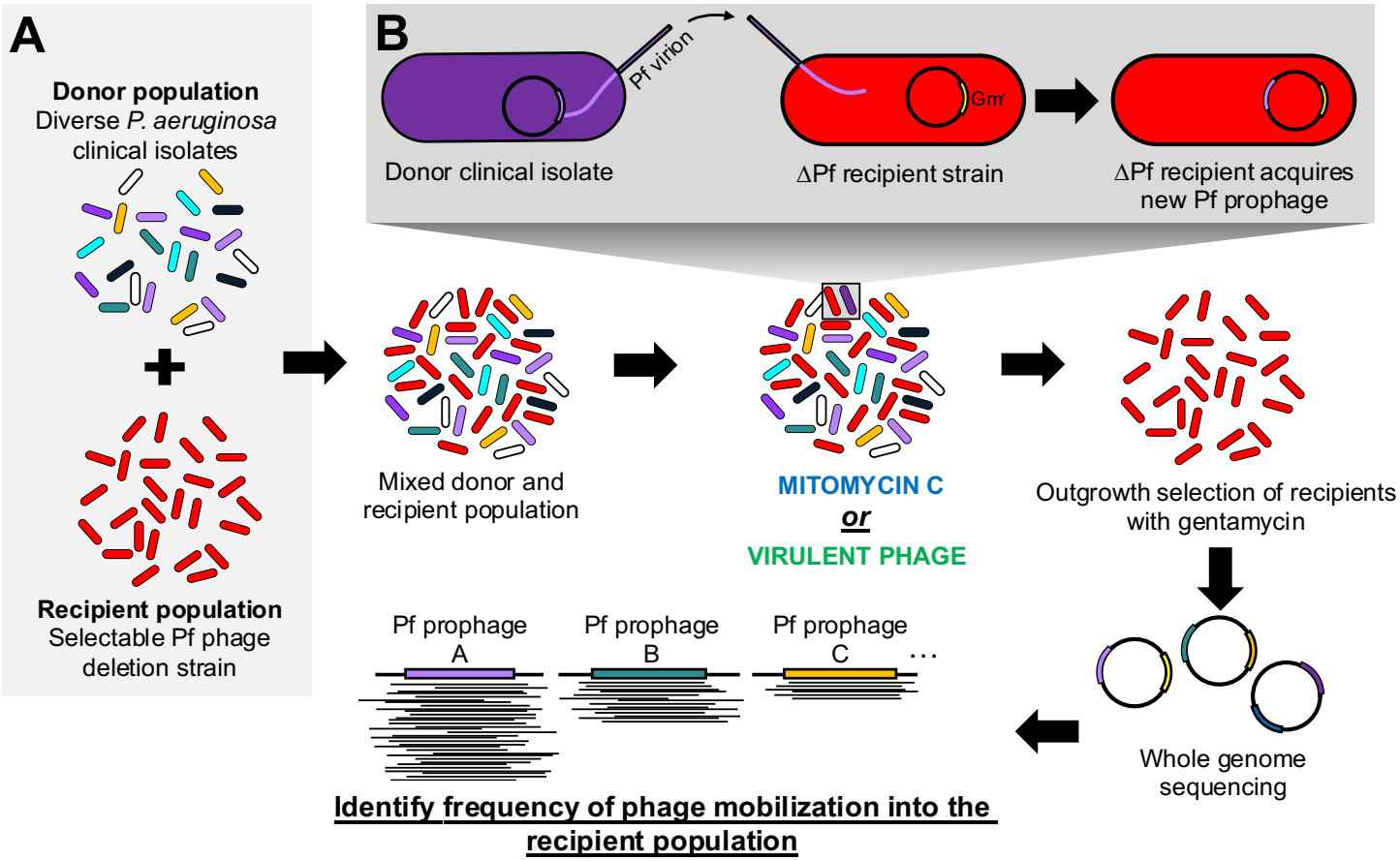

Figure 4- 3. Experimental design employed to assess transmission of Pf phage from donor clinical isolates into a recipient population. (A) Donor population, composed of 200 diverse clinical isolates isolated from chronic wounds, non-Cystic Fibrosis (CF) and CF lung infections, and medical hardware were pooled and combined with recipient population PAO1 ΔPf4ΔPf6-miniTn7TGmR::*gfp* and cocultured for 18h at 37ºC with agitation. **(B)** This experimental design aims to prompt prophage excision, replication, and resulting in infection of the recipient strain. Subsequent gDNA extraction, sequencing, and analysis of long-read Whole-Genome Sequencing (Oxford Nanopore) by alignment to concatemer of Pf phages originating form sequenced donor population allows for the assessment of Pf phage transmission.

A well-established method of prophage induction uses sub-inhibitory concentrations of mitomycin C to exert genotoxic stress through crosslinking of DNA. Mitomycin C induces prophage production in many bacterial pathogens, including *P. aeruginosa* (214, 215). First, we sought to determine if prophages mobilize from clinical isolates into the recipient strain, PAO1$_{\Delta Pf4/Pf6}$::pUC18-miniTn7Gm-*gfp.* To this end, the mixed donor/recipient population were incubated with a sub-inhibitory concentration of mitomycin C overnight. Gentamycin was then added to select for recipient cells, and recipient cells were recovered for ~4h, at which time cells were pelleted, washed, and gDNA was extracted. A DNA sequencing library was prepared according to Oxford Nanopore Technologies recommendation for use with Native Barcoding Kit (*v10.4 chemistry*) and sequenced on a MinION device. Resulting long reads were basecalled and demultiplexed via Guppy, filtered for QC with Filtlong, and reads were mapped to a concatemer of all known prophages within the 'donor' pool (**Table 4- 2**, **Table 4- 4**).

As anticipated, addition of mitomycin C increases the diversity of prophages mobilized from the donor clinical isolate population into the prophage-free recipient strain 10-fold in comparison to the LB control (**Figure 4- 4A/B**). Next, we sought to characterize the impact of exogenous polyamines, a recently identified lysis danger signal, on prophage mobilization (216). The polyamine putrescine is a four-carbon alkane-α,ω-diamine and is a fundamental metabolite for all life (217). When cells lyse, vast quantities of polyamine are released (218, 219). The subsequent import of putrescine into neighboring *P. aeruginosa* cells modulates quorum sensing through the Gac-Rsm pathway and is hypothesized to increase phage-tolerance response (216). We find that putrescine at 50mM is sufficient to increase diversity of prophage mobilized into the recipient strain (**Figure 4- 4C**). We noted that the Pf phages mobilized collectively encode at least 138 phage defense systems, only 19 of which are defined (**Table 4- 4**).

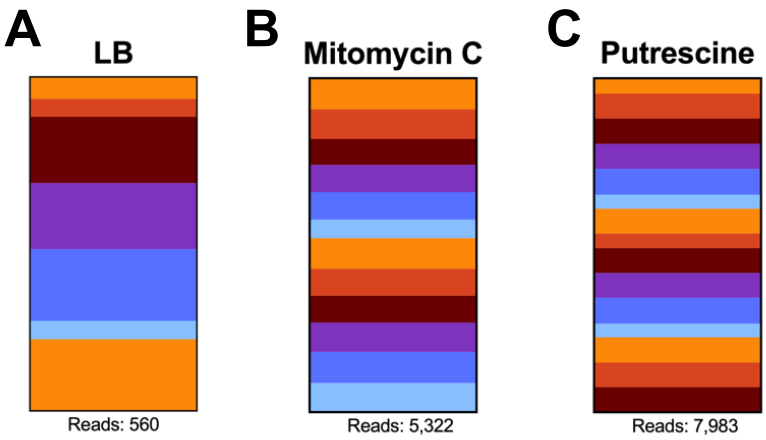

Figure 4- 4. Mitomycin C and exogenous polyamines increase phage mobilized from clinical isolates. (A) Recipient ($PAO1_{\Delta Pf4/Pf6}$-miniTn7TGmR::GFP) and donor (clinical isolate pools) populations were co-incubated in LB as a control for basal level of Pf mobility. **(B)** Donor and recipient (as in Figure 4- 4A) populations were co-incubated in LB with the addition of mitomycin C at 2 $\mu g/ml^{-1}$ overnight (18h). Recipient population was selected for with the addition gentamycin to a final concentration of 30 $\mu g/ml^{-1}$. Sequencing library was prepared with ONT SQK-NBK114 and performed on a MinION flow cell. Resulting reads were mapped to a concatemer of known prophage sequences from the donor population, and % reads per phage was calculated. **(C)** The same methodology was followed, and putrescine was added at a 50mM final concentration. Resulting reads were analyzed as previously described. *Colors represent distinct phage genome.*

Based on these observations we hypothesized that stress stimuli, such as virulent phage predation, would reduce overall diversity surviving cells and the prophages they harbor. We anticipated that prophages which provide a protective advantage against virulent phages would predominate in the surviving population. Phages which encode phage defense genes, as we observed many prophages within our donor population do (**Figure 4-2**), would then propagate, and spread through the recipient population, allowing for host survival.

To test this, purified lytic phages CMS1 or DMS3*vir* were added to the donor/recipient population at a multiplicity of infection (MOI) of 1. Our findings indicate that when *P. aeruginosa* is challenged with virulent phage Pf phages encoding specific defense systems replicate and are horizontally transmitted throughout the bacterial population, protecting the host from lysis (**Figure 4-5**).

4.2.3.2. Trial v02

Prior work and Trial v01 establish that subinhibitory concentrations of mitomycin C induce the bacterial SOS-response which activates Pf production (**Figure 4- 4B**) (220). To determine if Pf phages function to mobilize and spread advantageous genes through bacterial populations, we sought to create a pan-immune population comprised of the PAO1$_{\Delta Pf4/Pf6}$::pUC18-miniTn7Gm-*gfp* recipient-strain harboring diverse prophages obtained from clinical isolates. Illustrated by the innate promiscuity and diversity of prophages from clinical isolates in Trial v01 (**Figure 4- 4A/B**), construction of this background would enable us to examine the function of Pf phages as pan-immune elements in a controlled experimental setting.

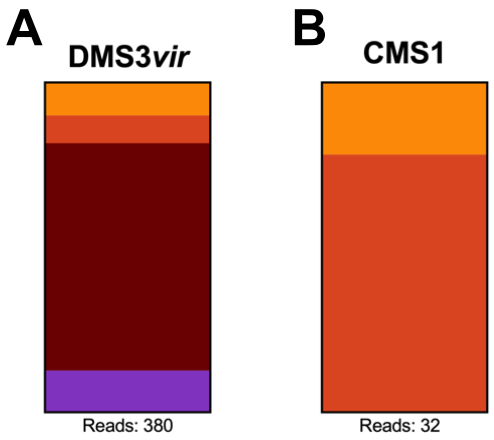

Figure 4- 5. Virulent phage predation reduces diversity of surviving recipient strains harboring prophages mobilized from clinical isolates. (A) Recipient (PAO1$_{\Delta Pf4/Pf6}$-miniTn7TGmR::GFP) and donor (clinical isolate pools) populations were co-incubated in LB. At OD600 0.2, purified virions of virulent phage DMS3*vir* was added at a multiplicity of infection (MOI) of 1 and incubated overnight (18h). Recipient population was selected for with the addition gentamycin to a final concentration of 30 μg ml^{-1}. Sequencing library was prepared with ONT SQK-NBK114 and performed on a MinION flow cell. Resulting reads were mapped to a concatemer of known prophage sequences from the donor population, and % reads per phage was calculated. **(B)** The same methodology as previously stated was followed. Purified CMS1 virions were added at an MOI of 1 and incubated overnight (18h).
Colors represent distinct phage genome.

To achieve this, we replicated the methodology outlined in Trial v01 (**Figure 4- 6**). Briefly, we subcultured overnights of the recipient strain, and at OD_{600} 0.2 combined it with the revived clinical isolate pools (**Table 4- 4**, **Table 4- 5**). We leveraged mitomycin C to induce prophage production and following overnight incubation selected for recipient cells with addition of gentamycin. Recipient cells were recovered, pelleted, washed, resuspended in LB Glycerol, aliquoted, and immediately placed at -80ºC for future use. gDNA was extracted and a DNA sequencing library was prepared using native barcodes to identify three biological replicates. The DNA library was sequenced on a MinION device, and sequencing data was basecalled with Epi2Me, reads were demultiplexed and trimmed with Porechop, and prophage reads were identified (**Figure 4- 6B**).

We began selection experiments in a growth curve format so we could monitor the recovery of cells allowing us to strike the delicate balance between enough selective pressure and too much. First, we tested virulent phages DMS3*vir* and CMS1. DMS3*vir* is a Type IV pili (T4P) dependent filamentous phage (221). CMS1 has an uncharacterized cell-surface receptor hypothesized to be LPS as it is capable of infecting PAO1$^{\Delta PilA}$ (222). While the recipient strain backbone (PAO1$_{\Delta Pf4/Pf6}$::pUC18-miniTn7Gm-*gfp*) was susceptible to both phages at a

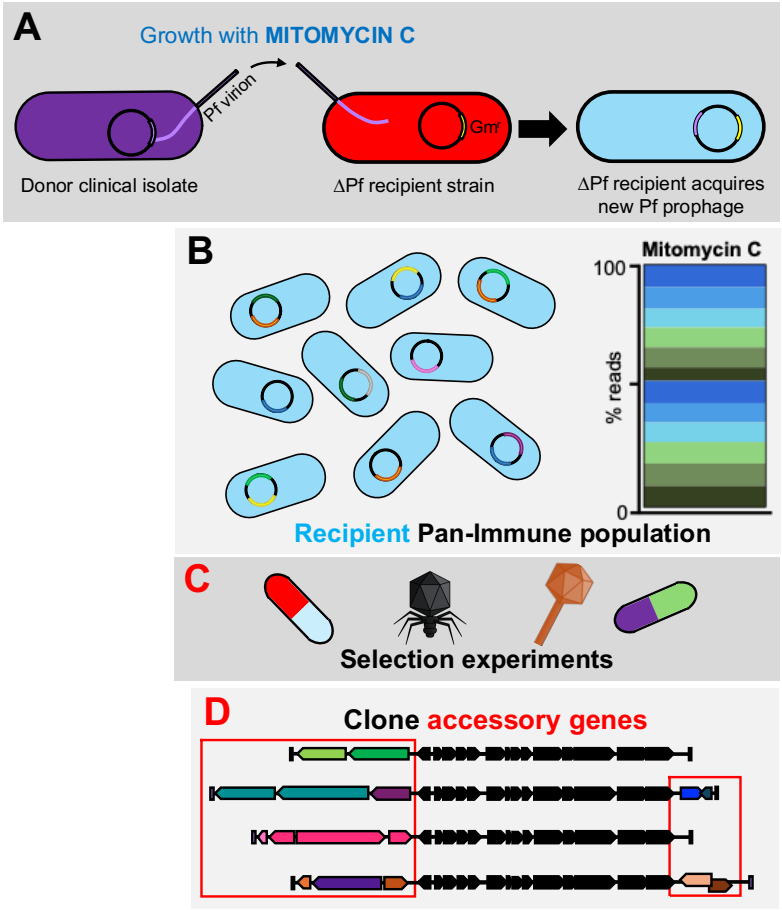

Figure 4- 6. Generation of a pan-immune population allows for streamlined examination of selection outcomes. (A) Overnight cultures of the recipient strain (PAO1$_{\Delta Pf4/Pf6}$-miniTn7TGmR*::gfp)* were subcultured into fresh media and incubated until an OD_{600} 0.2 was reached. Donor strain pools (Table 4- 4, Table 4- 5) were thawed from -80ºC, resuspended in LB (3mL) and revived for 30min at 37ºC with agitation. Recipient subcultures were combined it with the revived clinical isolate pools in a 3:1 ratio and mitomycin C was added (2 µg ml^{-1}) to induce prophage production. Following overnight co-incubation, recipient cells were selected for with the addition of gentamycin (30 µg ml^{-1}). Recipient cells were recovered for ~4h, pelleted, washed 3x in 1XPBS. Genomic DNA was extracted (NEB Monarch), a DNA sequencing library was prepared (ONT SQK-NBK114.24) using native barcodes to identify three biological replicates. **(B)** Library was subsequently sequenced on a MinION device, sequencing data was basecalled in Epi2Me, reads were demultiplexed and trimmed with Porechop (v0.2.4), and prophage reads were identified. *All experiments performed in biological triplicate.* ***Panels C and D remain untested.***

multiplicity of infection (MOI) of 0.5, the pan-immune strain was resistant to both phages at MOIs of 0.5, 1, and 50 (**Figure 4- 7B/C, Figure S4- 1, A-D**).

Next we tested susceptibility of the recipient strain and the pan-immune population to clinically relevant antibiotics ciprofloxacin and rifampin, often used in combination to *P. aeruginosa* infections (223). Ciprofloxacin, a fluoroquinolone, functions to inhibit bacterial replication through binding and inhibition of DNA gyrase and topoisomerase IV which are enzymes required for transcription, translation, DNA repair and recombination (224). Without function of these enzymes, bacterial DNA damage leads to induction of SOS response which we hypothesized would likely induce prophage harbored by our recipient strain. The model strain *P. aeruginosa* PAO1 is not intrinsically resistant to ciprofloxacin. At concentrations spanning 10-40 µg/ml^{-1} the pan-immune population was resistant to ciprofloxacin (**Figure 4- 7D, Figure S4- 1E/F**).

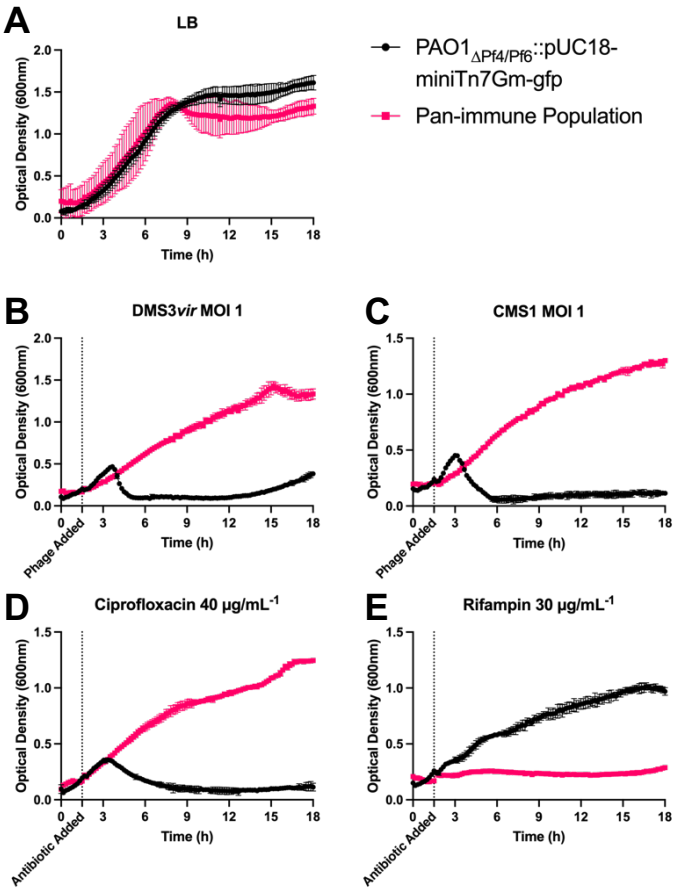

Figure 4- 7. Trial v02 pan-immune population tolerant to ciprofloxacin, rifampin, and virulent phages DMS3*vir* and CMS1. (A) Overnight cultures of the indicated *P. aeruginosa* strains were diluted with LB to an OD_{600} of 0.05. Growth curves over 18h are shown. OD_{600} was measured in a CLARIOstar (BMG Labtech) plate reader at 37ºC with shaking prior to each measurement. Cells were infected with virulent phage DMS3*vir* **(B)** or CMS1 **(C)** an OD_{600} of 0.2 1.5h post-inoculation (dotted line) at a MOI of 1. Antibiotics ciprofloxacin **(D)** or rifampin **(E)** were added to the indicated final concentration at an OD_{600} of 0.2, 1.5h post-inoculation (dotted line). Results are mean ± SD of three experiments.

Rifampin, sometimes referred to as rifampicin, inhibits initial RNA chain formation by targeting bacterial DNA-dependent RNA polymerase (DdRp) (225). The most common mechanism of bacterial resistance to rifampin is mutation of to the ß subunit of DdRp (223). Surprisingly, the pan-immune population was susceptible to rifampin at 7.5-30 µg/ml^{-1} however the backbone recipient strain was not (**Figure 4- 7E, Figure S4- 1G/H**).

These observations indicate that the pan-immune background bore significant differences to the parental prophage-free recipient strain, which was susceptible phages DMS3vir and CMS1, and ciprofloxacin (**Figure 4- 7, B-D**). Indeed, alignment of sequencing reads to the parental backbone revealed two large chromosomal deletions encompassing nearly 20kb (**Figure 4- 8**).

The two regions of genomic deletion are referred to hereafter as Gap A and Gap B (**Figure 4-8**). Gap A begins with truncation of the gene *hsdM*, a type I HsdM methyltransferase (226), followed by two transcriptional regulators (**Figure 4- 8**). The transcriptional activator encoded by gene *soxR* is redox-sensitive and is activated by pyocyanin (227). Interestingly, the deletion of SoxR in strain PAO1 has been demonstrated to have no impact on oxidative stress response, and SoxR appears to exert positive regulation on the efflux pump-encoding operon mexGHI-opmD (227). However SoxR deletion has been reported to have no impact on resistance of strain PAO1 to antibiotics[4] (227). Gene *ihfA* encodes an integration host factor gene (228). The last gene impacted by the chromosomal deletion Gap A is a 5' truncation of gene *pheT* which encodes the phenylalanine tRNA ligase (PheT) subunit β. PheT is essential in *P. aeruginosa* PAO1 and broadly conserved (229). While assessing the genes deleted in Gap A, we noted that many of them were involved in translation. Encouragingly, genes *soxR*, *pheT,* and *ihfA* were

[4] The relevant data in the cited paper is not shown, and it is unclear in which antibiotics were tested to contrast PAO1 with PAO1$^{\Delta soxR}$.

recently shown to frequently associate with anti-phage defense hot-spots (defense islands) in the *P. aeruginosa* chromosome (213). This finding suggests that the Gap A deletion could be the biproduct of robust predation by the phages produced by the clinical isolate pools.

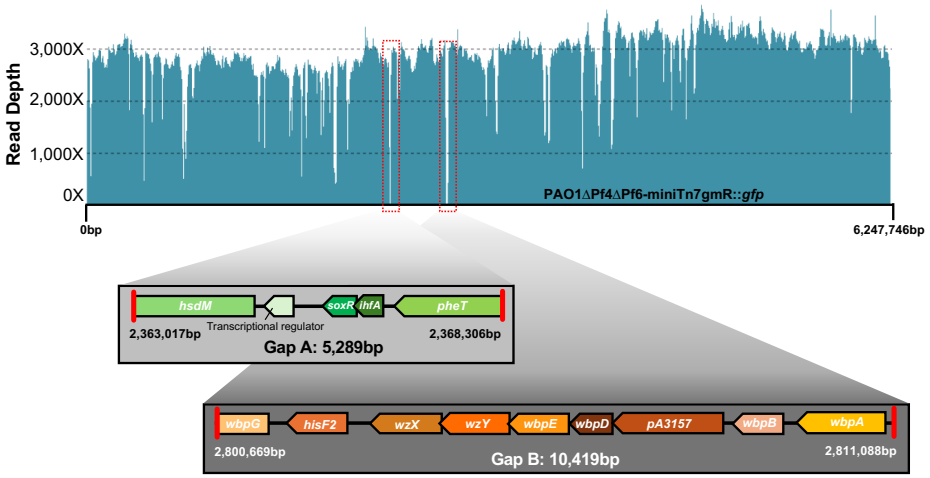

Figure 4- 8. Trial v02 sequencing reads mapped to pan-immune population backbone. Sequencing (PAO1ΔPf4ΔPf6-miniTn7::GFPgmR). Cells were recovered for ~4h, pelleted at 12,000xg for 2min, and washed 3x in 1XPBS. gDNA was extracted (NEB Monarch), and a DNA sequencing library was prepared (ONT SQK-NBK114.24) using native barcodes to identify three biological replicates. Library was subsequently sequenced on a MinION device. Sequencing data was basecalled in Epi2Me and reads were demultiplexed and trimmed with Porechop (*v0.2.4*). Reads were filtered for read quality with Filtlong (*v.0.2.1*) with parameters for minimum read length set to 1000 and keep precent set to 90. Filtered reads were mapped to the pan-immune backbone (PAO1ΔPf4ΔPf6-miniTn7::GFPgmR) in Epi2Me.

The second chromosomal deletion we observed encompasses genes *wbpA*, *wbpB*, *pA3157*, *wbpE*, *wzy*, *wzx*, *hisF2*, and *wbpG* which is truncated at its 3' end (**Figure 4- 8**). As a Gram- negative bacterium, *P. aeruginosa* has an outer membrane composed of lipopolysaccharide (LPS). LPS is organized into three discrete regions: lipid A, the core oligosaccharide, and the O-antigen. Lipid A is highly immunogenic and often serves as the pathogen-associated molecular pattern which mammalian innate immune systems recognize (230). The outermost layer, the O-antigen, can be further divided into the A-band and the B-band. The A-band is the common polysaccharide antigen comprised of a repeating tri-saccharide of –D– rhamnose. The B-band is serotype-specific and highly variable contributing to immune evasion. In *P. aeruginosa* serotype O5, the serotype of model strain PAO1, the B-band LPS gene cluster is encoded by genes *wzy*, *wzx*, *wbpA-wbpN, hisH*, *hisF*, and *uvrB* (231).

Genes *wbpA* and *wbpB* encode enzymes that are essential for biosynthesis of the unusual di-N-acetyl-d-mannosaminuronic acid-derived sugar nucleotides which form the B-band of serotype O5 (232). The function of WbpB relies on the enzyme produced by *wbpE,* a transaminase, to complete its coupled enzyme-substrate reaction (233). The substrate produced by WbpE is the precursor for the reaction catalyzed by WbpD, an N-acetyltransferase enzyme (233). Genes *wzy* and *wzx* encode an O-antigen polymerase and an O-antigen flippase, respectively. Wzy facilitates polymerization of the repeating sugar units into a long chain, forming the mature O-antigen while Wzx is responsible for the transport of the newly synthesized O-antigen across the inner membrane (234).

Modification of the B-band through *wzy* mutation has been shown to occur as a resistance mechanism to virulent phages (235). Although B-band modification can change the permeability of the outer membrane

rendering some antibiotics ineffective, it is more likely that the deletions within Gap A are responsible for rendering the pan-immune strain resistant to ciprofloxacin through upregulation of the Mex efflux pump (236). We concluded that these large deletions were the cause of the antibiotic and phage resistance we observed and were the result of predation by virulent phages produced by the strains within the clinical isolate pool.

4.2.3.3. Suggested Methodology for Trial v03

Trial v02 revealed that clinical isolates within our donor pool produced far more phage than anticipated. Although we identified filamentous Inovirus sequences (Pf) in our sequencing data, it is likely that more virulent phages are also being induced by genotoxic stress and polyamines.

To control for this, we modified our approach whereby induction of clinical isolate pools is undertaken separately from infection of recipient strain (PAO1$_{\Delta Pf4/Pf6}$::pUC18-miniTn7Gm-*gfp*) (**Figure 4- 9 A/B**). As Pf phages use Type IV Pili (T4P) as a cell-surface receptor, adsorption of T4P-independent phages to PAO1$^{\Delta pilA}$ selects for Pf (**Figure 4- 9D**). Virions are then purified to remove any residual mitomycin C and polyamine, as well as other potentially harmful molecules (**Figure 4- 9F**). Between each step titers are monitored with qPCR of highly conserved Pf gene *pfsE* (**Figure 4- 9C, E**). Finally, the recipient strain is infected with purified Pf obtained from clinical isolate pools (**Figure 4- 9G**). Initially it is advisable to test multiple MOIs to ensure genomic mutations and phage resistance do not occur when infecting the recipient strain to form a pan-immune population.

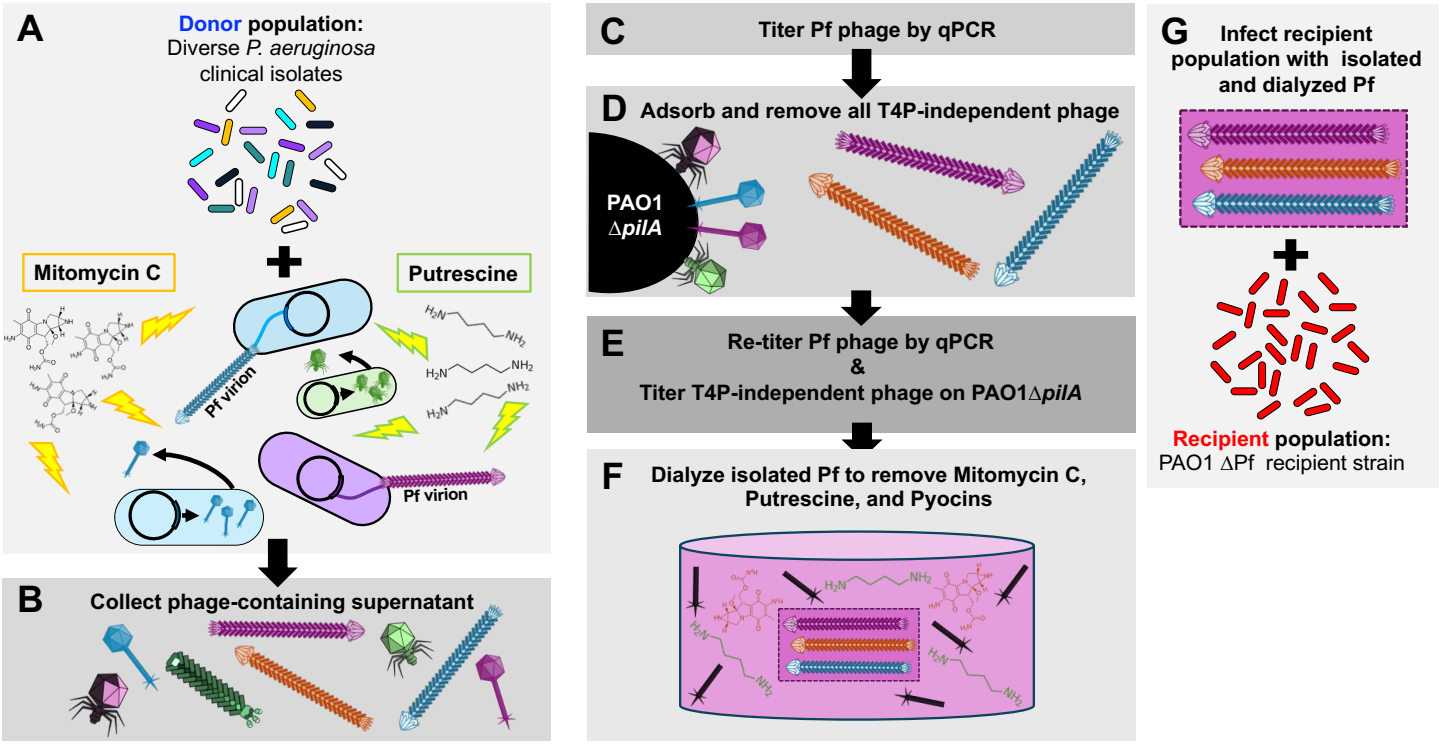

Figure 4- 9. Suggested approach to generate a pan-immune population for Trial v03.

4.3. Discussion

Recent studies of the arms race between bacteria and lytic phages illustrate the localization of phage defense systems into mobile defense islands (206). This discovery has led to contradictory observations: individual bacteria often encode multiple defense systems, yet these systems which are potentially vital for bacterial survival are frequently lost on short evolutionary time scales.

The model of the bacterial pan-immune system suggests that mobile elements, such as Pf phage, impose a significant fitness burden on their bacterial hosts (202). Thus, it is untenable for each bacterium to harbor more than a few. Rather, each bacterium harbors a unique subset of mobile elements, which they disseminate as needed to neighboring kin-cells. This cooperation between bacterial cells results in an 'effective' immune system that is the sum of its parts, which broadly shape bacterial evolution (21). Pf phages are uniquely well equipped to function as elements of a pan-immune system, as they produce virions without killing their host, can accommodate a large genome, and can spread rapidly throughout susceptible bacterial populations. In this work we sought to provide insight into how filamentous Inoviruses and the defense systems they encode constitute a pan-immune system that protects *P. aeruginosa* from diverse and ever-changing threats.

4.4. Future Directions

This model allows for the interrogation of mechanisms by which temperate phage protect their bacterial hosts from virulent phage predation. In the last decade, numerous scientific advances have originated from the study of bacterial phage defense, such as CRISPR-Cas9. Examination of temperate phage-mediated defense against virulent phage is relatively underdeveloped and has the potential to yield countless novel biotechnologies. As phages have broadly shaped bacterial evolution, this work would help contextualize our current understanding of evolution as a whole. Furthermore, with the rise of microbial resistance to antibiotics this work is more vital than ever and would inform development of effective therapies to combat antibiotic resistant bacterial infections.

Future work will be aimed at generating a population, in the same recipient background outlined here, which harbors diverse prophages mobilized from clinical isolates. This Pan-Immune population, produced with the aid of mitomycin C to induce prophage excision and replication, has the benefit of testing selective pressures in the same bacterial background while maintaining the diversity of prophages. We will also determine whether other stresses, not tested here, enrich specific prophages. Many auxiliary prophage genes encode toxins or other proteins that may affect virulence, host colonization, antibiotic tolerance, etc. We hypothesize that the benefits of the Pan-Immune system span far beyond phage defense. We plan to challenge this system with bacterivorous nematode *C. elegans* as well as a murine model to test for selection of prophage-

encoded virulence genes. Lastly, this model can be applied more broadly to test the utility of filamentous Inoviruses in enteric pathogens such as *E. coli*, *Salmonella*, and *Shigella*.

4.5. Materials and Methods

4.5.1. Strains, plasmids, and growth conditions

Strains, plasmids, and their sources are listed in **Table 4- 1**. Unless otherwise indicated, bacteria were grown in lysogeny broth (LB) at 37℃ with 230 rpm shaking and supplemented with gentamicin (Sigma) where appropriate, at 30 μg ml^{-1}. LB was supplemented with mitomycin C at a final concentration of 2 μg ml^{-1}. LB was supplemented with putrescine at a final concentration of 50mM.

Table 4- 1. Strains, bacteriophage, and plasmids used in this study.

Strain	Description	Source
Escherichia coli		
DH5α	Cloning strain	New England Biolabs
P. aeruginosa		
PAO1	Wild type	(102)
$PAO1_{\Delta Pf4/Pf6}$	Deletion of Pf4 and Pf6 prophage from PAO1	(237)
$PAO1_{\Delta Pf4/Pf6}$:: miniTn7-gfp	Prophage mutant strain with Tn7 insertion of GFP	This study
Bacteriophage		
DMS3*vir*	Siphoviridae	(166)
Plasmids		
pTNS2	Mini-Tn7 helper, Addgene plasmid #64968	(238)
pUC18-miniTn7-gfp	Mini-Tn7 element GmR, Gift from Boo Shan Tseng	(238)

Table 4- 2. Clinical Isolate Prophage Donor Strains, used in Trial v01.

Strain Names			
CPA0001	CPA0053	CPA0067	CPA0086
CPA0007	CPA0054	CPA0068	CPA0089
CPA0010	CPA0055	CPA0071	CPA0091
CPA0013	CPA0058	CPA0073	PAO1[*▲]
CPA0035	CPA0059[▲]	CPA0075	E80[*]
CPA0038	CPA0060	CPA0078	PA14[*]
CPA0041	CPA0061	CPA0082	E90[*▲]
CPA0042	CPA0062	CPA0085	LESB58[*]

[▲] Coinfected strain
[*] Model strain

Table 4- 3. Clinical Isolate Prophage Donor Strains, used in Trial v02.

Strain Names												
CPA0162	CPA0276	CPA0285	CPA0486	CPA0117	CPA0431	CPA0187	CPA0040	CPA0067	CPA0089	U813	S1226	U872
CPA0163	CPA0410	CPA0473	CPA0271	CPA0178	CPA0457	CPA0274	CPA0041	CPA0068	CPA0091	DDRC13	B12487	DDRC3
CPA0164	CPA0444	CPA0416	CPA0300	CPA0280	CPA0458	CPA0397	CPA0042	CPA0071	CPA0092	DDRC2	U6120	PA14*
CPA0257	CPA0445	CPA0487	CPA0303	CPA0361	CPA0119	CPA0001	CPA0053	CPA0073	2184	DDRC10	U5523	E90*
CPA0258	CPA0292	CPA0304	CPA0336	CPA0362	CPA0120	CPA0002	CPA0054	CPA0075	DDRC9	DDRC18	B6851	E80*
CPA0277	CPA0359	CPA0424	CPA0379	CPA0426	CPA0267	CPA0006	CPA0055	CPA0078	DDRC12	DDRC26	O2215	LESB58*
CPA0401	CPA0360	CPA0378	CPA0387	CPA0485	CPA0268	CPA0007	CPA0058	CPA0082	2181	P1550	S196	
CPA0402	CPA0460	CPA0398	CPA0393	CPA0158	CPA0329	CPA0010	CPA0059	CPA0085	DDRC1	DDRC4	1427	
CPA0305	CPA0463	CPA0450	CPA0452	CPA0192	CPA0453	CPA0013	CPA0060	CPA0086	DDRC7	2203	P1578	
CPA0435	CPA0135	CPA0224	CPA0464	CPA0265	CPA0454	CPA0035	CPA0061	CPA0087	DDRC17	2223	U8664	
CPA0193	CPA0390	CPA0239	CPA0467	CPA0430	CPA0186	CPA0038	CPA0062	CPA0088	DDRC 8	DDRC 6	2296	

KEY	
Pool	Sequencing
Felix	Full Prophage
Felix-Omega	Partial Prophage
Kumar	No Data

Table 4- 4. Clinical metadata and prophage traits associated with strains used in Trial v01 and Trial v02.

Patient ID	Collection Date	CPA#	Clinical	Pf?	Complete?	Attattachment (*att*)	Genes Divergent from Pf4 Core & Morons
80	6/27/20	CPA0001	lung transplant	Y	Y	tRNA-Met	ImmA Peptidase_M78
80	6/27/20	CPA0002	lung transplant	Y	Y	tRNA-Met	ImmA Peptidase_M78
137	*6/22/20*	*CPA0003*	*non CF*	*N*	*n/a*	*n/a*	*n/a*
3	*6/22/20*	*CPA0004*	*non CF*	*N*	*n/a*	*n/a*	*n/a*
93	*6/23/20*	*CPA0005*		*N*	*n/a*	*n/a*	*n/a*
93	6/23/20	CPA0006		Y	Y	tRNA-SeC	RT_Bac_retron_II, PHA03378 superfamily, PHA03247 superfamily
93	6/23/20	CPA0007		Y	Y	tRNA-SeC	RT_Bac_retron_II, PHA03378 superfamily, PHA03247 superfamily
93	*6/23/20*	*CPA0008*		*N*	*n/a*	*n/a*	*n/a*
93	*6/23/20*	*CPA0009*		*N*	*n/a*	*n/a*	*n/a*
93	6/23/20	CPA0010		Y	*N*	*?*	PHA03307 superfamily
48	*7/1/20*	*CPA0011*	*non CF*	*N*	*n/a*	*n/a*	*n/a*
107	*6/26/20*	*CPA0012*		*N*	*n/a*	*n/a*	*n/a*
127	6/26/20	CPA0013		Y	Y	tRNA-TtcA	P-loop_NTPase superfamily, DNA polymerase III subunits γ/τ
134	*7/3/20*	*CPA0014*		*N*	*n/a*	*n/a*	*n/a*
134	*7/3/20*	*CPA0015*		*N*	*n/a*	*n/a*	*n/a*
134	*7/3/20*	*CPA0016*		*N*	*n/a*	*n/a*	*n/a*
72	*7/6/20*	*CPA0017*		*N*	*n/a*	*n/a*	*n/a*
72	*7/6/20*	*CPA0018*		*N*	*n/a*	*n/a*	*n/a*
74	*7/9/20*	*CPA0019*	*lung transplant*	*N*	*n/a*	*n/a*	*n/a*
6	*7/16/20*	*CPA0020*		*N*	*n/a*	*n/a*	*n/a*
117	*7/16/20*	*CPA0021*	*non CF*	*N*	*n/a*	*n/a*	*n/a*
117	*7/16/20*	*CPA0022*	*non CF*	*N*	*n/a*	*n/a*	*n/a*
131	*8/3/20*	*CPA0023*		*N*	*n/a*	*n/a*	*n/a*
114	*8/6/20*	*CPA0024*	*lung transplant, high Pf in sputum*	*N*	*n/a*	*n/a*	*n/a*
64	*8/13/20*	*CPA0025*		*N*	*n/a*	*n/a*	*n/a*
54	*8/13/20*	*CPA0026*		*N*	*n/a*	*n/a*	*n/a*
78	*8/9/20*	*CPA0027*	*high levels of phage in sputum*	*N*	*n/a*	*n/a*	*n/a*

78	*8/9/20*	*CPA0028*	*high levels of phage in sputum*	*N*	*n/a*	*n/a*	*n/a*
78	*8/9/20*	*CPA0029*	*high levels of phage in sputum*	*N*	*n/a*	*n/a*	*n/a*
106	*8/10/20*	*CPA0030*		*N*	*n/a*	*n/a*	*n/a*
126	*8/12/20*	*CPA0031*		*N*	*n/a*	*n/a*	*n/a*
138	*8/13/20*	*CPA0032*		*N*	*n/a*	*n/a*	*n/a*
139	*8/13/20*	*CPA0033*		*N*	*n/a*	*n/a*	*n/a*
20	*8/19/20*	*CPA0034*		*N*	*n/a*	*n/a*	*n/a*
20	*8/19/20*	*CPA0035*		*N*	*n/a*	*n/a*	*n/a*
66	*8/9/20*	*CPA0036*		*N*	*n/a*	*n/a*	*n/a*
90	*8/18/20*	*CPA0037*		*N*	*n/a*	*n/a*	*n/a*
47	8/20/20	CPA0038		Y	Y	tRNA-Gly	Virul_fac_BrkB superfamily (hit spans *pfsE* to *coaB*)
76	*8/20/20*	*CPA0039*		*N*	*n/a*	*n/a*	*n/a*
78	8/16/20	CPA0040	high levels of phage in sputum	Y	Y	tRNA-TtcA	P-loop_NTPase superfamily, PHA03247 superfamily
78	8/16/20	CPA0041	high levels of phage in sputum	Y	Y	tRNA-TtcA / tRNA-Gly	DUF2523 superfamily (hit on IP)
17	8/19/20	CPA0042		Y	Y	tRNA-Gly	Cyt_C5_DNA_methylase superfamily (Dcm proximal to *PA0718*)
76	*8/20/20*	*CPA0043*		*N*	*n/a*	*n/a*	*n/a*
76	*8/20/20*	*CPA0044*		*N*	*n/a*	*n/a*	*n/a*
23	*8/25/20*	*CPA0045*	*sibling to patient 24*	*N*	*n/a*	*n/a*	*n/a*
23	*8/25/20*	*CPA0046*	*sibling to patient 24*	*N*	*n/a*	*n/a*	*n/a*
23	*8/25/20*	*CPA0047*	*sibling to patient 24*	*N*	*n/a*	*n/a*	*n/a*
135	*8/27/20*	*CPA0048*		*N*	*n/a*	*n/a*	*n/a*
132	*8/26/20*	*CPA0049*		*N*	*n/a*	*n/a*	*n/a*
132	8/26/20	CPA0050		Y	*N*	tRNA-TtcA	
147	*8/28/20*	*CPA0051*	*first time Pa+ (nosocomial)*	*N*	*n/a*	*n/a*	*n/a*
65	*9/2/20*	*CPA0052*		*N*	*n/a*	*n/a*	*n/a*
112	8/31/20	CPA0053		Y	Y	tRNA-TtcA	
112	8/31/20	CPA0054		Y	Y	tRNA-TtcA	DNA polymerase III subunits γ/τ, PHA03247 superfamily (large tegument protein UL36)
45	9/16/20	CPA0055	non CF	Y	*N*	tRNA-Met	ImmA Peptidase_M78
131	*9/8/20*	*CPA0056*		*N*	*n/a*	*n/a*	*n/a*
28	*10/14/20*	*CPA0057*		*N*	*n/a*	*n/a*	*n/a*
57	10/12/20	CPA0058		Y	*N*	tRNA-Met	*DNA polymerase III subunits γ/τ. NOTE: No attR detected. Possibly incomplete prophage.*
88	10/12/20	CPA0059		Y	Y	tRNA-Met	Cytosine-C5 specific DNA methylase (*Dcm),* MutL-like homologue (involved in MMR)
101	10/15/20	CPA0060		Y	Y	tRNA-Met	Cytosine-C5 specific DNA methylase (Dcm)
118	10/26/20	CPA0061	first time Pa+/early in Pa infection	Y	*N*	tRNA-Met	?
20	11/5/20	CPA0062		Y	*N*	tRNA-Gly	*No domain hits*
23	*11/18/20*	*CPA0063*	*sibling to patient 24*	*N*	*n/a*	*n/a*	*n/a*
23	*11/18/20*	*CPA0064*	*sibling to patient 24*	*N*	*n/a*	*n/a*	*n/a*
23	*11/18/20*	*CPA0065*	*sibling to patient 24*	*N*	*n/a*	*n/a*	*n/a*

23	*11/18/20*	*CPA0066*	*sibling to patient 24*	*N*	*n/a*	*n/a*	*n/a*
4	11/19/20	CPA0067		Y	Y	tRNA-Met / tRNA-Gly	*Large tegument protein UL36/ pfam05109 Herpes virus major outer envelope glycoprotein (BLLF1)*
4	11/29/20	CPA0068		Y	Y	tRNA-Met	DNA polymerase III subunits γ/τ, PHA03247 superfamily (large tegument protein UL36)
39	*11/20/20*	*CPA0069*	*not CF*	*N*	*n/a*	*n/a*	*n/a*
39	*11/20/20*	*CPA0070*	*not CF*	*N*	*n/a*	*n/a*	*n/a*
62	11/19/20	CPA0071	non CF	Y	*N*	*?*	
62	*11/19/20*	*CPA0072*	*non CF*	*N*	*n/a*	*n/a*	*n/a*
62	11/19/20	CPA0073	non CF	Y	Y	tRNA-TtcA / tRNA-Met	
24	*11/18/20*	*CPA0074*	*sibling to patient 23*	*N*	*n/a*	*n/a*	*n/a*
6	11/17/20	CPA0075		Y	Y	tRNA-TtcA	
53	*11/18/20*	*CPA0076*		*N*	*n/a*	*n/a*	*n/a*
37	*11/20/20*	*CPA0077*		*N*	*n/a*	*n/a*	*n/a*
127	11/18/20	CPA0078		Y	Y	tRNA-Met / tRNA-TtcA	*(Met) partial*
75	*12/22/20*	*CPA0079*		*N*	*n/a*	*n/a*	*n/a*
29	*12/28/20*	*CPA0080*	*lung transplant*	*N*	*n/a*	*n/a*	*n/a*
10	*1/7/21*	*CPA0081*	*non CF*	*N*	*n/a*	*n/a*	*n/a*
10	1/7/21	CPA0082	non CF	Y	Y	tRNA-Gly	
134	*1/7/21*	*CPA0083*		*N*	*n/a*	*n/a*	*n/a*
134	*1/7/21*	*CPA0084*		*N*	*n/a*	*n/a*	*n/a*
1	1/15/21	CPA0085	non CF	Y	Y	tRNA-Gly	Complete Type II Toxin-Antitoxin system: ParE_toxin (pfam05016), PhdYeFM_antitox (pfam02604)
1	1/15/21	CPA0086	non CF	Y	Y	tRNA-Gly	Complete Type II Toxin-Antitoxin system: ParE_toxin (pfam05016), PhdYeFM_antitox (pfam02604)
62	1/13/21	CPA0087	non CF	Y	*N*	*?*	
62	1/13/21	CPA0088	non CF	Y	*N*	*?*	
85	1/15/21	CPA0089	non CF	Y	*N*	tRNA-Gly / tRNA-Met	*(Gly) partial,* Met complete and encodes AbiEii toxin (COG4938 superfamily) and UL36
20	*1/20/21*	*CPA0090*		*N*	*n/a*	*n/a*	*n/a*
20	1/20/21	CPA0091		Y	*N*	tRNA-Gly	
20	1/20/21	CPA0092		Y	*N*	tRNA-Met	
128	*2/1/21*	*CPA0093*		*N*	*n/a*	*n/a*	*n/a*
85	*1/31/20*	*CPA0094*	*non CF*	*N*	*n/a*	*n/a*	*n/a*

Table 4- 5. Clinical metadata and prophage traits associated with strains used in Trial v02.

Serial#	sFB#	CPA#	Patient ID	Encounter	Modulator	Clinical	Pf?	Complete?	Attattachment (*att*)	Accessory Genes (Morons)
1	*sFB1371*	*CPA0106*	*55*	*1*	*none*	*CF*	*N*	*n/a*	*n/a*	*n/a*
3	*sFB1427*	*CPA0432*	*55*	*3*	*ETI*	*CF*	*N*	*n/a*	*n/a*	*n/a*
4	sFB1325	CPA0162	84	1	none	CF	Y	Y	tRNA-Met	Anti-phage dCTP deaminase
5	sFB1326	CPA0163	84	1	none	CF	Y	Y	tRNA-Met	Anti-phage dCTP deaminase, restriction endonuclease
6	sFB1327	CPA0164	84	1	none	CF	Y	Y	tRNA-Met	Anti-phage dCTP deaminase, restriction endonuclease
7	sFB1455	CPA0257	84	2	ETI	CF	Y	N	tRNA-Met	PIN-8 domain-containing protein, DUF262 domain-containing protein
8	sFB1456	CPA0258	84	2	ETI	CF	Y	N	*n/a*	*n/a*

9	sFB1463	CPA0277	84	3	ETI	CF	Y	N	tRNA-Met	PIN-8 domain-containing protein, DUF262 domain-containing protein
10	sFB1416	CPA0401	84	4	ETI	CF	Y	Y	tRNA-Met	DUF4902 domain-containing protein, HEPN domain-containing protein, HNH endonuclease, EexN family lipoprotein
11	sFB1417	CPA0402	84	4	ETI	CF	Y	N	tRNA-Met	PIN-8 domain-containing protein, DUF262 domain-containing protein
12	sFB1473	CPA0305	131	1	TEZ/IVA	CF	Y	Y	tRNA-Gly	AraC family transcriptional regulator, DUF4365 domain-containing protein, AAA-15 domain-containing protein
13	sFB1430	CPA0435	131	2	ETI	CF	Y	Y	tRNA-Gly	AraC family transcriptional regulator, DUF4365 domain-containing protein, AAA-15 domain-containing protein
14	*sFB1388*	*CPA0129*	*19*	*2*	*ETI*	*CF*	*N*	*n/a*	*n/a*	*n/a*
15	*sFB1389*	*CPA0130*	*19*	*2*	*ETI*	*CF*	*N*	*n/a*	*n/a*	*n/a*
17	*sFB1450*	*CPA0219*	*19*	*4*	*ETI*	*CF*	*N*	*n/a*	*n/a*	*n/a*
19	*sFB1490*	*CPA0392*	*19*	*6*	*ETI*	*CF*	*N*	*n/a*	*n/a*	*n/a*
20	*sFB1428*	*CPA0433*	*19*	*7*	*ETI*	*CF*	*N*	*n/a*	*n/a*	*n/a*
22	*sFB1319*	*CPA0156*	*25*	*2*	*ETI*	*CF*	*N*	*n/a*	*n/a*	*n/a*
23	*sFB1320*	*CPA0157*	*25*	*2*	*ETI*	*CF*	*N*	*n/a*	*n/a*	*n/a*
24	*sFB1454*	*CPA0244*	*25*	*3*	*ETI*	*CF*	*N*	*n/a*	*n/a*	*n/a*
25	*sFB1474*	*CPA0309*	*25*	*4*	*ETI*	*CF*	*N*	*n/a*	*n/a*	*n/a*
26	*sFB1475*	*CPA0310*	*25*	*4*	*ETI*	*CF*	*N*	*n/a*	*n/a*	*n/a*
27	*sFB1476*	*CPA0311*	*25*	*4*	*ETI*	*CF*	*N*	*n/a*	*n/a*	*n/a*
28	*sFB1397*	*CPA0343*	*25*	*5*	*ETI*	*CF*	*N*	*n/a*	*n/a*	*n/a*
30	*sFB1420*	*CPA0412*	*25*	*6*	*ETI*	*CF*	*N*	*n/a*	*n/a*	*n/a*
31	*sFB1421*	*CPA0413*	*25*	*6*	*ETI*	*CF*	*N*	*n/a*	*n/a*	*n/a*
32	*sFB1398*	*CPA0480*	*25*	*7*	*ETI*	*CF*	*N*	*n/a*	*n/a*	*n/a*
33	*sFB1399*	*CPA0481*	*25*	*7*	*ETI*	*CF*	*N*	*n/a*	*n/a*	*n/a*
34	sFB1349	CPA0193	94	1	ETI	CF	Y2	N	*n/a*	*n/a*
35	sFB1462	CPA0276	94	2	ETI	CF	Y	N	tRNA-Met / tRNA-TtcA	*n/a*
37	sFB1418	CPA0410	94	4	ETI	CF	Y	N	tRNA-Met	*n/a*
38	sFB1432	CPA0444	94	5	ETI	CF	Y	N	tRNA-Met / tRNA-TtcA	*n/a*
39	sFB1433	CPA0445	94	5	ETI	CF	Y	N	tRNA-Met / tRNA-TtcA	*n/a*
42	sFB1469	CPA0292	26	3	TEZ/IVA	CF	Y	Y	tRNA-Gly	NACHT domain-containing protein, NYN domain-containing protein
43	sFB1486	CPA0359	26	4	TEZ/IVA	CF	Y	Y	tRNA-Gly	NACHT domain-containing protein, NYN domain-containing protein
44	sFB1487	CPA0360	26	5	TEZ/IVA	CF	Y	Y	tRNA-Gly	NACHT domain-containing protein, NYN domain-containing protein
45	sFB1440	CPA0460	20	5	ETI	CF	Y	Y	tRNA-Gly	Hypothetical proteins, nucleotidyltransferase domain-containing protein, pentapeptide repeat-containing protein
46	sFB1441	CPA0463	21	9	ETI	CF	Y	N	tRNA-Gly	Nucleotidyltransferase domain-containing protein, pentapeptide repeat-containing protein
48	*sFB1444*	*CPA0475*	*29*	*4*	*ETI*	*CF*	*N*	*n/a*	*n/a*	*n/a*
49	sFB1394	CPA0135	31	3	ETI	CF	Y	Y	tRNA-TtcA	HEPN-RiboL-PSP domain-containing protein, ParA family protein
51	sFB1400	CPA0390	52	2	ETI	CF	Y	N	*n/a*	*n/a*
52	*sFB1402*	*CPA0339*	*64*	*3*	*ETI*	*CF*	*N*	*n/a*	*n/a*	*n/a*
53	sFB1467	CPA0285	66	3	ETI	CF	Y	N	*n/a*	*n/a*
54	sFB1403	CPA0473	68	5	ETI	CF	Y	Y	tRNA-SeC	Hypothetical proteins
55	sFB1422	CPA0416	69	5	ETI	CF	Y	Y	tRNA-TtcA	Transposase, Hypothetical protein
58	*sFB1401*	*CPA0395*	*75*	*3*	*ETI*	*CF*	*N*	*n/a*	*n/a*	*n/a*
59	sFB1404	CPA0487	80	4	ETI	CF	Y	N	*n/a*	*n/a*
60	sFB1472	CPA0304	82	3	ETI	CF	Y	N	*n/a*	*n/a*
61	sFB1423	CPA0424	85	4	ETI	CF	Y	Y	tRNA-Met	Hypothetical proteins, restriction endonuclease, anti-phage dCTP deaminase
62	sFB1489	CPA0378	90	3	ETI	CF	Y	N	*n/a*	*n/a*
63	*sFB1465*	*CPA0281*	*91*	*2*	*ETI*	*CF*	*N*	*n/a*	*n/a*	*n/a*
64	sFB1405	CPA0398	99	2	ETI	CF	Y	N2	tRNA-Met/ tRNA-TtcA	Hypothetical proteins
65	sFB1434	CPA0450	105	3	ETI	CF	Y	N	tRNA-Gly	Hypothetical proteins

66	*sFB1468*	*CPA0286*	*106*	*2*	*ETI*	*CF*	*N*	*n/a*	*n/a*	*n/a*
67	*sFB1431*	*CPA0438*	*109*	*4*	*ETI*	*CF*	*N*	*n/a*	*n/a*	*n/a*
68	sFB1451	CPA0224	110	1	ETI	CF	Y	N	*n/a*	*n/a*
70	sFB1453	CPA0239	116	1	ETI	CF	Y	Y	tRNA-SeC	Hypothetical protein, DUF4263 domain-containing protein
71	sFB1448	CPA0486	125	5	ETI	CF	Y	N	tRNA-Met / tRNA-Gly	Hypothetical proteins
72	sFB1460	CPA0271	126	1	ETI	CF	Y	N	*n/a*	*n/a*
73	*sFB1406*	*CPA0488*	*128*	*5*	*ETI*	*CF*	*N*	*n/a*	*n/a*	*n/a*
74	sFB1470	CPA0300	129	1	ETI	CF	Y	N	*n/a*	*n/a*
75	sFB1471	CPA0303	130	1	ETI	CF	Y	Y	tRNA-Gly	Hypothetical proteins, Phosphotransferase domain-containing protein
76	*sFB1477*	*CPA0319*	*135*	*1*	*ETI*	*CF*	*N*	*n/a*	*n/a*	*n/a*
77	sFB1407	CPA0336	138	1	ETI	CF	Y	N	*n/a*	*n/a*
78	sFB1485	CPA0353	140	2	ETI	CF	Y	Y	tRNA-Met	Hypothetical proteins, EexN family lipoprotein
78	sFB1485	CPA0353	140	2	ETI	CF	Y	Y	tRNA-SeC	DUF4393 domain-containing protein
79	*sFB1483*	*CPA0351*	*142*	*1*	*ETI*	*CF*	*N*	*n/a*	*n/a*	*n/a*
80	sFB1408	CPA0379	148	1	ETI	CF	Y	Y	tRNA-Met	Hypothetical proteins, EexN family lipoprotein
81	sFB1409	CPA0385	151	1	ETI	CF	Y	N	*n/a*	*n/a*
82	sFB1410	CPA0387	152	1	ETI	CF	Y	N	*n/a*	*n/a*
83	sFB1411	CPA0393	154	1	ETI	CF	Y	N	*n/a*	*n/a*
84	*sFB1429*	*CPA0434*	*159*	*1*	*ETI*	*CF*	*N*	*n/a*	*n/a*	*n/a*
85	sFB1435	CPA0452	164	1	ETI	CF	Y	N	*n/a*	*n/a*
86	sFB1442	CPA0464	166	1	ETI	CF	Y	N	*n/a*	*n/a*
87	sFB1443	CPA0467	167	1	ETI	CF	Y	N	*n/a*	*n/a*
88	sFB1376	CPA0117	16	3	none	CF	Y	N	*n/a*	*n/a*
89	sFB1336	CPA0178	16	4	none	CF	Y	N	*n/a*	*n/a*
90	sFB1464	CPA0280	16	5	none	CF	Y	N	*n/a*	*n/a*
91	sFB1488	CPA0361	16	6	none	CF	Y	N	*n/a*	*n/a*
92	sFB1412	CPA0362	16	6	none	CF	Y	N	*n/a*	*n/a*
93	sFB1424	CPA0426	16	7	none	CF	Y	N	*n/a*	*n/a*
94	sFB1447	CPA0485	16	8	none	CF	Y	N	*n/a*	*n/a*
95	*sFB1366*	*CPA0095*	*27*	*3*	*none*	*CF*	*N*	*n/a*	*n/a*	*n/a*
96	*sFB1466*	*CPA0284*	*27*	*4*	*none*	*CF*	*N*	*n/a*	*n/a*	*n/a*
97	*sFB1478*	*CPA0322*	*27*	*5*	*none*	*CF*	*N*	*n/a*	*n/a*	*n/a*
98	*sFB1479*	*CPA0323*	*27*	*5*	*none*	*CF*	*N*	*n/a*	*n/a*	*n/a*
100	*sFB1415*	*CPA0400*	*27*	*6*	*none*	*CF*	*N*	*n/a*	*n/a*	*n/a*
101	sFB1321	CPA0158	50	2	none	CF	Y	N	*n/a*	*n/a*
102	sFB1348	CPA0192	50	3	none	CF	Y	N	*n/a*	*n/a*
103	sFB1457	CPA0265	50	4	none	CF	Y	N	*n/a*	*n/a*
105	sFB1425	CPA0430	50	6	none	CF	Y	N	*n/a*	*n/a*
106	sFB1426	CPA0431	50	6	none	CF	Y	N	*n/a*	*n/a*
107	sFB1438	CPA0457	50	7	none	CF	Y	N	*n/a*	*n/a*
108	sFB1439	CPA0458	50	7	none	CF	Y	Y	tRNA-Met	Hypothetical proteins, HNH endonuclease, EexN family lipoprotein
109	sFB1378	CPA0119	62	1	none	CF	Y	Y	tRNA-Gly	Nucleotide-binding protein, DUF3278 domain-containing protein, Transposase
110	sFB1379	CPA0120	62	1	none	CF	Y	N	*n/a*	*n/a*
111	sFB1458	CPA0267	62	2	none	CF	Y	N	*n/a*	*n/a*
112	sFB1459	CPA0268	62	2	none	CF	Y	Y	tRNA-Met	Hypothetical proteins
113	sFB1482	CPA0329	62	3	none	CF	Y	N	*n/a*	*n/a*
114	sFB1436	CPA0453	62	4	none	CF	Y	N	*n/a*	*n/a*
115	sFB1437	CPA0454	62	4	none	CF	Y	Y	tRNA-SeC	Transposase, Hypothetical protein
116	sFB1344	CPA0186	92	1	none	CF	Y	Y	tRNA-Met	Mrr-cat domain-containing protein
117	sFB1345	CPA0187	92	1	none	CF	Y	Y	tRNA-Met	Mrr-cat domain-containing protein
118	sFB1461	CPA0274	92	2	none	CF	Y	Y	tRNA-Met	Mrr-cat domain-containing protein, Hypothetical proteins
119	sFB1413	CPA0397	92	3	none	CF	Y	Y	tRNA-Met	Mrr-cat domain-containing protein

4.5.2. Construction of PAO1$_{\Delta Pf4\Delta Pf6}$::pUC18-miniTn7-*gfp*

P. aeruginosa strain PAO1 was cured of prophages Pf4 and Pf6 through allelic exchange targeting *pflM,* as previously described (237). A 3mL culture of strain PAO1$_{\Delta Pf4/Pf6}$ was incubated in LB for 18h under standard conditions. PAO1$_{\Delta Pf4/Pf6}$ was then pelleted at 16,000xg, supernatant was removed, and pellet was resuspended and washed with 1mL 300mM sucrose to make electrocompetent. Following the third wash, pellet was resuspended in 200µL 300mM sucrose and placed on ice. Mini preps of plasmids pTNS2 and pUC18-miniTn7-gfp (**Table 4-1**) were prepared with the Monarch® Plasmid Miniprep Kit (NEB #T1110) and electroporated into PAO1$_{\Delta Pf4/Pf6}$:miniTn7-gfp in a 2mm-gap electroporation cuvette (BioRad #1652086) via an Eppendorf Eporator at 25µF, 200Ω, 2.5 kV, time constant <5ms. Cells were selected for with gentamycin (30 µg ml^{-1}) and screened for successful Tn7 insertion via PCR and microscopy to confirm endogenous GFP expression.

4.5.3. Construction of a pan-immune Population

4.5.3.1. Trial v01

Prophage 'donor' clinical isolates with Pf phage listed in **Table 4- 2** were tested for resistance to gentamicin at 30 µg ml^{-1}. Sensitive donor strains were individually inoculated into 3mL LB, incubated for 18h at 37ºC 230rpm. Donor strains were then pelleted at 12,000xg for 2min, washed 3 times in 1XPBS to remove exogenous virions, and pellets were resuspended in 1mL LB Glycerol (2:1 v/v). Donor cultures were then combined in equal volume, aliquoted, and immediately frozen at -80ºC. For each following experiment, individual donor pools were thawed in biological triplicate, revived in 9mL LB at 37ºC with agitation for 30min. Recipient strain (PAO1$_{\Delta Pf4/Pf6}$::pUC18-miniTn7Gm-*gfp*) overnight cultures were subcultured into 9mL fresh LB, and grown to OD$_{600}$ 0.2. Recipient and donor were then combined at a 1:3 ratio (3mL donor : 9mL recipient), and incubated for 18h at 37ºC with agitation. LB was supplemented as indicated. Recipient strain PAO1$_{\Delta Pf4/Pf6}$::pUC18-miniTn7Gm-*gfp* selection for through addition of gentamycin to a final concentration of 30 µg ml^{-1} was incubated for ~4h. Genomic DNA extraction, library preparation, and sequence analyses were all performed as indicated.

4.5.3.2. Trial v02

Trial v03 methodology mirrors that of Trial v01 for generation of the pan-immune population, however a larger pool of clinical isolate strains were used (**Table 4- 3**), many of which were unsequenced. We sought to sequence the pan-immune population with depth significant enough (~3,000x chromosomal coverage) to identify prophage all sequences. Another significant difference from Trial v01 was the sequencing data analyses as we did not have a concatemer of known prophage sequences to align raw reads back to. As the program Guppy, used in Trial v01, was no longer recommended by Oxford Nanopore Technologies, sequencing data was basecalled in the recommended platform (*Epi2Me*) and reads were demultiplexed and trimmed with Porechop (*v0.2.4*), This

approach was successful, and prophage reads were identified through methodology outline in section 4.5.5 (**Table 4- 4**, **Table 4- 5**). We intended to then create a concatemer of trimmed prophage sequences identified in the pan-immune population to use for diversity analyses.

4.5.3.3. Suggested approach for Trial v03

See protocol entitled *'AKS 20231213_PanImmuneT3.0_MakingPanImmunePop'* for detailed suggested methodology.

4.5.4. Assembly of Clinical Isolate PacBio Whole-Genome sequencing

PacBio whole-genome sequencing was performed by Felix Biotech in collaboration with the Bollyky Lab at Stanford University. Felix biotech assembled their sequencing data independently, and these assemblies were used when discovered prophage sequences were intact. However, when prophage sequences were incomplete, which is often the case because many assemblers detect complementarity of the attachment (*att*) sites and designate these reads as duplicates, we re-filtered and re-assembled. Reads were filtered for read quality with Filtlong (*v.0.2.1*) with parameters for minimum read length set to 1000 and keep precent set to 90. Filtered reads were assembled using the Trycycler pipeline (211, 212), with dependencies minimap2 (*v2.24-r1122*), Flye (*v2.9.1*), Raven (v1.8.3), and Velvet (*v7.0.4*). Assemblies were manually curated in Bandage (*v0.8.1*), polished using Medaka (*v1.8.0*), and annotated using Bakta (*v1.6.1*) and RAST (*https://rast.nmpdr.org/*). Prophage sequences within assembled genomes were then identified by searching for the highly conserved Pf gene *pfsE* (*PA0721*). Prophage *att* sites were then determined, and prophage sequences were trimmed, as described in section **4.5.5.**

4.5.5. Identification of Pf genomes and prophage trimming

The below code was written and ran in R studio (v. 2023.12.1+402), and provides an example of the methodology used to trim prophage sequences which contain an internal marker (highly conserved prophage gene *pfsE*, in the context of this work) flanked by two external markers (*att* sites in the context of this work).

```
///
###Define sequences to search for where external markers are att sites and internal markers are highly
conserved prophage gene(s) within the 'core' genome, such as Pf gene pfsE (PA0721).

sequences <- DNAStringSet(c("ACGTACGTTAAAGGACGATCGATCGTAGGGGCTAGCTAGCTAGCTAGCGCGCGCG",
"AGCTAGCTAGCAAATAGCTAGCTAGCTAGCGGGCTAGCTAGCTAGCTAGCTAGAAACTAGC",
"CGCGCGCGGGGCGCGCGCGCGCGCGCGCGCGAAACGCGCGCGCGCGCGCGCGCGCGCGC",
"ACGACGAAACGACGACGACGACGACGGGACGACGACGACGACGACGACGACGAAACGAC",
"ACGACGAAACGACGACGACGACGACGACGACGACGACGACGACGACGAAACGAC"))

external_marker <- "AAA"
internal_marker <- "GGG"
```

###Number of mismatches = 5 for actual analysis

```
mismatches <- 0
```

###Matches of the external marker for all sequences

```
external_matches <- vmatchPattern(external_marker, sequences, max.mismatch = mismatches)
```

###Matches of the internal marker for all sequences

```
internal_matches <- vmatchPattern(internal_marker, sequences, max.mismatch = mismatches)
```

###Return indices that have at least *two* external marker hits and at least *one* internal marker hit

```
valid_indices <- which(lengths(external_matches) >= 2 & lengths(internal_matches) >= 1)

valid_seq <- sequences[valid_indices]

trimmed <- gsub(".*(AAA.*AAA).*", "\\1", valid_seq)
```

###Save as a **.fasta* file containing trimmed sequences

```
file_conn <- file("<file path>.fasta", "w")
for (i in seq_along(trimmed)) {
  new_names <- paste0("<seq name>_", i) #change sequence names
  writeLines(paste0(">", new_names), con = file_conn)
  writeLines(trimmed[i], con = file_conn)
  writeLines("", con = file_conn)  #add an empty line between sequences
}
close(file_conn)
```

###If working correctly, your **.fasta* file should contain trimmed "prophage" sequences which contain exactly *two* external markers (these are your *att* sites) **and *one* internal marker** (this is your highly conserved prophage gene) **like in the example 'prophages' below:**

```
>seq_1
AAATAGCTAGCTAGCTAGCGGGCTAGCTAGCTAGCTAGCTAGAAA
>seq_2
AAACGACGACGACGACGACGGGACGACGACGACGACGACGACGACGAAA
```

/// end.

4.5.6. Genomic DNA Extraction and Quantification

Genomic DNA was extracted using NEB Monarch gDNA isolation kits (*NEB #T3010*) according to manufacturer specification. gDNA was eluted in 30µL heated (55ºC) UltraPure™ DNase/RNase-Free Distilled Water (*Thermo #10977015*). DNA purity was determined with a NanoDrop One Microvolume UV-Vis Spectrophotometer (*Thermo #ND-ONE-W4*) and quantified with and AccuBlue dsDNA quantitation kit (*Biotium #31006*). To gauge gDNA fragment size 100ng of purified gDNA was run on a 0.25% agarose gel with a 1 kb Extend DNA Ladder (*NEB #N3239S*) and imaged on a GelDoc Go System (*BioRad #12009077*).

4.5.7. DNA Library Preparation and Long Read Whole-Genome Sequencing

gDNA ends were repaired with the NEBNext FFPE DNA Repair Mix (*NEB #E7360*) and NEBNext Ultra II End Repair / dA-tailing Module (*NEB #E7595*). End-prepped gDNA was quantified with the AccuBlue dsDNA quantitation kit (*Biotium #31006*) and concentration was normalized across all replicates. Next, gDNA was barcoded using NEB Blunt/TA Ligase Master Mix (*NEB #M0367L*) and Oxford Nanopore Technologies Native Barcoding Kit (*ONT SQK-NBD114.24*). Native sequencing adapters provided in the Native Barcoding Kit were ligated with the NEBNext Quick Ligation Reaction Module (*NEB #E6056*) and pellet was washed with the Long Fragment Buffer (LFB), also provided in the SQK-NBD114.24 kit. DNA concentration of eluate (1µL) was again quantified using the AccuBlue High Sensitivity dsDNA Quantitation Kit (*Biotium #31006*). Library fmols were calculated with the following formulae: *moles dsDNA (mol)* = mass of dsDNA (g)/((length of dsDNA (bp) x 615.96 g/mol/bp) + 36.04 g/mol), *moles of dsDNA ends* = moles dsDNA (mol) x 2, *DNA copy number* = moles of dsDNA x 6.022e23 molecules/mol. Per Oxford Nanopore Technologies recommendation for R10.4.1 flow cells, DNA libraries were made up to a concentration of 10-20fmol in 12µL. Whole-genome sequencing of pan-immune populations was performed using an Oxford Nanopore Technologies MinION Mk1B device and DNA (R 10.4.1) FLO-MIN114 flow cells.

4.5.8. Pan-immune Whole-Genome Sequencing Quality Control and Analyses

Raw Reads were basecalled with Guppy Basecalling Software (*v 6.4.8+31becc941*). Bascealled reads were demultiplexed and trimmed with Porechop (*v0.2.4.*). Quality control was performed with Filtlong (*v.0.2.1*) with parameters for minimum read length set to 1000 and keep precent set to 90. Reads were then mapped to the pan-immune backbone, strain PAO1$_{\Delta Pf4\Delta Pf6}$::pUC18-miniTn7-*gfp* (**Table 4- 1**) with minimap2 (*v2.24-r1122*). Reads that did <u>not</u> map to the backbone were retained using Samtools (*v1.18*). These reads were then aligned to a concatemer of all prophage sequences from the clinical isolates used as prophage donors.

4.5.9. Statistical Analyses and Graphing

GraphPad Prism version 9.4.1 (GraphPad Software, San Diego, CA) was used for all analyses.

CHAPTER FIVE Conclusions

In 1915 British microbiologist Frederick Twort observed “glassy and transparent” spots appearing on his *E. coli* streak plates (239). Shortly thereafter, French-Canadian microbiologist Felix d’Herelle published similar findings of an “invisible microbe endowed with antagonistic properties toward a pathogenic bacillus” (240). Twort concurred with d’Herelle and suggested that these spots could be the result of an “ultra-microscopic virus”. This was a radical notion for the time and soon Twort abandoned the hypothesis. However, persistent and eccentric d’Herelle was convinced that he had discovered a new type of virus; a virus that infected bacteria. So, he called them bacteriophages; phage meaning "to devour, consume, destroy, or to eat" in Latin.

It has been a hair over a century since Twort and d’Herelle’s initial observations. Phages are now known to be the most diverse and abundant biological entity on the planet; a simultaneously daunting and thrilling fact. These bacteria-eaters have been entangled in the coevolutionary arms-race with their bacterial hosts on a timescale that is difficult for the human brain to comprehend. Consequently, phages are responsible for shaping every microbial community, and thus, much of the life on earth. Elements of bacterial phage defenses have even been proposed to be some of the earliest known elements our mammalian innate immune systems (241). Gut flora, present in virtually every species with a gut, are shaped by phage predation(242). Although phages are often considered to be simpler than their bacterial the interactions they engage in are infinitely complex. Packed into a genome 5 orders of magnitude smaller than that of a human (Pf4’s measly 12 Kbp compared to 3 Gbp), are genes like *pfsE,* which modify bacterial behavior and ultimately microbial pathogenesis.

In Chapter II, we uncovered that the highly-conserved Pf4 gene *pfsE* functions to suppress twitch motility, and elaborated that it can (and does!) also inhibit *pqs* signaling (11). Initially we undertook this research to make sense of the transient loss of twitch motility, mediated by Type IV Pili (T4P), in Pf4-infected cultures. We found that PfsE inhibits T4P-dependent twitch motility by interacting with the T4P subunit PilC, preventing pilus extension. Furthermore, we discover that interaction between PfsE and PilC is mediated by three highly conserved aromatic residues which, when modified to non-polar residues, abrogate PfsE-mediated loss of twitch motility and PfsE/PilC interaction. Importantly, loss of twitch motility by *pfsE* expression is transient; T4P function is restored following subculture into phage-free media. This transient suppression of T4P likely assists *P. aeruginosa* in biofilm dispersal. PfsE is emblematic of the olive branch filamentous Inoviruses so often extend to their bacterial hosts; demonstrative of the delicate balance these phages strike between obligate parasitism and mutualism.

In Chapter III we discover that deletion of Pf4 gene *pflM* results in prophage excision and lack of replication. We determine that functionality of this gene remains conserved across diverse clinical isolates, and leverage this finding to generate prophage-free mutants. Using these prophage mutants, we uncover the intricate and diverse ways in which Pf phages puppeteer their bacterial hosts. We observed diverse interactions between

Pf and *P. aeruginosa* quorum sensing, biofilm formation and pigment production. Furthermore, we find that *C. elegans* are consistently biased towards Pf-free bacteria as a food source, which broadly implicates Pf phage in virulence against bacterivorous nematodes.

Lastly, in Chapter IV I present preliminary findings which support the model of filamentous Inoviruses as elements of a bacterial Pan-Immune system, whereby phages serve as a community resource for the mobilization of advantageous genes. In support of this hypothesis, hot-off-the-press research from the Tomás Lab at Universidad de A Coruña (UDC) find that novel Pf phage, isolated from Cystic Fibrosis patients, encode functional anti-phage defense systems (243). This research establishes the role of Pf in conferring resistance to virulent phage and mobilizing Pf-encoded defenses in response to virulent phage predation, as asserted in Chapter IV of this work.

Taken together, this work supports findings within current literature (66), pointing to Pf phage modulating *P. aeruginosa* behavior and virulence potential. Inhibition of T4P and *pqs* signaling, two canonical virulence factors which *pfsE* targets, could improve patient outcomes fighting *P. aeruginosa* infection. Future research into phenotypic changes resulting from prophage 'deletion', as discussed in Chapter III have the potential to yield novel therapeutics, and personalized treatments. Importantly, this body of work emphasizes the pleiotropy of phage genes which often, as demonstrated with *pfsE,* are incredibly multifaceted.

Painting a clear picture of the interactions between Filamentous Inoviruses and their bacterial hosts is vital to understanding and ultimately combatting bacterial infection in an increasingly antimicrobial resistant world. This body of work serves to meaningfully advance our understanding of the biology which underpins Filamentous Inovirus:bacterial interaction.

Though phages are not themselves living, they have shaped the world around us. We will likely never understand them in their entirety, but we will sure try.

SUPPLEMENTARY MATERIAL

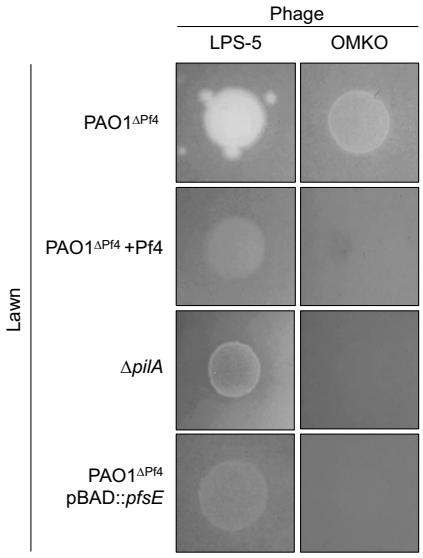

Figure S2- 1. Pf4 superinfection and expression of PfsE promotes resistance to type IV pili (T4P)-dependent lytic bacteriophages. Representative images of *P. aeruginosa* PAO1 lawns spotted with 10^6 PFUs OMKO (T4P-dependent lytic phage), or LPS-5 (a T4P-independent lytic phage). Note plaques are visualized as bright spots in these images.

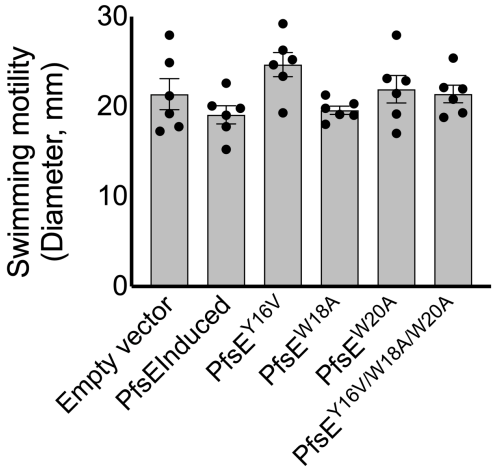

Figure S2- 2. PfsE expression does not affect swimming motility in *P. aeruginosa*. Swimming motility of *P. aeruginosa* growing on swim agar was measured in PAO1$^{\Delta Pf4}$ expressing wild-type or modified PfsE or an empty expression vector (pHERD20T). Results are mean 6 SEM of 6 experiments, unpaired Student's t test.

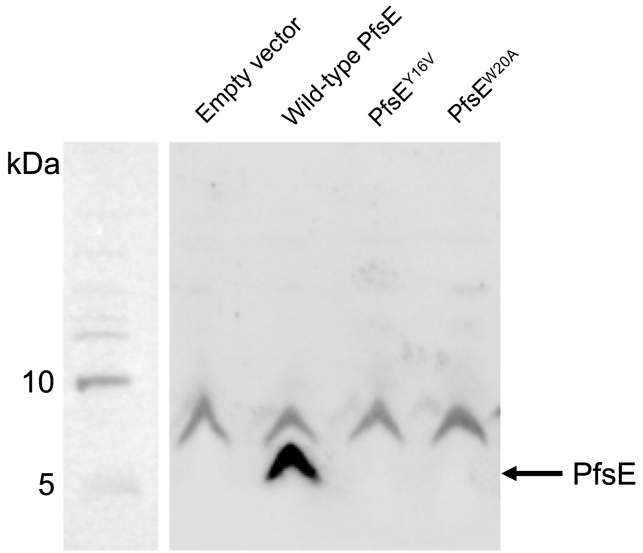

Figure S2- 3. Wild-type PfsE protein is expressed in *E. coli*, but not the point mutants PfsE^{Y16V} or PfsE^{W20A}. A His tag was cloned onto the N-terminus of wild-type or mutant PfsE in a pETDuet vector. Proteins were then expressed in *E. coli* BTH101. Protein was then run on SDS-PAGE, blotted, and detected using anti-His antibodies. A representative gel from triplicate experiments is shown.

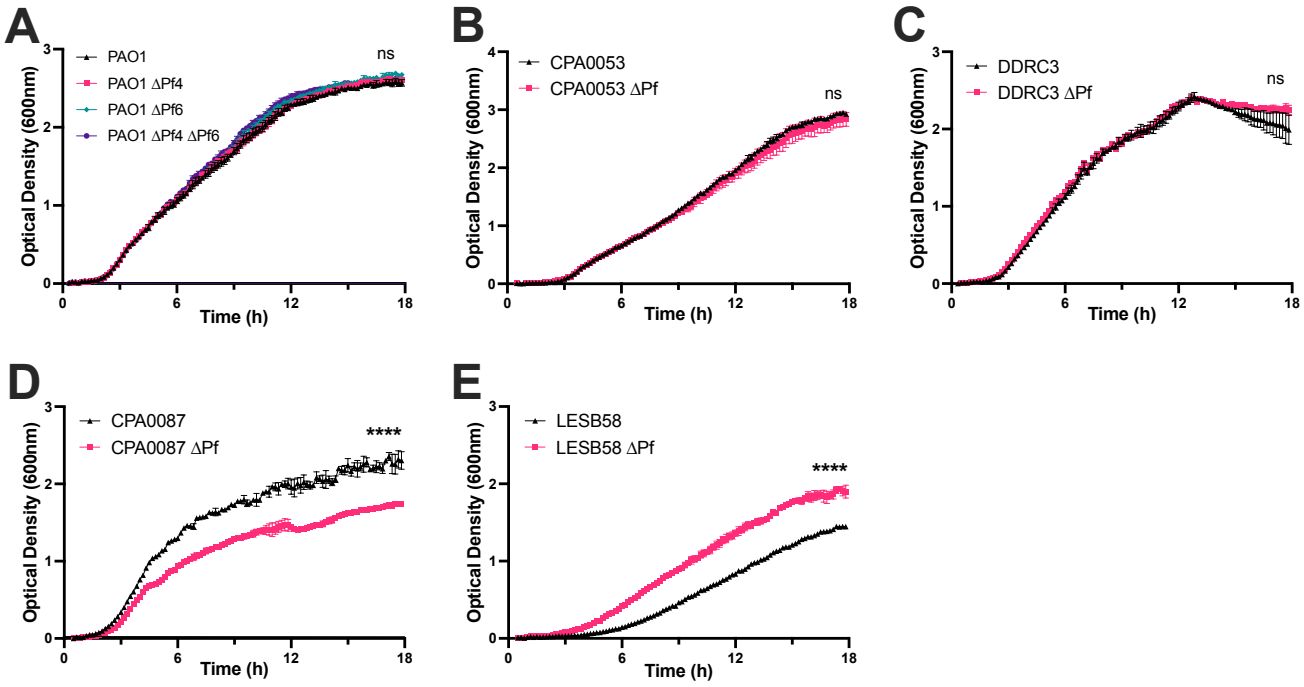

Figure S3- 1. Prophage presence has variable impact on host growth. Individual colonies were picked and used to inoculate overnight cultures. The following day, overnight cultures were subcultured into fresh LB. Optical density was monitored for 18h. n = 4. Statistical analyses was performed in GraphPad Prism (v10.2.0) by three-way or two-way ANOVA as appropriate and employing the Geisser-Greenhouse correction for sphericity. ****P<0.0001.

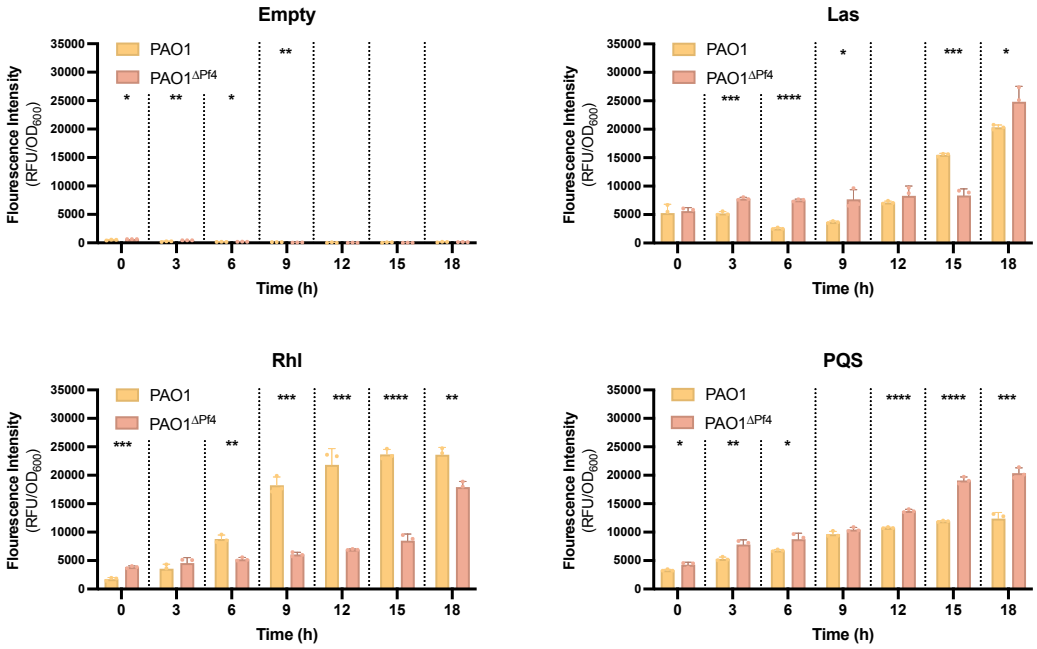

Figure S3- 2. Pf4 modulates *P. aeruginosa* PAO1 quorum sensing. Fluorescence intensity from the transcriptional reporters P*rsaL*-*gfp* (Las), P*rhlA*-*gfp* (Rhl), or P*pqsA*-*gfp* (PQS) was measured in the indicated strains after 18 hours of growth. Fluorescence intensity was normalized to cell density (OD_{600}) at each timepoint. Data are the mean ±SEM of three biological replicates. *P<0.05, **P<0.01, ***P<0.001, ****P<0.0001, Student's *t*-test comparing ΔPf strains to the wild-type parent at each time point.

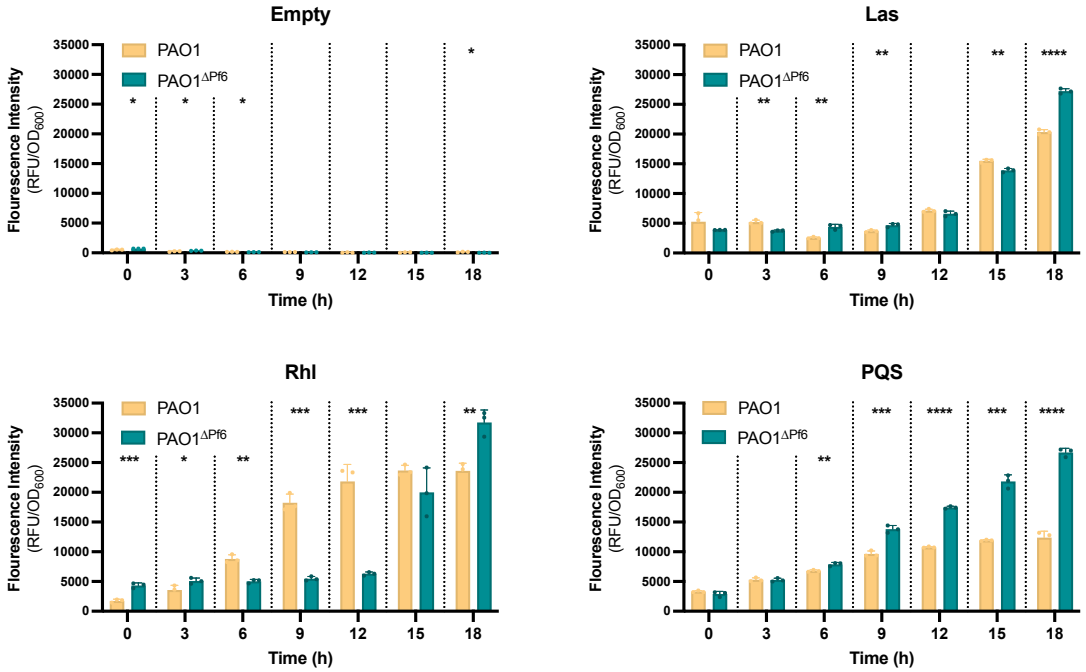

Figure S3- 3. Pf6 modulates *P. aeruginosa* PAO1 quorum sensing. Fluorescence intensity from the transcriptional reporters P*rsaL*-*gfp* (Las), P*rhlA*-*gfp* (Rhl), or P*pqsA*-*gfp* (PQS) was measured in the indicated strains after 18 hours of growth. Fluorescence intensity was normalized to cell density (OD_{600}) at each timepoint. Data are the mean ±SEM of three biological replicates. *P<0.05, **P<0.01, ***P<0.001, ****P<0.0001, Student's *t*-test comparing ΔPf strains to the wild-type parent at each time point.

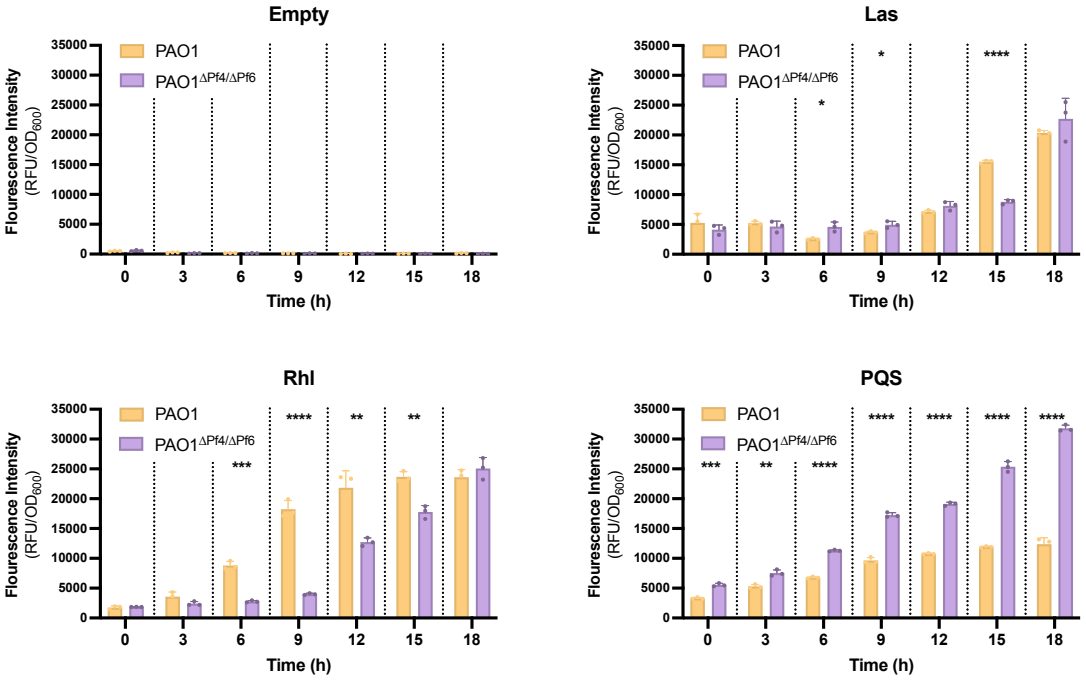

Figure S3- 4. Pf4 and Pf6 modulate *P. aeruginosa* PAO1 quorum sensing. Fluorescence intensity from the transcriptional reporters P*rsaL*-*gfp* (Las), P*rhlA*-*gfp* (Rhl), or P*pqsA*-*gfp* (PQS) was measured in the indicated strains after 18 hours of growth. Fluorescence intensity was normalized to cell density (OD_{600}) at each timepoint. Data are the mean ±SEM of three biological replicates. *P<0.05, **P<0.01, ***P<0.001, ****P<0.0001, Student's *t*-test comparing ΔPf strains to the wild-type parent at each time point.

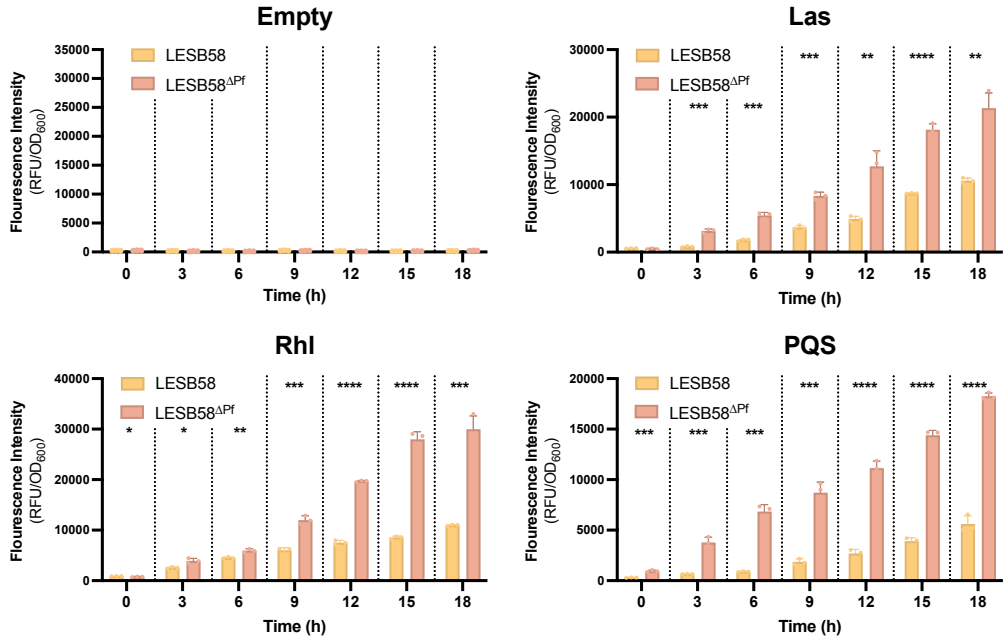

Figure S3- 5. Pf phage modulate *P. aeruginosa* LESB58 quorum sensing. Fluorescence intensity from the transcriptional reporters P*rsaL*-*gfp* (Las), P*rhlA*-*gfp* (Rhl), or P*pqsA*-*gfp* (PQS) was measured in the indicated strains after 18 hours of growth. Fluorescence intensity was normalized to cell density (OD_{600}) at each timepoint. Data are the mean ±SEM of three biological replicates. *P<0.05, **P<0.01, ***P<0.001, ****P<0.0001, Student's *t*-test comparing ΔPf strains to the wild-type parent at each time point.

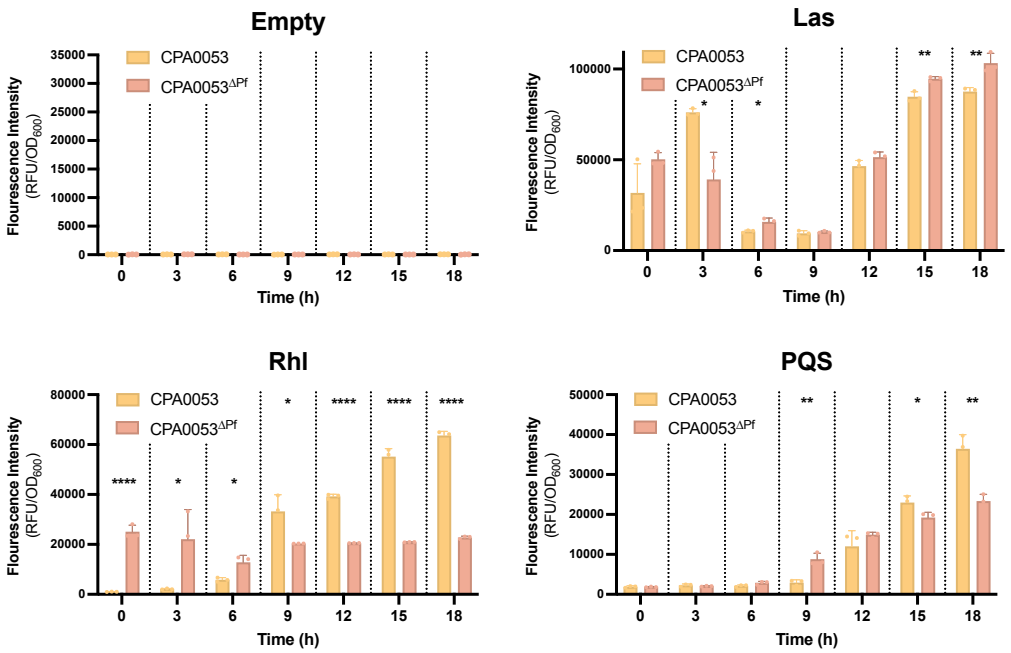

Figure S3- 6. Pf phage modulate *P. aeruginosa* CPA0053 quorum sensing. Fluorescence intensity from the transcriptional reporters P*rsaL*-*gfp* (Las), P*rhlA*-*gfp* (Rhl), or P*pqsA*-*gfp* (PQS) was measured in the indicated strains after 18 hours of growth. Fluorescence intensity was normalized to cell density (OD_{600}) at each timepoint. Data are the mean ±SEM of three biological replicates. *P<0.05, **P<0.01, ***P<0.001, ****P<0.0001, Student's *t*-test comparing ΔPf strains to the wild-type parent at each time point.

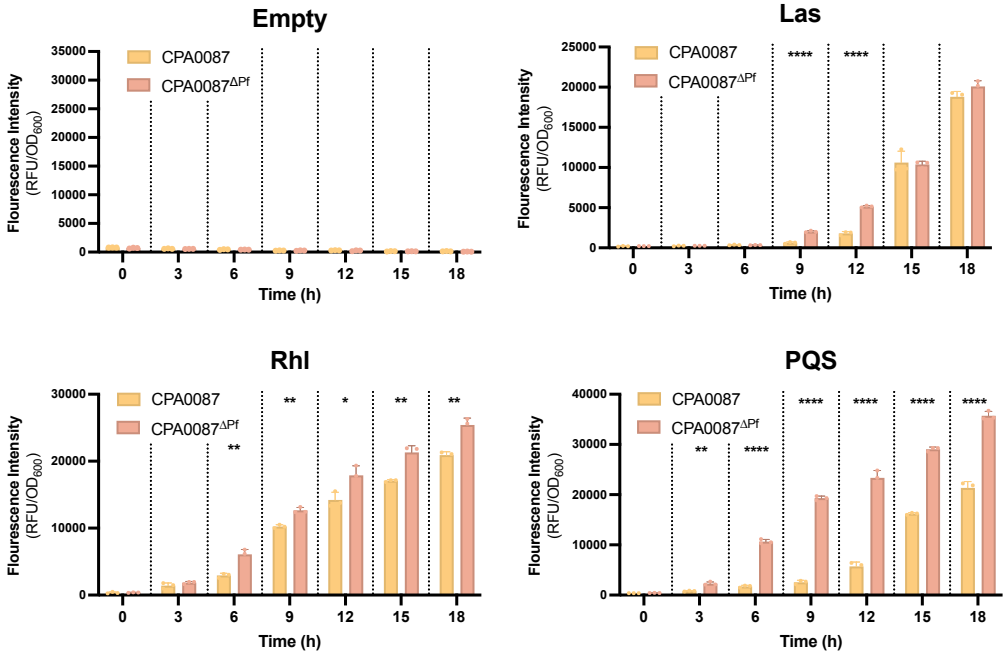

Figure S3- 7. Pf phage modulate *P. aeruginosa* CPA0087 quorum sensing. Fluorescence intensity from the transcriptional reporters P*rsaL*-*gfp* (Las), P*rhlA*-*gfp* (Rhl), or P*pqsA*-*gfp* (PQS) was measured in the indicated strains after 18 hours of growth. Fluorescence intensity was normalized to cell density (OD_{600}) at each timepoint. Data are the mean ±SEM of three biological replicates. *P<0.05, **P<0.01, ***P<0.001, ****P<0.0001, Student's *t*-test comparing ΔPf strains to the wild-type parent at each time point.

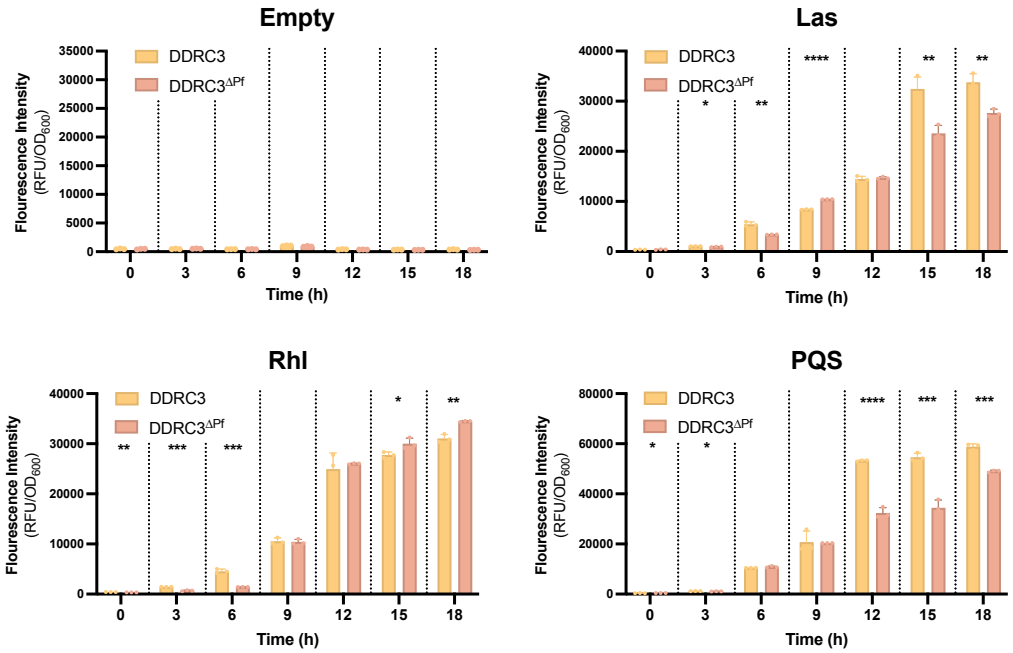

Figure S3- 8. Pf phage modulate *P. aeruginosa* DDRC3 quorum sensing Fluorescence intensity from the transcriptional reporters P_{rsaL}-*gfp* (Las), P_{rhlA}-*gfp* (Rhl), or P_{pqsA}-*gfp* (PQS) was measured in the indicated strains after 18 hours of growth. Fluorescence intensity was normalized to cell density (OD_{600}) at each timepoint. Data are the mean ±SEM of three biological replicates. *P<0.05, **P<0.01, ***P<0.001, ****P<0.0001, Student's *t*-test comparing ΔPf strains to the wild-type parent at each time point.

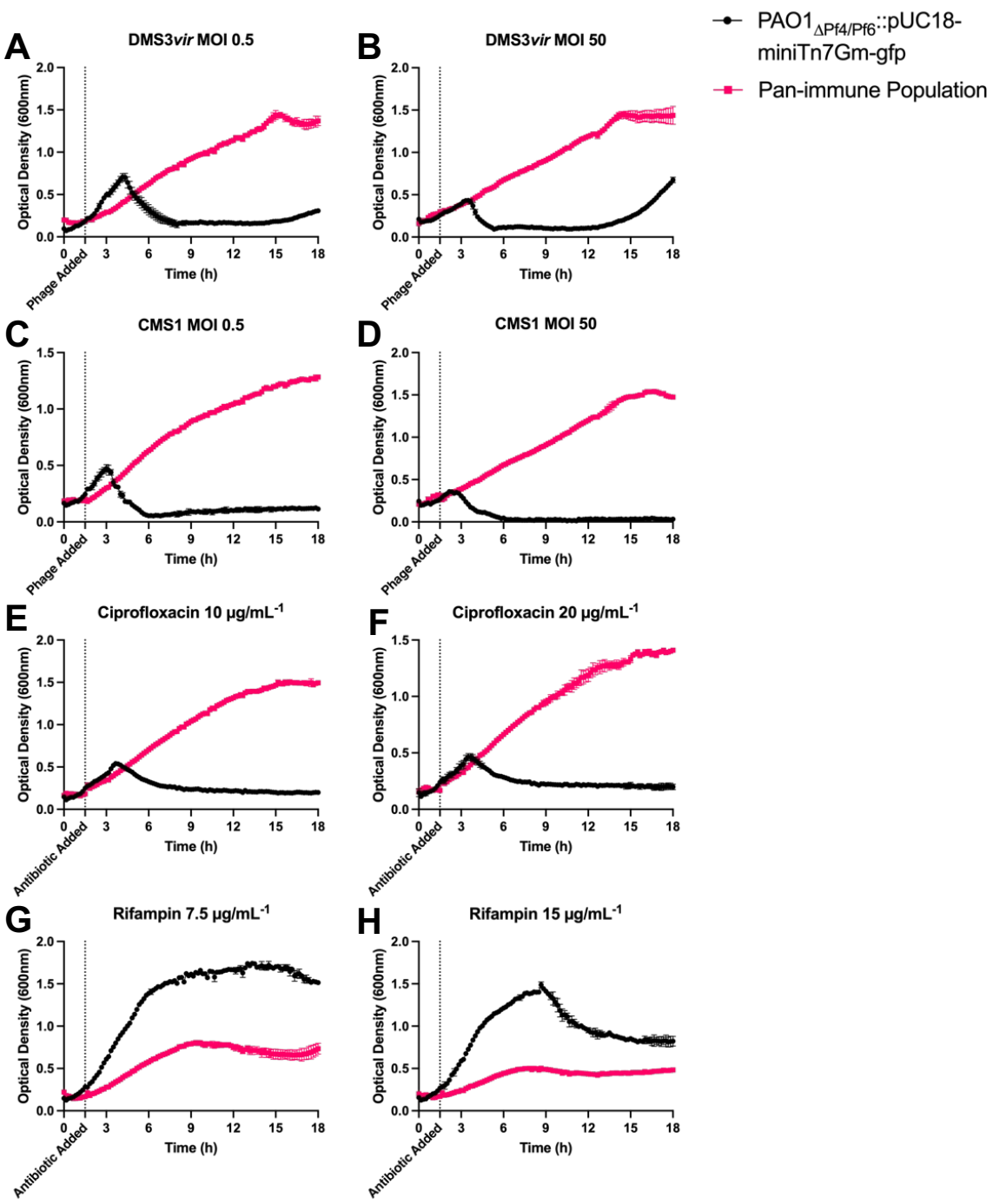

Figure S4- 1: Trial v02 pan-immune population tolerant to ciprofloxacin, rifampin, and virulent phages DMS3*vir* and CMS1. Overnight cultures of the indicated *P. aeruginosa* strains were diluted with LB to an OD_{600} of 0.05. Growth curves over 18h are shown. OD_{600} was measured in a CLARIOstar (BMG Labtech) plate reader at 37ºC with shaking prior to each measurement. Cells were infected with virulent phage DMS3*vir* **(A/B)** or CMS1 **(C/D)** an OD_{600} of 0.2, 1.5h post-inoculation (dotted line) at a MOI of 0.5 or 50. Antibiotics ciprofloxacin **(E/F)** or rifampin **(G/H)** were added to the indicated final concentration at an OD_{600} of 0.2, 1.5h post-inoculation (dotted line). Results are mean ± SD of three experiments.

REFRENCES

1. Taylor VL, Fitzpatrick AD, Islam Z, Maxwell KL. 2019. The Diverse Impacts of Phage Morons on Bacterial Fitness and Virulence. Adv Virus Res 103:1-31.
2. Chang YW, Kjær A, Ortega DR, Kovacikova G, Sutherland JA, Rettberg LA, Taylor RK, Jensen GJ. 2017. Architecture of the Vibrio cholerae toxin-coregulated pilus machine revealed by electron cryotomography. Nat Microbiol 2:16269.
3. Li Y, Liu X, Tang K, Wang P, Zeng Z, Guo Y, Wang X. 2019. Excisionase in Pf filamentous prophage controls lysis-lysogeny decision-making in Pseudomonas aeruginosa. Mol Microbiol 111:495-513.
4. Paget MS, Helmann JD. 2003. Genome Biology 4:203.
5. Ismail MH, Michie KA, Goh YF, Noorian P, Kjelleberg S, Duggin IG, McDougald D, Rice SA. 2021. The repressor C protein, Pf4r, controls superinfection of Pseudomonas aeruginosa PAO1 by the Pf4 filamentous phage and regulates host gene expression. Viruses 13:1614.
6. Conners R, León-Quezada RI, McLaren M, Bennett NJ, Daum B, Rakonjac J, Gold VAM. 2023. Cryo-electron microscopy of the f1 filamentous phage reveals insights into viral infection and assembly. Nature Communications 14:2724.
7. Crooks GE, Hon G, Chandonia JM, Brenner SE. 2004. WebLogo: a sequence logo generator. Genome Res 14:1188-90.
8. Winsor GL, Griffiths EJ, Lo R, Dhillon BK, Shay JA, Brinkman FS. 2016. Enhanced annotations and features for comparing thousands of Pseudomonas genomes in the Pseudomonas genome database. Nucleic acids research 44:D646-53.
9. McLeod SM, Kimsey HH, Davis BM, Waldor MK. 2005. CTXφ and *Vibrio cholerae*: exploring a newly recognized type of phage–host cell relationship. Molecular Microbiology 57:347-356.
10. Davis BM, Waldor MK. 2003. Filamentous phages linked to virulence of Vibrio cholerae. Current Opinion in Microbiology 6:35-42.
11. Schwartzkopf CM, Taylor VL, Groleau MC, Faith DR, Schmidt AK, Lamma TL, Brooks DM, Déziel E, Maxwell KL, Secor PR. 2024. Inhibition of PQS signaling by the Pf bacteriophage protein PfsE enhances viral replication in *Pseudomonas aeruginosa*. Molecular Microbiology 121:116-128.
12. Castang S, Dove SL. 2012. Basis for the essentiality of H-NS family members in Pseudomonas aeruginosa. Journal of bacteriology 194:5101-9.
13. Jumper J, Evans R, Pritzel A, Green T, Figurnov M, Ronneberger O, Tunyasuvunakool K, Bates R, Zidek A, Potapenko A, Bridgland A, Meyer C, Kohl SAA, Ballard AJ, Cowie A, Romera-Paredes B, Nikolov S, Jain R, Adler J, Back T, Petersen S, Reiman D, Clancy E, Zielinski M, Steinegger M, Pacholska M, Berghammer T, Bodenstein S, Silver D, Vinyals O, Senior AW, Kavukcuoglu K, Kohli P, Hassabis D. 2021. Highly accurate protein structure prediction with AlphaFold. Nature doi:10.1038/s41586-021-03819-2.

14. McCallum M, Tammam S, Little DJ, Robinson H, Koo J, Shah M, Calmettes C, Moraes TF, Burrows LL, Howell PL. 2016. PilN Binding Modulates the Structure and Binding Partners of the Pseudomonas aeruginosa Type IVa Pilus Protein PilM. J Biol Chem 291:11003-15.
15. Martinez E, Campos-Gomez J. 2016. Pf Filamentous Phage Requires UvrD for Replication in Pseudomonas aeruginosa. mSphere 1.
16. Schmidt AK, Fitzpatrick AD, Schwartzkopf CM, Faith DR, Jennings LK, Coluccio A, Hunt DJ, Michaels LA, Hargil A, Chen Q, Bollyky PL, Dorward DW, Wachter J, Rosa PA, Maxwell KL, Secor PR. 2022. A Filamentous Bacteriophage Protein Inhibits Type IV Pili To Prevent Superinfection of Pseudomonas aeruginosa. mBio 13:e02441-21.
17. Secor PR, Burgener EB, Kinnersley M, Jennings LK, Roman-Cruz V, Popescu M, Van Belleghem JD, Haddock N, Copeland C, Michaels LA, de Vries CR, Chen Q, Pourtois J, Wheeler TJ, Milla CE, Bollyky PL. 2020. Pf Bacteriophage and Their Impact on Pseudomonas Virulence, Mammalian Immunity, and Chronic Infections. Front Immunol 11:244.
18. Loeb T. 1960. Isolation of a bacteriophage specific for the F plus and Hfr mating types of *Escherichia coli* K-12. Science 131:932-3.
19. Hofschneider PH, Preuss A. 1963. M13 bacteriophage liberation from intact bacteria as revealed by electron microscopy. Journal of Molecular Biology 7:450-IN5.
20. Marvin DA, Hoffmann-Berling H. 1963. Physical and Chemical Properties of Two New Small Bacteriophages. Nature 197:517-518.
21. Roux S, Krupovic M, Daly RA, Borges AL, Nayfach S, Schulz F, Sharrar A, Matheus Carnevali PB, Cheng JF, Ivanova NN, Bondy-Denomy J, Wrighton KC, Woyke T, Visel A, Kyrpides NC, Eloe-Fadrosh EA. 2019. Cryptic inoviruses revealed as pervasive in bacteria and archaea across Earth's biomes. Nat Microbiol 4:1895-1906.
22. Hay ID, Lithgow T. 2019. Filamentous phages: masters of a microbial sharing economy. Embo Reports 20.
23. Knezevic P, Adriaenssens EM, Consortium IR. 2021. ICTV Virus Taxonomy Profile: Inoviridae. The Journal of General Virology 102.
24. Jia K, Peng Y, Chen X, Jian H, Jin M, Yi Z, Su M, Dong X, Yi M. 2022. A Novel Inovirus Reprograms Metabolism and Motility of Marine *Alteromonas*. Microbiology Spectrum 10:e03388-22.
25. Xu J, Dayan N, Goldbourt A, Xiang Y. 2019. Cryo-electron microscopy structure of the filamentous bacteriophage IKe. Proceedings of the National Academy of Sciences 116:5493-5498.
26. Böhning J, Graham M, Letham SC, Davis LK, Schulze U, Stansfeld PJ, Corey RA, Pearce P, Tarafder AK, Bharat TAM. 2023. Biophysical basis of filamentous phage tactoid-mediated antibiotic tolerance in *P. aeruginosa*. Nature Communications 14:8429.
27. Mai-Prochnow A, Hui JG, Kjelleberg S, Rakonjac J, McDougald D, Rice SA. 2015. 'Big things in small packages: the genetics of filamentous phage and effects on fitness of their host'. FEMS Microbiol Rev 39:465-87.
28. Bertozzi Silva J, Storms Z, Sauvageau D. 2016. Host receptors for bacteriophage adsorption. FEMS Microbiol Lett 363.

29. Jin X, Marshall JS. 2020. Mechanics of biofilms formed of bacteria with fimbriae appendages. PLOS ONE 15:e0243280.
30. Chen F-J, Chan C-H, Huang Y-J, Liu K-L, Peng H-L, Chang H-Y, Liou G-G, Yew T-R, Liu C-H, Hsu KY, Hsu L. 2011. Structural and Mechanical Properties of *Klebsiella pneumoniae* Type 3 Fimbriae. Journal of Bacteriology 193:1718-1725.
31. Burrows LL. 2012. Pseudomonas aeruginosa twitching motility: type IV pili in action. Annu Rev Microbiol 66:493-520.
32. Averhoff B, Friedrich A. 2003. Type IV pili-related natural transformation systems: DNA transport in mesophilic and thermophilic bacteria. Archives of microbiology 180:385-393.
33. Reguera G, McCarthy KD, Mehta T, Nicoll JS, Tuominen MT, Lovley DR. 2005. Extracellular electron transfer via microbial nanowires. Nature 435:1098-1101.
34. Click EM, Webster RE. 1997. Filamentous phage infection: required interactions with the TolA protein. Journal of bacteriology 179:6464-6471.
35. Holliger P, Riechmann L. 1997. A conserved infection pathway for filamentous bacteriophages is suggested by the structure of the membrane penetration domain of the minor coat protein g3p from phage fd. Structure 5:265-275.
36. Rakonjac J, Bennett NJ, Spagnuolo J, Gagic D, Russel M. 2011. Filamentous bacteriophage: biology, phage display and nanotechnology applications. Current issues in molecular biology 13:51-76.
37. Smilowitz H. 1974. Bacteriophage f1 Infection: Fate of the Parental Major Coat Protein. Journal of Virology 13:94-99.
38. Higashitani A, Higashitani N, Horiuchi K. 1997. Minus-strand origin of filamentous phage versus transcriptional promoters in recognition of RNA polymerase. Proceedings of the National Academy of Sciences 94:2909-2914.
39. Zenkin N, Naryshkina T, Kuznedelov K, Severinov K. 2006. The mechanism of DNA replication primer synthesis by RNA polymerase. Nature 439:617-620.
40. Horiuchi K. 1997. Initiation mechanisms in replication of filamentous phage DNA. Genes to Cells 2:425-432.
41. Fiedoruk K, Zakrzewska M, Daniluk T, Piktel E, Chmielewska S, Bucki R. 2020. Two Lineages of Pseudomonas aeruginosa Filamentous Phages: Structural Uniformity over Integration Preferences. Genome Biology and Evolution 12:1765-1781.
42. Davis BM, Waldor MK. 2000. CTXφ contains a hybrid genome derived from tandemly integrated elements. Proceedings of the National Academy of Sciences 97:8572-8577.
43. Moyer KE, Kimsey HH, Waldor MK. 2001. Evidence for a rolling-circle mechanism of phage DNA synthesis from both replicative and integrated forms of CTXφ. Molecular Microbiology 41:311-323.
44. Das B, Bischerour J, Barre F-X. 2011. VGJϕ integration and excision mechanisms contribute to the genetic diversity of *Vibrio cholerae* epidemic strains. Proceedings of the National Academy of Sciences 108:2516-2521.
45. Askora A, Kawasaki T, Fujie M, Yamada T. 2011. Resolvase-like serine recombinase mediates integration/excision in the bacteriophage ϕRSM. Journal of Bioscience and Bioengineering 111:109-116.

46. Martínez E, Paly E, Barre F-X. 2015. CTXφ Replication Depends on the Histone-Like HU Protein and the UvrD Helicase. PLOS Genetics 11:e1005256.
47. Horabin JI, Webster RE. 1986. Morphogenesis of f1 filamentous bacteriophage. Increased expression of gene I inhibits bacterial growth. J Mol Biol 188:403-13.
48. Horabin JI, Webster RE. 1988. An amino acid sequence which directs membrane insertion causes loss of membrane potential. J Biol Chem 263:11575-83.
49. Russel M. 1995. Moving through the membrane with filamentous phages. Trends Microbiol 3:223-8.
50. Pratt D, Tzagoloff H, Erdahl WS. 1966. Conditional lethal mutants of the small filamentous coliphage M13: I. Isolation, complementation, cell killing, time of cistron action. Virology 30:397-410.
51. Marvin DA, Hohn B. 1969. Filamentous bacterial viruses. Bacteriological Reviews 33:172-209.
52. Bondy-Denomy J, Qian J, Westra ER, Buckling A, Guttman DS, Davidson AR, Maxwell KL. 2016. Prophages mediate defense against phage infection through diverse mechanisms. Isme Journal 10:2854-2866.
53. Karaolis DKR, Somara S, Maneval DR, Johnson JA, Kaper JB. 1999. A bacteriophage encoding a pathogenicity island, a type-IV pilus and a phage receptor in cholera bacteria. Nature 399:375-379.
54. Zhou S, Liu Z, Song J, Chen Y. 2023. Disarm The Bacteria: What Temperate Phages Can Do. Current Issues in Molecular Biology 45:1149-1167.
55. Varani AM, Monteiro-Vitorello CB, Nakaya HI, Van Sluys MA. 2013. The role of prophage in plant-pathogenic bacteria. Annu Rev Phytopathol 51:429-51.
56. Ilyina TS. 2015. Filamentous Bacteriophages and Their Role in the Virulence and Evolution of Pathogenic Bacteria. Molecular Genetics Microbiology and Virology 30:1-9.
57. Secor PR, Sweere JM, Michaels LA, Malkovskiy AV, Lazzareschi D, Katznelson E, Rajadas J, Birnbaum ME, Arrigoni A, Braun KR, Evanko SP, Stevens DA, Kaminsky W, Singh PK, Parks WC, Bollyky PL. 2015. Filamentous Bacteriophage Promote Biofilm Assembly and Function. Cell Host Microbe 18:549-59.
58. Bille E, Meyer J, Jamet A, Euphrasie D, Barnier JP, Brissac T, Larsen A, Pelissier P, Nassif X. 2017. A virulence-associated filamentous bacteriophage of Neisseria meningitidis increases host-cell colonisation. PLoS Pathog 13:e1006495.
59. Bondy-Denomy J, Davidson AR. 2014. When a Virus is not a Parasite: The Beneficial Effects of Prophages on Bacterial Fitness. Journal of Microbiology 52:235-242.
60. Chung IY, Jang HJ, Bae HW, Cho YH. 2014. A phage protein that inhibits the bacterial ATPase required for type IV pilus assembly. Proceedings of the National Academy of Sciences of the United States of America 111:11503-11508.
61. Snyder JA, Haugen BJ, Lockatell CV, Maroncle N, Hagan EC, Johnson DE, Welch RA, Mobley HLT. 2005. Coordinate Expression of Fimbriae in Uropathogenic *Escherichia coli*. Infection and Immunity 73:7588-7596.
62. Hornick DB, Allen BL, Horn MA, Clegg S. 1992. Adherence to respiratory epithelia by recombinant *Escherichia coli* expressing *Klebsiella pneumoniae* type 3 fimbrial gene products. Infection and Immunity 60:1577-1588.
63. Anger R, Pieulle L, Shahin M, Valette O, Le Guenno H, Kosta A, Pelicic V, Fronzes R. 2023. Structure of a heteropolymeric type 4 pilus from a monoderm bacterium. Nature Communications 14.

64. Knezevic P, Voet M, Lavigne R. 2015. Prevalence of Pf1-like (pro)phage genetic elements among Pseudomonas aeruginosa isolates. Virology 483:64-71.
65. Goldbourt A, Gross BJ, Day LA, McDermott AE. 2007. Filamentous phage studied by magic-angle spinning NMR: Resonance assignment and secondary structure of the coat protein in Pf1. Journal of the American Chemical Society 129:2338-2344.
66. Secor PR, Burgener EB, Kinnersley M, Jennings LK, Roman-Cruz V, Popescu M, Van Belleghem JD, Haddock N, Copeland C, Michaels LA. 2020. Pf bacteriophage and their impact on Pseudomonas virulence, mammalian immunity, and chronic infections. Frontiers in Immunology 11:244.
67. Takeya K, Amako K. 1966. A rod-shaped Pseudomonas phage. Virology 28:163-165.
68. Harms A, Diard M. 2019. Crowd Controlled-Host Quorum Sensing Drives Phage Decision. Cell Host Microbe 25:179-181.
69. Maxwell KL. 2019. Phages Tune in to Host Cell Quorum Sensing. Cell 176:7-8.
70. Silpe JE, Bassler BL. 2019. A Host-Produced Quorum-Sensing Autoinducer Controls a Phage Lysis-Lysogeny Decision. Cell 176:268-280 e13.
71. Lee Y, Song S, Sheng L, Zhu L, Kim J-S, Wood TK. 2018. Substrate binding protein DppA1 of ABC transporter DppBCDF increases biofilm formation in Pseudomonas aeruginosa by inhibiting Pf5 prophage lysis. Frontiers in microbiology 9:30.
72. Castang S, McManus HR, Turner KH, Dove SL. 2008. H-NS family members function coordinately in an opportunistic pathogen. Proceedings of the National Academy of Sciences of the United States of America 105:18947-52.
73. Li C, Wally H, Miller SJ, Lu C-D. 2009. The Multifaceted Proteins MvaT and MvaU, Members of the H-NS Family, Control Arginine Metabolism, Pyocyanin Synthesis, and Prophage Activation in Pseudomonas aeruginosa PAO1. Journal of Bacteriology 191:6211-6218.
74. Guo Y, Tang K, Sit B, Gu J, Chen R, Lin J, Lin S, Liu X, Wang W, Gao X. 2022. Dual control of lysogeny and phage defense by a phosphorylation-based toxin/antitoxin system. bioRxiv:2022.09. 05.506569.
75. Castang S, McManus HR, Turner KH, Dove SL. 2008. H-NS family members function coordinately in an opportunistic pathogen. Proc Natl Acad Sci U S A 105:18947-52.
76. Castang S, Dove SL. 2012. Basis for the essentiality of H-NS family members in Pseudomonas aeruginosa. Journal of bacteriology 194:5101-5109.
77. Wei Q, Le Minh PN, Dötsch A, Hildebrand F, Panmanee W, Elfarash A, Schulz S, Plaisance S, Charlier D, Hassett D. 2012. Global regulation of gene expression by OxyR in an important human opportunistic pathogen. Nucleic acids research 40:4320-4333.
78. Martínez E, Campos-Gómez J. 2016. Pf filamentous phage requires UvrD for replication in Pseudomonas aeruginosa. MSphere 1:e00104-15.
79. Chen M, Samuelson JC, Jiang F, Muller M, Kuhn A, Dalbey RE. 2002. Direct interaction of YidC with the Sec-independent Pf3 coat protein during its membrane protein insertion. Journal of Biological Chemistry 277:7670-7675.

80. Liu DJ, Day LA. 1994. Pf1 virus structure: helical coat protein and DNA with paraxial phosphates. Science 265:671-674.
81. Tsao Y-F, Taylor VL, Kala S, Bondy-Denomy J, Khan AN, Bona D, Cattoir V, Lory S, Davidson AR, Maxwell KL. 2018. Phage morons play an important role in Pseudomonas aeruginosa phenotypes. Journal of bacteriology 200.
82. Shah M, Taylor VL, Bona D, Tsao Y, Stanley SY, Pimentel-Elardo SM, McCallum M, Bondy-Denomy J, Howell PL, Nodwell JR, Davidson AR, Moraes TF, Maxwell KL. 2021. A phage-encoded anti-activator inhibits quorum sensing in Pseudomonas aeruginosa. Mol Cell doi:10.1016/j.molcel.2020.12.011.
83. Chung IY, Jang HJ, Bae HW, Cho YH. 2014. A phage protein that inhibits the bacterial ATPase required for type IV pilus assembly. Proc Natl Acad Sci U S A 111:11503-8.
84. Rice SA, Tan CH, Mikkelsen PJ, Kung V, Woo J, Tay M, Hauser A, McDougald D, Webb JS, Kjelleberg S. 2009. The biofilm life cycle and virulence of Pseudomonas aeruginosa are dependent on a filamentous prophage. ISME J 3:271-82.
85. Hui JGK, Mai-Prochnow A, Kjelleberg S, McDougald D, Rice SA. 2014. Environmental cues and genes involved in establishment of the superinfective Pf4 phage of Pseudomonas aeruginosa. Frontiers in Microbiology 5.
86. Webb JS, Lau M, Kjelleberg S. 2004. Bacteriophage and phenotypic variation in Pseudomonas aeruginosa biofilm development. J Bacteriol 186:8066-73.
87. Webb JS, Thompson LS, James S, Charlton T, Tolker-Nielsen T, Koch B, Givskov M, Kjelleberg S. 2003. Cell death in Pseudomonas aeruginosa biofilm development. J Bacteriol 185:4585-92.
88. Whitchurch CB, Tolker-Nielsen T, Ragas PC, Mattick JS. 2002. Extracellular DNA required for bacterial biofilm formation. Science 295:1487-1487.
89. Saunders SH, Edmund C, Yates MD, Otero FJ, Trammell SA, Stemp ED, Barton JK, Tender LM, Newman DK. 2020. Extracellular DNA promotes efficient extracellular electron transfer by pyocyanin in Pseudomonas aeruginosa biofilms. Cell 182:919-932. e19.
90. Barraud N, Hassett DJ, Hwang S-H, Rice SA, Kjelleberg S, Webb JS. 2006. Involvement of nitric oxide in biofilm dispersal of Pseudomonas aeruginosa. Journal of bacteriology 188:7344-7353.
91. McElroy KE, Hui JG, Woo JK, Luk AW, Webb JS, Kjelleberg S, Rice SA, Thomas T. 2014. Strain-specific parallel evolution drives short-term diversification during Pseudomonas aeruginosa biofilm formation. Proceedings of the National Academy of Sciences 111:E1419-E1427.
92. Heydorn A, Ersbøll B, Kato J, Hentzer M, Parsek MR, Tolker-Nielsen T, Givskov M, Molin S. 2002. Statistical analysis of Pseudomonas aeruginosa biofilm development: impact of mutations in genes involved in twitching motility, cell-to-cell signaling, and stationary-phase sigma factor expression. Applied and Environmental Microbiology 68:2008-2017.
93. Klausen M, Heydorn A, Ragas P, Lambertsen L, Aaes-Jørgensen A, Molin S, Tolker-Nielsen T. 2003. Biofilm formation by Pseudomonas aeruginosa wild type, flagella and type IV pili mutants. Molecular microbiology 48:1511-1524.

94. O'Toole GA, Kolter R. 1998. Flagellar and twitching motility are necessary for Pseudomonas aeruginosa biofilm development. Molecular microbiology 30:295-304.
95. Hauser AR, Jain M, Bar-Meir M, McColley SA. 2011. Clinical significance of microbial infection and adaptation in cystic fibrosis. Clin Microbiol Rev 24:29-70.
96. Pang Z, Raudonis R, Glick BR, Lin TJ, Cheng Z. 2019. Antibiotic resistance in Pseudomonas aeruginosa: mechanisms and alternative therapeutic strategies. Biotechnol Adv 37:177-192.
97. Ramos GP, Rocha JL, Tuon FF. 2013. Seasonal humidity may influence Pseudomonas aeruginosa hospital-acquired infection rates. International Journal of Infectious Diseases 17:E757-E761.
98. Quinton PM. 2008. Cystic fibrosis: impaired bicarbonate secretion and mucoviscidosis. Lancet 372:415-7.
99. Burgener EB, Sweere JM, Bach MS, Secor PR, Haddock N, Jennings LK, Marvig RL, Johansen HK, Rossi E, Cao X, Tian L, Nedelec L, Molin S, Bollyky PL, Milla CE. 2019. Filamentous bacteriophages are associated with chronic Pseudomonas lung infections and antibiotic resistance in cystic fibrosis. Sci Transl Med 11.
100. Folkesson A, Jelsbak L, Yang L, Johansen HK, Ciofu O, Hoiby N, Molin S. 2012. Adaptation of *Pseudomonas aeruginosa* to the cystic fibrosis airway: an evolutionary perspective. Nature reviews Microbiology 10:841-51.
101. Asokan GV, Ramadhan T, Ahmed E, Sanad H. 2019. WHO Global Priority Pathogens List: A Bibliometric Analysis of Medline-PubMed for Knowledge Mobilization to Infection Prevention and Control Practices in Bahrain. Oman Med J 34:184-193.
102. Rice SA, Tan CH, Mikkelsen PJ, Kung V, Woo J, Tay M, Hauser A, McDougald D, Webb JS, Kjelleberg S. 2009. The biofilm life cycle and virulence of Pseudomonas aeruginosa are dependent on a filamentous prophage. The ISME journal 3:271-82.
103. Tarafder AK, von Kugelgen A, Mellul AJ, Schulze U, Aarts D, Bharat TAM. 2020. Phage liquid crystalline droplets form occlusive sheaths that encapsulate and protect infectious rod-shaped bacteria. Proc Natl Acad Sci U S A 117:4724-4731.
104. Burgener EB, Sweere JM, Bach MS, Secor PR, Haddock N, Jennings LK, Marvig RL, Johansen HK, Rossi E, Cao X. 2019. Filamentous bacteriophages are associated with chronic Pseudomonas lung infections and antibiotic resistance in cystic fibrosis. Science translational medicine 11:eaau9748.
105. Sweere JM, Van Belleghem JD, Ishak H, Bach MS, Popescu M, Sunkari V, Kaber G, Manasherob R, Suh GA, Cao X, de Vries CR, Lam DN, Marshall PL, Birukova M, Katznelson E, Lazzareschi DV, Balaji S, Keswani SG, Hawn TR, Secor PR, Bollyky PL. 2019. Bacteriophage trigger antiviral immunity and prevent clearance of bacterial infection. Science 363.
106. Whiteley M, Bangera MG, Bumgarner RE, Parsek MR, Teitzel GM, Lory S, Greenberg EP. 2001. Gene expression in Pseudomonas aeruginosa biofilms. Nature 413:860-4.
107. Papenfort K, Bassler BL. 2016. Quorum sensing signal-response systems in Gram-negative bacteria. Nat Rev Microbiol 14:576-88.
108. Smith P, Schuster M. 2022. Antiactivators prevent self-sensing in Pseudomonas aeruginosa quorum sensing. Proceedings of the National Academy of Sciences 119:e2201242119.

109. Schuster M, Greenberg EP. 2006. A network of networks: quorum-sensing gene regulation in Pseudomonas aeruginosa. Int J Med Microbiol 296:73-81.
110. Lee J, Zhang L. 2015. The hierarchy quorum sensing network in Pseudomonas aeruginosa. Protein Cell 6:26-41.
111. Pearson JP, Gray KM, Passador L, Tucker KD, Eberhard A, Iglewski BH, Greenberg EP. 1994. Structure of the autoinducer required for expression of Pseudomonas aeruginosa virulence genes. Proc Natl Acad Sci U S A 91:197-201.
112. Pearson JP, Passador L, Iglewski BH, Greenberg EP. 1995. A second N-acylhomoserine lactone signal produced by Pseudomonas aeruginosa. Proc Natl Acad Sci U S A 92:1490-4.
113. Diggle SP, Matthijs S, Wright VJ, Fletcher MP, Chhabra SR, Lamont IL, Kong X, Hider RC, Cornelis P, Cámara M. 2007. The Pseudomonas aeruginosa 4-quinolone signal molecules HHQ and PQS play multifunctional roles in quorum sensing and iron entrapment. Chemistry & biology 14:87-96.
114. Xiao G, Déziel E, He J, Lépine F, Lesic B, Castonguay MH, Milot S, Tampakaki AP, Stachel SE, Rahme LG. 2006. MvfR, a key Pseudomonas aeruginosa pathogenicity LTTR-class regulatory protein, has dual ligands. Molecular microbiology 62:1689-1699.
115. García-Reyes S, Soberón-Chávez G, Cocotl-Yanez M. 2020. The third quorum-sensing system of Pseudomonas aeruginosa: Pseudomonas quinolone signal and the enigmatic PqsE protein. Journal of medical microbiology 69:25-34.
116. Mukherjee S, Moustafa DA, Stergioula V, Smith CD, Goldberg JB, Bassler BL. 2018. The PqsE and RhlR proteins are an autoinducer synthase-receptor pair that control virulence and biofilm development in Pseudomonas aeruginosa. Proc Natl Acad Sci U S A 115:E9411-E9418.
117. Farrow III JM, Sund ZM, Ellison ML, Wade DS, Coleman JP, Pesci EC. 2008. PqsE functions independently of PqsR-Pseudomonas quinolone signal and enhances the rhl quorum-sensing system. Journal of bacteriology 190:7043-7051.
118. Lee J, Wu J, Deng Y, Wang J, Wang C, Wang J, Chang C, Dong Y, Williams P, Zhang LH. 2013. A cell-cell communication signal integrates quorum sensing and stress response. Nat Chem Biol 9:339-43.
119. Eickhoff MJ, Bassler BL. 2018. SnapShot: bacterial quorum sensing. Cell 174:1328-1328. e1.
120. Whiteley M, Lee KM, Greenberg E. 1999. Identification of genes controlled by quorum sensing in Pseudomonas aeruginosa. Proceedings of the National Academy of Sciences 96:13904-13909.
121. Kariminik A, Baseri-Salehi M, Kheirkhah B. 2017. Pseudomonas aeruginosa quorum sensing modulates immune responses: an updated review article. Immunology letters 190:1-6.
122. Taylor IR, Paczkowski JE, Jeffrey PD, Henke BR, Smith CD, Bassler BL. 2021. Inhibitor Mimetic Mutations in the Pseudomonas aeruginosa PqsE Enzyme Reveal a Protein–Protein Interaction with the Quorum-Sensing Receptor RhlR That Is Vital for Virulence Factor Production. ACS chemical biology 16:740-752.
123. Pierson LS, Pierson EA. 2010. Metabolism and function of phenazines in bacteria: impacts on the behavior of bacteria in the environment and biotechnological processes. Applied microbiology and biotechnology 86:1659-1670.

124. Meirelles LA, Newman DK. 2018. Both toxic and beneficial effects of pyocyanin contribute to the lifecycle of Pseudomonas aeruginosa. Mol Microbiol 110:995-1010.
125. Lau GW, Hassett DJ, Ran H, Kong F. 2004. The role of pyocyanin in Pseudomonas aeruginosa infection. Trends in molecular medicine 10:599-606.
126. Choi W, Choe S, Lin J, Borchers MT, Kosmider B, Vassallo R, Limper AH, Lau GW. 2020. Exendin-4 restores airway mucus homeostasis through the GLP1R-PKA-PPARγ-FOXA2-phosphatase signaling. Mucosal immunology 13:637-651.
127. Secor PR, Michaels LA, Smigiel KS, Rohani MG, Jennings LK, Hisert KB, Arrigoni A, Braun KR, Birkland TP, Lai Y, Hallstrand TS, Bollyky PL, Singh PK, Parks WC. 2017. Filamentous Bacteriophage Produced by Pseudomonas aeruginosa Alters the Inflammatory Response and Promotes Noninvasive Infection In Vivo. Infect Immun 85.
128. McElroy KE, Hui JG, Woo JK, Luk AW, Webb JS, Kjelleberg S, Rice SA, Thomas T. 2014. Strain-specific parallel evolution drives short-term diversification during Pseudomonas aeruginosa biofilm formation. Proceedings of the National Academy of Sciences of the United States of America 111:E1419-27.
129. Webb JS, Lau M, Kjelleberg S. 2004. Bacteriophage and phenotypic variation in Pseudomonas aeruginosa biofilm development. Journal of bacteriology 186:8066-73.
130. Webb JS, Thompson LS, James S, Charlton T, Tolker-Nielsen T, Koch B, Givskov M, Kjelleberg S. 2003. Cell death in Pseudomonas aeruginosa biofilm development. Journal of bacteriology 185:4585-92.
131. Petrova OE, Schurr JR, Schurr MJ, Sauer K. 2011. The novel Pseudomonas aeruginosa two-component regulator BfmR controls bacteriophage-mediated lysis and DNA release during biofilm development through PhdA. Molecular microbiology 81:767-83.
132. Tsao YF, Taylor VL, Kala S, Bondy-Denomy J, Khan AN, Bona D, Cattoir V, Lory S, Davidson AR, Maxwell KL. 2018. Phage Morons Play an Important Role in Pseudomonas aeruginosa Phenotypes. J Bacteriol 200.
133. Roux S, Krupovic M, Daly RA, Borges AL, Nayfach S, Schulz F, Sharrar A, Matheus Carnevali PB, Cheng JF, Ivanova NN, Bondy-Denomy J, Wrighton KC, Woyke T, Visel A, Kyrpides NC, Eloe-Fadrosh EA. 2019. Cryptic inoviruses revealed as pervasive in bacteria and archaea across Earth's biomes. Nat Microbiol doi:10.1038/s41564-019-0510-x.
134. Bondy-Denomy J, Qian J, Westra ER, Buckling A, Guttman DS, Davidson AR, Maxwell KL. 2016. Prophages mediate defense against phage infection through diverse mechanisms. ISME J 10:2854-2866.
135. Murray TS, Kazmierczak BI. 2008. Pseudomonas aeruginosa exhibits sliding motility in the absence of type IV pili and flagella. J Bacteriol 190:2700-8.
136. Burgener EB, Secor PR, Tracy MC, Sweere JM, Bik EM, Milla CE, Bollyky PL. 2020. Methods for Extraction and Detection of Pf Bacteriophage DNA from the Sputum of Patients with Cystic Fibrosis. Phage (New Rochelle) 1:100-108.
137. Lanzarotti E, Biekofsky RR, Estrin DA, Marti MA, Turjanski AG. 2011. Aromatic-aromatic interactions in proteins: beyond the dimer. J Chem Inf Model 51:1623-33.

138. Stahelin RV, Cho W. 2001. Differential roles of ionic, aliphatic, and aromatic residues in membrane-protein interactions: a surface plasmon resonance study on phospholipases A2. Biochemistry 40:4672-8.
139. Takhar HK, Kemp K, Kim M, Howell PL, Burrows LL. 2013. The platform protein is essential for type IV pilus biogenesis. J Biol Chem 288:9721-9728.
140. Lee YM, Tscherne DM, Yun SI, Frolov I, Rice CM. 2005. Dual mechanisms of pestiviral superinfection exclusion at entry and RNA replication. J Virol 79:3231-42.
141. Pourtois JD, Kratochvil MJ, Chen Q, Haddock NL, Burgener EB, De Leo GA, Bollyky PL. 2021. Filamentous Bacteriophages and the Competitive Interaction between Pseudomonas aeruginosa Strains under Antibiotic Treatment: a Modeling Study. mSystems 6:e0019321.
142. Comolli JC, Hauser AR, Waite L, Whitchurch CB, Mattick JS, Engel JN. 1999. Pseudomonas aeruginosa gene products PilT and PilU are required for cytotoxicity in vitro and virulence in a mouse model of acute pneumonia. Infection and immunity 67:3625-30.
143. Sauer K, Cullen MC, Rickard AH, Zeef LA, Davies DG, Gilbert P. 2004. Characterization of nutrient-induced dispersion in Pseudomonas aeruginosa PAO1 biofilm. Journal of bacteriology 186:7312-26.
144. Sauer K, Camper AK, Ehrlich GD, Costerton JW, Davies DG. 2002. Pseudomonas aeruginosa displays multiple phenotypes during development as a biofilm. Journal of bacteriology 184:1140-54.
145. Wright A, Hawkins CH, Anggard EE, Harper DR. 2009. A controlled clinical trial of a therapeutic bacteriophage preparation in chronic otitis due to antibiotic-resistant Pseudomonas aeruginosa; a preliminary report of efficacy. Clin Otolaryngol 34:349-57.
146. Bruttin A, Brussow H. 2005. Human volunteers receiving Escherichia coli phage T4 orally: a safety test of phage therapy. Antimicrob Agents Chemother 49:2874-8.
147. Rhoads DD, Wolcott RD, Kuskowski MA, Wolcott BM, Ward LS, Sulakvelidze A. 2009. Bacteriophage therapy of venous leg ulcers in humans: results of a phase I safety trial. J Wound Care 18:237-8, 240-3.
148. Schooley RT, Biswas B, Gill JJ, Hernandez-Morales A, Lancaster J, Lessor L, Barr JJ, Reed SL, Rohwer F, Benler S, Segall AM, Taplitz R, Smith DM, Kerr K, Kumaraswamy M, Nizet V, Lin L, McCauley MD, Strathdee SA, Benson CA, Pope RK, Leroux BM, Picel AC, Mateczun AJ, Cilwa KE, Regeimbal JM, Estrella LA, Wolfe DM, Henry MS, Quinones J, Salka S, Bishop-Lilly KA, Young R, Hamilton T. 2017. Development and Use of Personalized Bacteriophage-Based Therapeutic Cocktails To Treat a Patient with a Disseminated Resistant Acinetobacter baumannii Infection. Antimicrob Agents Chemother 61.
149. Dedrick RM, Guerrero-Bustamante CA, Garlena RA, Russell DA, Ford K, Harris K, Gilmour KC, Soothill J, Jacobs-Sera D, Schooley RT, Hatfull GF, Spencer H. 2019. Engineered bacteriophages for treatment of a patient with a disseminated drug-resistant Mycobacterium abscessus. Nat Med 25:730-733.
150. Aslam S, Courtwright AM, Koval C, Lehman SM, Morales S, Furr CL, Rosas F, Brownstein MJ, Fackler JR, Sisson BM, Biswas B, Henry M, Luu T, Bivens BN, Hamilton T, Duplessis C, Logan C, Law N, Yung G, Turowski J, Anesi J, Strathdee SA, Schooley RT. 2019. Early clinical experience of bacteriophage therapy in 3 lung transplant recipients. Am J Transplant 19:2631-2639.

151. Oechslin F. 2018. Resistance Development to Bacteriophages Occurring during Bacteriophage Therapy. Viruses 10.
152. Loc Carrillo C, Atterbury RJ, el-Shibiny A, Connerton PL, Dillon E, Scott A, Connerton IF. 2005. Bacteriophage therapy to reduce Campylobacter jejuni colonization of broiler chickens. Appl Environ Microbiol 71:6554-63.
153. Scott AE, Timms AR, Connerton PL, Loc Carrillo C, Adzfa Radzum K, Connerton IF. 2007. Genome dynamics of Campylobacter jejuni in response to bacteriophage predation. PLoS Pathog 3:e119.
154. Carvalho CM, Gannon BW, Halfhide DE, Santos SB, Hayes CM, Roe JM, Azeredo J. 2010. The in vivo efficacy of two administration routes of a phage cocktail to reduce numbers of Campylobacter coli and Campylobacter jejuni in chickens. BMC Microbiol 10:232.
155. Chung IY, Kim BO, Han JH, Park J, Kang HK, Park Y, Cho YH. 2021. A phage protein-derived antipathogenic peptide that targets type IV pilus assembly. Virulence 12:1377-1387.
156. Hmelo LR, Borlee BR, Almblad H, Love ME, Randall TE, Tseng BS, Lin C, Irie Y, Storek KM, Yang JJ, Siehnel RJ, Howell PL, Singh PK, Tolker-Nielsen T, Parsek MR, Schweizer HP, Harrison JJ. 2015. Precision-engineering the Pseudomonas aeruginosa genome with two-step allelic exchange. Nature protocols 10:1820-41.
157. Li Y, Liu X, Tang K, Wang W, Guo Y, Wang X. 2020. Prophage encoding toxin/antitoxin system PfiT/PfiA inhibits Pf4 production in Pseudomonas aeruginosa. Microb Biotechnol 13:1132-1144.
158. Qiu D, Damron FH, Mima T, Schweizer HP, Yu HD. 2008. PBAD-based shuttle vectors for functional analysis of toxic and highly regulated genes in Pseudomonas and Burkholderia spp. and other bacteria. Appl Environ Microbiol 74:7422-6.
159. Semmler AB, Whitchurch CB, Mattick JS. 1999. A re-examination of twitching motility in Pseudomonas aeruginosa. Microbiology 145 (Pt 10):2863-73.
160. Choi KH, Schweizer HP. 2006. mini-Tn7 insertion in bacteria with single attTn7 sites: example Pseudomonas aeruginosa. Nature protocols 1:153-61.
161. Pettersen EF, Goddard TD, Huang CC, Meng EC, Couch GS, Croll TI, Morris JH, Ferrin TE. 2021. UCSF ChimeraX: Structure visualization for researchers, educators, and developers. Protein Sci 30:70-82.
162. Holloway BW, Krishnapillai V, Morgan AF. 1979. Chromosomal genetics of Pseudomonas. Microbiological reviews 43:73-102.
163. Zhao K, Tseng BS, Beckerman B, Jin F, Gibiansky ML, Harrison JJ, Luijten E, Parsek MR, Wong GC. 2013. Psl trails guide exploration and microcolony formation in Pseudomonas aeruginosa biofilms. Nature 497:388-91.
164. Jennings LK, Storek KM, Ledvina HE, Coulon C, Marmont LS, Sadovskaya I, Secor PR, Tseng BS, Scian M, Filloux A, Wozniak DJ, Howell PL, Parsek MR. 2015. Pel is a cationic exopolysaccharide that cross-links extracellular DNA in the Pseudomonas aeruginosa biofilm matrix. Proc Natl Acad Sci U S A 112:11353-8.
165. Cruz RL, Asfahl KL, Van den Bossche S, Coenye T, Crabbe A, Dandekar AA. 2020. RhlR-Regulated Acyl-Homoserine Lactone Quorum Sensing in a Cystic Fibrosis Isolate of Pseudomonas aeruginosa. mBio 11.
166. Budzik JM, Rosche WA, Rietsch A, O'Toole GA. 2004. Isolation and characterization of a generalized transducing phage for Pseudomonas aeruginosa strains PAO1 and PA14. J Bacteriol 186:3270-3.

167. Chan BK, Sistrom M, Wertz JE, Kortright KE, Narayan D, Turner PE. 2016. Phage selection restores antibiotic sensitivity in MDR Pseudomonas aeruginosa. Sci Rep 6:26717.
168. Fiedoruk K, Zakrzewska M, Daniluk T, Piktel E, Chmielewska S, Bucki R. 2020. Two Lineages of Pseudomonas aeruginosa Filamentous Phages: Structural Uniformity over Integration Preferences. Genome Biol Evol 12:1765-1781.
169. Janmey PA, Slochower DR, Wang YH, Wen Q, Cebers A. 2014. Polyelectrolyte properties of filamentous biopolymers and their consequences in biological fluids. Soft Matter 10:1439-1449.
170. Schwartzkopf CM, Robinson AJ, Ellenbecker M, Faith DR, Schmidt AK, Brooks DM, Lewerke L, Voronina E, Dandekar AA, Secor PR. 2023. Tripartite interactions between filamentous Pf4 bacteriophage, Pseudomonas aeruginosa, and bacterivorous nematodes. PLoS Pathog 19:e1010925.
171. Schwartzkopf CM, Taylor VL, Groleau MC, Faith DR, Schmidt AK, Lamma TL, Brooks DM, Deziel E, Maxwell KL, Secor PR. 2023. Inhibition of PQS signaling by the Pf bacteriophage protein PfsE enhances viral replication in Pseudomonas aeruginosa. bioRxiv doi:10.1101/2023.08.25.554831.
172. Schmidt AK, Fitzpatrick AD, Schwartzkopf CM, Faith DR, Jennings LK, Coluccio A, Hunt DJ, Michaels LA, Hargil A, Chen Q, Bollyky PL, Dorward DW, Wachter J, Rosa PA, Maxwell KL, Secor PR. 2022. A Filamentous Bacteriophage Protein Inhibits Type IV Pili To Prevent Superinfection of Pseudomonas aeruginosa. mBio doi:10.1128/mbio.02441-21:e0244121.
173. Secor PR, Sass G, Nazik H, Stevens DA. 2017. Effect of acute predation with bacteriophage on intermicrobial aggression by Pseudomonas aeruginosa. PLoS One 12:e0179659.
174. Klockgether J, Munder A, Neugebauer J, Davenport CF, Stanke F, Larbig KD, Heeb S, Schock U, Pohl TM, Wiehlmann L, Tummler B. 2010. Genome diversity of Pseudomonas aeruginosa PAO1 laboratory strains. J Bacteriol 192:1113-21.
175. Breg JN, van Opheusden JH, Burgering MJ, Boelens R, Kaptein R. 1990. Structure of Arc repressor in solution: evidence for a family of beta-sheet DNA-binding proteins. Nature 346:586-9.
176. Vershon AK, Youderian P, Susskind MM, Sauer RT. 1985. The bacteriophage P22 arc and mnt repressors. Overproduction, purification, and properties. J Biol Chem 260:12124-9.
177. Tortuel D, Tahrioui A, David A, Cambronel M, Nilly F, Clamens T, Maillot O, Barreau M, Feuilloley MGJ, Lesouhaitier O, Filloux A, Bouffartigues E, Cornelis P, Chevalier S. 2022. Pf4 Phage Variant Infection Reduces Virulence-Associated Traits in Pseudomonas aeruginosa. Microbiology Spectrum 10:e01548-22.
178. Schwartzkopf CM, Taylor VL, Groleau MC, Faith DR, Schmidt AK, Lamma TL, Brooks DM, Deziel E, Maxwell KL, Secor PR. 2023. Inhibition of PQS signaling by the Pf bacteriophage protein PfsE enhances viral replication in Pseudomonas aeruginosa. Mol Microbiol doi:10.1111/mmi.15202.
179. Secor PR, Jennings LK, Michaels LA, Sweere JM, Singh PK, Parks WC, Bollyky PL. 2015. Biofilm assembly becomes crystal clear - filamentous bacteriophage organize the Pseudomonas aeruginosa biofilm matrix into a liquid crystal. Microb Cell 3:49-52.
180. O'Toole GA. 2011. Microtiter dish biofilm formation assay. Journal of visualized experiments : JoVE doi:10.3791/2437.

181. Dietrich LE, Price-Whelan A, Petersen A, Whiteley M, Newman DK. 2006. The phenazine pyocyanin is a terminal signalling factor in the quorum sensing network of Pseudomonas aeruginosa. Mol Microbiol 61:1308-21.
182. Schwartzkopf CM, Robinson AJ, Ellenbecker M, Faith DR, Schmidt AK, Brooks DM, Lewerke L, Voronina E, Dandekar AA, Secor PR. 2023. Tripartite interactions between filamentous Pf4 bacteriophage, Pseudomonas aeruginosa, and bacterivorous nematodes. PLOS Pathogens 19:e1010925.
183. Hilbi H, Weber SS, Ragaz C, Nyfeler Y, Urwyler S. 2007. Environmental predators as models for bacterial pathogenesis. Environ Microbiol 9:563-75.
184. Schulenburg H, Felix MA. 2017. The Natural Biotic Environment of Caenorhabditis elegans. Genetics 206:55-86.
185. Filipowicz A, Lalsiamthara J, Aballay A. 2021. TRPM channels mediate learned pathogen avoidance following intestinal distention. eLife 10:e65935.
186. Kaletsky R, Moore RS, Vrla GD, Parsons LR, Gitai Z, Murphy CT. 2020. C. elegans interprets bacterial non-coding RNAs to learn pathogenic avoidance. Nature 586:445-451.
187. Ghosh DD, Lee D, Jin X, Horvitz HR, Nitabach MN. 2021. *C. elegans* discriminates colors to guide foraging. Science 371:1059-1063.
188. Hao Y, Yang W, Ren J, Hall Q, Zhang Y, Kaplan JM. 2018. Thioredoxin shapes the C. elegans sensory response to Pseudomonas produced nitric oxide. eLife 7:e36833.
189. Wei Q, Minh PN, Dotsch A, Hildebrand F, Panmanee W, Elfarash A, Schulz S, Plaisance S, Charlier D, Hassett D, Haussler S, Cornelis P. 2012. Global regulation of gene expression by OxyR in an important human opportunistic pathogen. Nucleic Acids Res 40:4320-33.
190. Mooij MJ, Drenkard E, Llamas MA, Vandenbroucke-Grauls CM, Savelkoul PH, Ausubel FM, Bitter W. 2007. Characterization of the integrated filamentous phage Pf5 and its involvement in small-colony formation. Microbiology 153:1790-8.
191. Moura-Alves P, Puyskens A, Stinn A, Klemm M, Guhlich-Bornhof U, Dorhoi A, Furkert J, Kreuchwig A, Protze J, Lozza L, Pei G, Saikali P, Perdomo C, Mollenkopf HJ, Hurwitz R, Kirschhoefer F, Brenner-Weiss G, Weiner J, 3rd, Oschkinat H, Kolbe M, Krause G, Kaufmann SHE. 2019. Host monitoring of quorum sensing during Pseudomonas aeruginosa infection. Science 366.
192. Moura-Alves P, Fae K, Houthuys E, Dorhoi A, Kreuchwig A, Furkert J, Barison N, Diehl A, Munder A, Constant P, Skrahina T, Guhlich-Bornhof U, Klemm M, Koehler AB, Bandermann S, Goosmann C, Mollenkopf HJ, Hurwitz R, Brinkmann V, Fillatreau S, Daffe M, Tummler B, Kolbe M, Oschkinat H, Krause G, Kaufmann SH. 2014. AhR sensing of bacterial pigments regulates antibacterial defence. Nature 512:387-92.
193. Winstanley C, Langille MG, Fothergill JL, Kukavica-Ibrulj I, Paradis-Bleau C, Sanschagrin F, Thomson NR, Winsor GL, Quail MA, Lennard N, Bignell A, Clarke L, Seeger K, Saunders D, Harris D, Parkhill J, Hancock RE, Brinkman FS, Levesque RC. 2009. Newly introduced genomic prophage islands are critical determinants of in vivo competitiveness in the Liverpool Epidemic Strain of Pseudomonas aeruginosa. Genome research 19:12-23.
194. Feltner JB, Wolter DJ, Pope CE, Groleau MC, Smalley NE, Greenberg EP, Mayer-Hamblett N, Burns J, Deziel E, Hoffman LR, Dandekar AA. 2016. LasR Variant Cystic Fibrosis Isolates Reveal an Adaptable Quorum-Sensing Hierarchy in Pseudomonas aeruginosa. mBio 7.

195. Smalley NE, Schaefer AL, Asfahl KL, Perez C, Greenberg EP, Dandekar AA. 2022. Evolution of the Quorum Sensing Regulon in Cooperating Populations of Pseudomonas aeruginosa. mBio 13:e00161-22.
196. Burgener EB, Secor PR, Tracy MC, Sweere JM, Bik EM, Milla CE, Bollyky PL. 2020. Methods for Extraction and Detection of Pf Bacteriophage DNA from the Sputum of Patients with Cystic Fibrosis. Phage: Therapy, Applications, and Research 1:100-108.
197. McKitterick AC, Seed KD. 2018. Anti-phage islands force their target phage to directly mediate island excision and spread. Nat Commun 9:2348.
198. Essar DW, Eberly L, Hadero A, Crawford IP. 1990. Identification and characterization of genes for a second anthranilate synthase in Pseudomonas aeruginosa: interchangeability of the two anthranilate synthases and evolutionary implications. J Bacteriol 172:884-900.
199. Choi K-H, Kumar A, Schweizer HP. 2006. A 10-min method for preparation of highly electrocompetent Pseudomonas aeruginosa cells: Application for DNA fragment transfer between chromosomes and plasmid transformation. Journal of Microbiological Methods 64:391-397.
200. Tesson F, Hervé A, Mordret E, Touchon M, d'Humières C, Cury J, Bernheim A. 2022. Systematic and quantitative view of the antiviral arsenal of prokaryotes. Nature Communications 13:2561.
201. Oromi-Bosch A, Antani JD, Turner PE. 2023. Developing Phage Therapy That Overcomes the Evolution of Bacterial Resistance. Annu Rev Virol doi:10.1146/annurev-virology-012423-110530.
202. Bernheim A, Sorek R. 2019. The pan-immune system of bacteria: antiviral defence as a community resource. Nat Rev Microbiol doi:10.1038/s41579-019-0278-2.
203. Partridge SR, Kwong SM, Firth N, Jensen SO. 2018. Mobile Genetic Elements Associated with Antimicrobial Resistance. Clinical Microbiology Reviews 31.
204. Rankin DJ, Rocha EPC, Brown SP. 2011. What traits are carried on mobile genetic elements, and why? Heredity 106:1-10.
205. Nogueira T, Rankin DJ, Touchon M, Taddei F, Brown SP, Rocha EP. 2009. Horizontal gene transfer of the secretome drives the evolution of bacterial cooperation and virulence. Curr Biol 19:1683-91.
206. Doron S, Melamed S, Ofir G, Leavitt A, Lopatina A, Keren M, Amitai G, Sorek R. 2018. Systematic discovery of antiphage defense systems in the microbial pangenome. Science 359.
207. Duncan-Lowey B, Kranzusch PJ. 2022. CBASS phage defense and evolution of antiviral nucleotide signaling. Curr Opin Immunol 74:156-163.
208. Millman A, Bernheim A, Stokar-Avihail A, Fedorenko T, Voichek M, Leavitt A, Oppenheimer-Shaanan Y, Sorek R. 2020. Bacterial Retrons Function In Anti-Phage Defense. Cell 183:1551-1561 e12.
209. Koonin EV, Makarova KS, Wolf YI. 2017. Evolutionary Genomics of Defense Systems in Archaea and Bacteria. Annu Rev Microbiol 71:233-261.
210. Goldfarb T, Sberro H, Weinstock E, Cohen O, Doron S, Charpak-Amikam Y, Afik S, Ofir G, Sorek R. 2015. BREX is a novel phage resistance system widespread in microbial genomes. EMBO J 34:169-83.
211. Wick RR, Judd LM, Gorrie CL, Holt KE. 2017. Unicycler: Resolving bacterial genome assemblies from short and long sequencing reads. PLOS Computational Biology 13:e1005595.

212. Wick RR, Judd LM, Cerdeira LT, Hawkey J, Méric G, Vezina B, Wyres KL, Holt KE. 2021. Trycycler: consensus long-read assemblies for bacterial genomes. Genome Biology 22.
213. Johnson MC, Laderman E, Huiting E, Zhang C, Davidson A, Bondy-Denomy J. 2023. Core defense hotspots within Pseudomonas aeruginosa are a consistent and rich source of anti-phage defense systems. Nucleic Acids Research doi:10.1093/nar/gkad317.
214. Owen SV, Wenner N, Dulberger CL, Rodwell EV, Bowers-Barnard A, Quinones-Olvera N, Rigden DJ, Rubin EJ, Garner EC, Baym M, Hinton JCD. 2021. Prophages encode phage-defense systems with cognate self-immunity. Cell Host & Microbe 29:1620-1633.e8.
215. Fillol-Salom A, Rostøl JT, Ojiogu AD, Chen J, Douce G, Humphrey S, Penadés JR. 2022. Bacteriophages benefit from mobilizing pathogenicity islands encoding immune systems against competitors. Cell 185:3248-3262.e20.
216. de Mattos CD, Faith DR, Nemudryi AA, Schmidt AK, Bublitz DC, Hammond L, Kinnersley MA, Schwartzkopf CM, Robinson AJ, Joyce A, Michaels LA, Brzozowski RS, Coluccio A, Xing DD, Uchiyama J, Jennings LK, Eswara P, Wiedenheft B, Secor PR. 2023. Polyamines and linear DNA mediate bacterial threat assessment of bacteriophage infection. Proceedings of the National Academy of Sciences 120:e2216430120.
217. Seiler N, Eichentopf B. 1975. 4-aminobutyrate in mammalian putrescine catabolism. Biochem J 152:201-10.
218. Wu D, Lim SC, Dong Y, Wu J, Tao F, Zhou L, Zhang L-H, Song H. 2012. Structural Basis of Substrate Binding Specificity Revealed by the Crystal Structures of Polyamine Receptors SpuD and SpuE from *Pseudomonas aeruginosa*. Journal of Molecular Biology 416:697-712.
219. Zhou L, Wang J, Zhang L-H. 2007. Modulation of Bacterial Type III Secretion System by a Spermidine Transporter Dependent Signaling Pathway. PLOS ONE 2:e1291.
220. Gavric D, Knezevic P. 2022. Filamentous Pseudomonas Phage Pf4 in the Context of Therapy-Inducibility, Infectivity, Lysogenic Conversion, and Potential Application. Viruses 14:1261.
221. Shah M, Taylor VL, Bona D, Tsao Y, Stanley SY, Pimentel-Elardo SM, McCallum M, Bondy-Denomy J, Howell PL, Nodwell JR, Davidson AR, Moraes TF, Maxwell KL. 2021. A phage-encoded anti-activator inhibits quorum sensing in Pseudomonas aeruginosa. Molecular Cell 81:571-583.e6.
222. Faith D, Kinnersley M, Schwartzkopf CM, Mattos CDd, Schmidt AK, Secor PR. 2022. Complete Genome Sequence of the N4-like Pseudomonas aeruginosa Bacteriophage vB_PaeP_CMS1. Microbiology Resource Announcements 11:e00239-22.
223. Chin NX, Neu HC. 1987. Synergy of imipenem--a novel carbapenem, and rifampin and ciprofloxacin against *Pseudomonas aeruginosa*, *Serratia marcescens* and *Enterobacter* species. Chemotherapy 33:183-8.
224. Shariati A, Arshadi M, Khosrojerdi MA, Abedinzadeh M, Ganjalishahi M, Maleki A, Heidary M, Khoshnood S. 2022. The resistance mechanisms of bacteria against ciprofloxacin and new approaches for enhancing the efficacy of this antibiotic. Front Public Health 10:1025633.
225. Campbell EA, Korzheva N, Mustaev A, Murakami K, Nair S, Goldfarb A, Darst SA. 2001. Structural mechanism for rifampicin inhibition of bacterial rna polymerase. Cell 104:901-12.
226. Fischer S, Römling U, Tümmler B. 2019. A unique methylation pattern by a type I HsdM methyltransferase prepares for DpnI rare cutting sites in the Pseudomonas aeruginosa PAO1 genome. FEMS Microbiol Lett 366.

227. Palma M, Zurita J, Ferreras JA, Worgall S, Larone DH, Shi L, Campagne F, Quadri LE. 2005. *Pseudomonas aeruginosa* SoxR does not conform to the archetypal paradigm for SoxR-dependent regulation of the bacterial oxidative stress adaptive response. Infect Immun 73:2958-66.
228. Calb R, Davidovitch A, Koby S, Giladi H, Goldenberg D, Margalit H, Holtel A, Timmis K, Sanchez-Romero JM, de Lorenzo V, Oppenheim AB. 1996. Structure and function of the *Pseudomonas putida* integration host factor. J Bacteriol 178:6319-26.
229. Poulsen BE, Yang R, Clatworthy AE, White T, Osmulski SJ, Li L, Penaranda C, Lander ES, Shoresh N, Hung DT. 2019. Defining the core essential genome of *Pseudomonas aeruginosa*. Proceedings of the National Academy of Sciences 116:10072-10080.
230. Whitfield C, Williams DM, Kelly SD. 2020. Lipopolysaccharide O-antigens-bacterial glycans made to measure. J Biol Chem 295:10593-10609.
231. Burrows LL, Charter DF, Lam JS. 1996. Molecular characterization of the *Pseudomonas aeruginosa* serotype O5 (PAO1) B-band lipopolysaccharide gene cluster. Mol Microbiol 22:481-95.
232. Miller WL, Wenzel CQ, Daniels C, Larocque S, Brisson JR, Lam JS. 2004. Biochemical characterization of WbpA, a UDP-N-acetyl-D-glucosamine 6-dehydrogenase involved in O-antigen biosynthesis in Pseudomonas aeruginosa PAO1. J Biol Chem 279:37551-8.
233. Westman EL, McNally DJ, Charchoglyan A, Brewer D, Field RA, Lam JS. 2009. Characterization of WbpB, WbpE, and WbpD and reconstitution of a pathway for the biosynthesis of UDP-2,3-diacetamido-2,3-dideoxy-D-mannuronic acid in Pseudomonas aeruginosa. J Biol Chem 284:11854-62.
234. Weckener M, Woodward LS, Clarke BR, Liu H, Ward PN, Le Bas A, Bhella D, Whitfield C, Naismith JH. 2023. The lipid linked oligosaccharide polymerase Wzy and its regulating co-polymerase, Wzz, from enterobacterial common antigen biosynthesis form a complex. Open Biol 13:220373.
235. Li G, Shen M, Yang Y, Le S, Li M, Wang J, Zhao Y, Tan Y, Hu F, Lu S. 2018. Adaptation of Pseudomonas aeruginosa to Phage PaP1 Predation via O-Antigen Polymerase Mutation. Frontiers in Microbiology 9.
236. Delcour AH. 2009. Outer membrane permeability and antibiotic resistance. Biochimica et biophysica acta 1794:808-16.
237. Schmidt AK, Schwartzkopf CM, Pourtois JD, Burgener EB, Faith DR, Joyce A, Lamma T, Kumar G, Bollyky PL, Secor PR. 2024. Targeted deletion of Pf prophages from diverse *Pseudomonas aeruginosa* isolates has differential impacts on quorum sensing and virulence traits. Journal of Bacteriology 206:e00402-23.
238. Choi KH, Gaynor JB, White KG, Lopez C, Bosio CM, Karkhoff-Schweizer RR, Schweizer HP. 2005. A Tn7-based broad-range bacterial cloning and expression system. Nat Methods 2:443-8.
239. Twort FW. 1936. Further Investigations on the Nature of Ultra-Microscopic Viruses and their Cultivation. Journal of Hygiene 36:204-235.
240. D'Herelle F. 2007. On an invisible microbe antagonistic toward dysenteric bacilli: brief note by Mr. F. D'Herelle, presented by Mr. Roux. Research in Microbiology 158:553-554.
241. Culbertson EM, Levin TC. 2023. Eukaryotic antiviral immune proteins arose via convergence, horizontal transfer, and ancient inheritance doi:10.1101/2023.06.27.546753. Cold Spring Harbor Laboratory.

242. Silpe JE, Wong JWH, Owen SV, Baym M, Balskus EP. 2022. The bacterial toxin colibactin triggers prophage induction. Nature 603:315-320.

243. Blasco L, Barrio-Pujante A, Lopez-Causape C, Arman L, Bleriot I, Pacios O, Fernandez-Garcia L, Ortiz-Cartagena C, Ibarguren-Quiles C, Canton R, Oliver A, Tomas M. 2024. Involvement of Pf-like phages in resistance to phage infection in clinical isolates of P. aeruginosa from cystic fibrosis patients doi:10.1101/2024.05.03.592413. Cold Spring Harbor Laboratory.